Charles University

Faculty of Science

Study programme: Environmental Science



Mgr. Josef Brůna

Use of remote sensing data for monitoring of long-term vegetation dynamics on the landscape scale

Využití dat dálkového průzkumu Země pro sledování dlouhodobé dynamiky vegetace na krajinném měřítku

Type of thesis:

Doctoral thesis

Supervisor: doc. Ing. Jan Wild Ph.D.

Prague, 2018

Prohlášení:

Prohlašuji, že jsem závěrečnou práci zpracoval samostatně a že jsem uvedl všechny použité informační zdroje a literaturu. Tato práce ani její podstatná část nebyla předložena k získání jiného nebo stejného akademického titulu.

Declaration:

Hereby I declare that I worked out this thesis independently, using the listed sources and literature. I have not submitted this thesis, or any significant part thereof, to obtain the same or any other academic degree.

V Praze / In Prague 14.06.2018

.....

Josef Brůna

Table of contents

Acknowledgments 5
List of publications and manuscripts included in the Ph.D. thesis 6
Author's contributions 7
Abstract in Czech 9
Abstract 10
Introduction 11
Aims of the thesis 11
Remote sensing of vegetation changes 12
Data 14
Methods of processing 17
Results 18
Use of presented papers on current environmental problems 20
Conclusions 22
References 23
Attached publications 28
Paper I
Paper II
Paper III
Paper IV
Paper V

Acknowledgments

I would like to express my gratefulness to my supervisor Jan Wild for his continuous support and friendship throughout my studies.

A substantial part of the presented research would not be possible without contributions and support from my colleagues from Institute of Botany, Department of GIS and RS, namely Jana Müllerová, Martin Kopecký, Martin Macek, Zdeňka Konopová, Matěj Man and others and co-authors from other institutions, namely Jaroslav Vojta, Martin Hais, Luděk Berec, Petr Dvořák, Tomáš Bartaloš and others.

I am also grateful for the support of my family and friends, especially in recent months.

Publications in this thesis were only possible thanks to support from research grants and their leaders throughout my long study: GAČR 526/06/0818 (T. Herben), MŽP SP/2D2/111/08 (J. Wild), GAUK 20310 (J. Brůna), GAČR 504/10/0843 (T. Herben), GAUK 630112 (E. Horčičková), COST FP 1304 (Ch. Reyer), TAČR TA04020455 (J. Müllerová), COST LD 15158 (J. Wild). My research also greatly benefited from institutional access to scientific literature and from the open access movement.

List of publications and manuscripts included in the Ph.D. thesis

Paper I

Brůna, J., Wild, J., Svoboda, M., Heurich, M., Müllerová, J. (2013) Impacts and underlying factors of landscape-scale, historical disturbance of mountain forest identified using archival documents. *Forest Ecology and Management* 305:294-306. doi: 10.1016/j.foreco.2013.06.017

Paper II

Brůna, J., Vojta, J. (manuscript) Landscape-scale forest succession on abandoned agricultural land is controlled by terrain topography, distance to seed source and previous land use

Manuscript prepared for Ecosystems

Paper III

Hais, M.; Wild, J.; Berec, L.; Brůna, J.; Kennedy, R.; Braaten, J.; Brož, Z. (2016) Landsat Imagery Spectral Trajectories — Important Variables for Spatially Predicting the Risks of Bark Beetle Disturbance. *Remote Sensing* 8: 1–22. doi: 10.3390/rs8080687

Paper IV

Müllerová, J., Bartaloš, T., Brůna, J., Dvořák, P., Vítková, M. (2017) Unmanned aircraft in nature conservation: an example from plant invasions. *International Journal of Remote Sensing* 38(8-10):2177-2198. doi: 10.1080/01431161.2016.1275059

Paper V

Müllerová, J., Brůna, J., Bartaloš, T., Dvořák, P., Vítková, M., Pyšek, P. (2017) Timing is important: unmanned aircraft versus satellite imagery in plant invasion monitoring. *Frontiers in Plant Science* 8 (May): 1-13. doi: 10.3389/fpls.2017.00887

Author's contributions

Paper I JB participated in data preparation, computed all statistical analyses and led the writing of the paper.

Paper II JB prepared all data, computed all statistical analyses and led the writing of the manuscript.

Paper III JB participated in data preparations and the writing of the paper.

Paper IV JB participated in the field data collection, performed some of the analyses and participated in the writing of the paper.

Paper V JB participated in the field data collection, performed statistical analyses on one of the species (*Reynoutria sp.*) and participated in the writing of the paper.

The supervisor of this Ph.D. thesis, Jan Wild, confirms the contributions of Josef Brůna as stated above.

Jan Wild

The main authors of the papers confirm these contributions as stated above.

Paper IV and V

Jana Müllerová

Paper III

Martin Hais

Abstract in Czech

Tato disertační práce se věnuje především využití dat dálkového průzkumu pro sledování a studium změn vegetace. Díky archivním materiálům můžeme dnes provádět rozsáhlé studie na úrovni krajiny i celého světa bez potřeby rozsáhlých nebo archivních terénních dat. Od středověku se můžeme opřít o různé typy map, pro studium vegetace především lesnických. Od 30. let 20. století jsou v Evropě dostupné letecké snímky a od 70. let pak snímky satelitní, jejichž dostupnost a kvalita v době mého studia rapidně vzrostla. Nejnovějším příspěvkem v této oblasti jsou bezpilotní prostředky a metody jejich zpracování, které umožňují detailní mapování rozsáhlých ploch s nízkými náklady. Kromě výzkumných ekologických otázek, mají zde prezentované práce i environmentální rozměr a různou měrou přispívají k řešení aktuální problémů české ochrany životního prostředí od ochrany přírody v národních parcích a chráněných oblastech až po monitoring rostlinných invazí.

Archivní lesnické mapy jsem využil k rekonstrukci a analýze rozsáhlých disturbancí (polomů a následné gradace lýkožrouta smrkového) v lesích Šumavy a Bavorského lesa v letech 1868-1870. Analyzována byla nejen druhová skladba, ale i faktory prostředí odvozené z digitálního modelu terénu. Stejnému tématu se pak věnovala analýza predispozic lesa k napadení lýkožroutem smrkovým využívající archivu dat satelitů Landsat. Archivní a současné letecké snímky jsem využil pro modelování zarůstání opuštěné krajiny v Doupovských horách, kde jsem opět využíval faktory prostředí odvozené z digitálního modelu terénu. Analýza vývoje od roku 1952 ukazuje změny prostředí, které by během terénních prací nebylo možné postihnout. I zde je cenným zdrojem informací mapa původního využití půdy, která nahrazuje terénní průzkum v době zániku sídel.

Díky rozvoji bezpilotních prostředků je dnes možné monitorovat výskyt jednotlivých druhů rostlin, čemuž jsme se věnovali v článcích věnujících se detekci invazních rostlin. Zde jsou důležitým zdrojem dat především terénní data o výskytu jednotlivých druhů pro kalibraci a validaci. Současné pokroky strojového zpracování velkého množství obrazových dat slibují značný rozvoj tohoto oboru v nadcházejících desetiletích. I nadále však budou archivní data důležitá pro pochopení předchozího vývoje.

Abstract

This thesis deals with the use of remote sensing data for studying and monitoring vegetation changes. Thanks to archival materials, we can now make extensive studies at the landscape and global level without the need for large-scale old field data. From the Middle Ages, we can rely on different types of maps, for vegetation studies, these are mainly forestry maps. Since the 1930's, aerial photographs have been available in Europe, and satellite imagery was available since the 1970's. Availability and quality of satellite imagery had increased rapidly during my study. The most recent data source are unmanned aerial systems and methods of processing their data, which allow inexpensive detailed mapping of large areas. The presented publications do not only solve ecological research questions, but also contribute to solving current environmental problems in the Czech Republic, from nature conservation in National Parks and protected areas to monitoring of plant invasions.

I have used archival forest maps for the reconstruction and analysis of large disturbances (windthrow and subsequent gradations of bark beetle) in forests of Šumava and the Bavarian Forest in 1868-1870. Species composition, as well as environmental factors derived from digital elevation model, were analyzed. The same topic was also studied in the current analysis of forest predisposition to bark beetle attack using the Landsat satellites data archive. I have used archival and contemporary aerial imagery for modeling of secondary succession of the abandoned landscape in the Doupov Mountains. Once again, environmental factors derived from the digital terrain model were used for analysis of development since 1952. The results show long-term changes in the environment that could not have been covered by fieldwork. Old cadastral map from the time of abandonment was also used here as a valuable source of data to understand the predispositions for change.

Thanks to the development of unmanned aerial systems it is now possible to monitor the occurrence of individual plant species, as we have done in articles dealing with the detection of invasive plants. This type of research relies on field data on the occurrence of individual species for calibration and validation. The current advances in machine processing of large amounts of image data promise considerable development in this field over the coming decades. However, archival data will continue to be important for understanding previous development.

Introduction

The occurrence of trees and plants is determined by environmental conditions, disturbance regime, competition between coexisting species, interactions with herbivores and others influences. However, the significance of some factors is evident on a larger spatial scale, particularly the importance of species spreading, historical species distribution and large-scale disturbances. Processes on a landscape scale can significantly modify local events or their outcomes. Knowledge of the landscape context is therefore necessary to understand the development of vegetation cover over longer periods of time. One possible approach is the mathematical modeling of natural processes based on knowledge of population-biological characteristics of species. The disadvantage of such an approach is that information is not always available. For example, if we do not have reliable information on the mutual competition of tree species, such models may erroneously predict the development of species composition under different disturbance conditions. Permanent study plots are often used to assess long-term vegetation chnages. They provide valuable data, but maintenance and data collection costs are high. Remote sensing (RS) and geographic information systems (GIS) can deliver data for similar studies even in places where long-term data collection has not taken place. In my thesis, I had used several available types of remote sensing data to answer various ecological questions relevant to current nature protection problems in the Czech Republic.

Aims of the thesis

The main aims of my thesis are methodological and ecological. Available processing methods are rarely ideal for the ecological question in mind. Therefore, for most studies that use remote sensing data, there are modifications and innovative processing needed to produce the best results.

- My first methodological aim was to adapt and use object-oriented classification of aerial images to derive relevant ecological data for monitoring vegetation changes semi-automatically.
    - I have focused on this aim in **Papers II**, **IV** and **V**.
- My second methodological aim was to process and use archival data to enable long-term studies even without old field data.
    - I have focused on this aim in **Papers I** (maps), **II** (aerial imagery) and **III** (satellite imagery).
- My third methodological aim was to prepare a method for practical application of unmanned aerial vehicle (UAV) for monitoring of invasive plant species in nature conservation.

- I have focused on this aim in **Papers IV** and **V**.

- The ecological questions of my thesis are connected to the spatial dimension of several ecological processes.
    1. Are large-scale disturbances part of a historical range of variability of central European mountain spruce forests? What are the drivers behind spatial differences of impacts of large-scale disturbances?
        - I have focused on this aim in **Papers I** and **III**.
    2. What are the main drivers behind secondary succession speed and course in an abandoned landscape?
        - I have focused on this aim in **Paper II**.

Remote sensing of vegetation changes

The first aerial photograph was captured in 1858 by a French photographer Gaspard-Félix Tournachon from a hot-air balloon from 80 m above ground. It captured an image of the of Bievre valley near Petit-Becetre, as a proof of an idea, Tournachon had patented 3 years earlier, to use this type of photography for mapmaking and surveying. Aerial photography was recognized as a useful method for mapping purposes during the beginning of 20th century as it delivers a vast amount of data about the landscape at a single point in time and later also about changes in time. The original purpose was usually military or economic, but it is also valuable for ecological research purposes. Repeated black and white aerial survey photography is available in many countries of Europe (Cousins and Ihse, 1998; Lofman and Kouki, 2001) and USA (Turner and Ruscher, 1988) since 1930's and was successfully used for ecological studies in boreal (Cousins, 2001), temperate (Godet and Thomas, 2013) and Mediterranean areas (Carmel and Kadmon, 1999, 1998; Pueyo and Beguería, 2007; Rocchini et al., 2006). Modern processing and classification techniques can help to derive even more data from this old imagery. This means that we now have a continuous source of information about large areas on a decadal or even shorter timestep for almost a century. This is a large source of spatially explicit information that can be used for long-term studies (Korpela, 2006; Miller et al., 2000). We have used old aerial imagery from every decade between 1952 and 2015 in **Paper II** to model landscape scale secondary succession of an abandoned agricultural landscape in Doupovské hory.

Infrared photography is widely used for vegetation mapping and assessment of vegetation health but was usually not captured, when the original aim of image acquisition was different and therefore this type of data is mostly missing in the archives or needs additional processing like recent orthoimages

from ČÚZK, where the infrared bands were not orthorectified. Infrared imagery is also provided by satellites that mostly includes one or several infra-red bands (Carreiras et al., 2006), although with lower spatial resolution than aerial imagery. The most significant benefit of satellite imagery is its spatial and temporal coverage. Landsat missions, for example, have coverage from 82° north latitude to 82° south latitude and imagery of the same area is captured every 16 days from one satellite and even more often when combining several satellites. The Landsat satellites have accumulated a vast data archive since 1972. Commercial satellites can offer even better coverage, and their resolution is up to 0.31 m (World-View 4). The military satellites date back even further, data from the recently declassified CORONA program cover 1960's and early 1970's and are also used in scientific studies (Fowler and Fowler, 2005). The cost of targeted acquisition of commercial high-resolution imagery is high, but it is still lower than a targeted aerial imagery acquisition (Bird et al., 2000; Comber et al., 2004). Aerial imagery is usually cheaper when comparing already acquired data from both sources.

During my studies, remote sensing options and techniques have developed rapidly. For a long time, the price of the images limited research and applications. The most substantial advance was made in 2008 when the US Geological Survey (USGS) made the data from the vast archive of Landsat missions freely available for everyone (United States Geological Survey (USGS), 2008; Woodcock et al., 2008). This revolutionized how Landsat data are used and accelerated the use of multitemporal data for change detection (Wulder et al., 2012) and resulted in a 100 fold increase in downloads and about 100,000 papers using this data were published since 2008 (Popkin, 2018) including Hansen et al. (2013) who used 654,178 Landsat scenes for a global forest study, or Zhu and Woodcock (2014) who used all 519 available images for a local study in New England. New approaches including time series and phenology help to derive more information even from its coarse resolution data. Our study (Hais et al., 2016, **Paper III**) was also made possible, although we have used only 16 scenes to derive the spectral trajectories. The freely available data and their impact inspired policies of European Earth observation program and all data from the ambitious Sentinel missions are free of charge (Butler, 2014).

Studies using remote sensing usually rely on field data for calibration and validation which enables the researchers to extrapolate the local knowledge to larger areas (Bird et al., 2000). To understand the context better, scientists use older imagery and archival data including old maps like land economic inventories (White and Mladenoff, 1994), topographic maps (Fuchs et al., 2015) or old military survey maps (Godet and Thomas, 2013; Skaloš et al., 2011). These maps were a primary source of spatial information before GIS and computer processing. Their purpose was mainly, management, economy or military related and results derived from them were mostly descriptive. Computer processing in GIS helped to derive new information from these maps (Cousins, 2001;

Skaloš et al., 2011) and statistical analysis of this type of data can answer more specific questions, than the original purpose. An excellent example of this is **Paper I**, where the archival maps and forestry books of the Czech part of Šumava were already processed manually by (Jelínek, 2005, 1988) but environmental factors behind the variability of disturbance intensity and the effect on stand age were not tested. We have added old maps from Bavarian Forest and joined all maps with information from forestry books to test possible drivers behind large scale disturbances in 19th century forests. These disturbances had a considerable impact on the current species and tree age distribution in the area. The management efforts after the disturbances included large-scale spruce plantations even in areas, with originally mixed forests and therefore large areas of forests became even aged.

The newest trend in remote sensing is the use of unmanned aerial vehicles (UAV) that combine the benefits of remote sensing with the flexibility of field data collection. They cannot compete with the spatial and temporal coverage of satellites, but they offer higher spatial and temporal resolution (Manfreda et al., 2018). They can even deliver data even in cloudy weather which is problematic with satellite data (Müllerová et al., 2016). The costs of this type of imagery are low, although the initial investment can be higher (Manfreda et al., 2018). We had used purposely built UAV for monitoring of invasive species in **Papers IV** and **V**. Combining imagery from several acquisitions across a vegetation season, we have used differences in phenology to distinguish several invasive species from similarly looking surrounding vegetation (white flowering *Heracleum mantegazzianum* and *Robinia psedoacacia* in May; dry *Reynoutria sp.* in November). The aircraft also carried a modified second consumer camera with a removed infrared filter which delivered imagery that includes information from the near infrared spectrum. This type of studies relies on field data for calibration and validation purposes, especially when using near infrared bands. Ideally, they need to be collected during the UAV missions and with a precise location. We have used a portable spectrometer to identify differences in spectral curves of several similar plants and mapped validation plots using a Global Navigation Satellite System (GNSS) equipped device.

Data

Data are a crucial part of ecological studies and methods are often based on the amount of data available. The lack of specific data is solved by using proxy data (e.g. pollen sediments for historical species distribution; topographical exposition for photosynthetically active radiation; soil type for available nutrients) or space for time substitution (Pickett, 1989) or models that derive information based on current knowledge like Ellis et al. (2010) who derived global historical anthropogenic transformation maps based on human population densities. All these methods are based on

assumption, that the influence of specific variables does not change during the time or doesn't change unexpectedly. The other problem is that no analog ecosystems or communities have existed and may exist in the future (Fox, 2007; Williams and Jackson, 2007) and the same problem comes up with climate (Veloz et al., 2012). Our results from **Paper I** concerning the factors behind large-scale disturbances certainly tell, that age of a forest stand increases disturbance probability, but our results concerning the influence of species diversity are not very useful since most of the forests have a different species composition today and it will probably be different in the future. Using a real series of repeated measurements can solve these problems, although it is harder to find the right data. We have classified several decades of aerial imagery to describe secondary succession over 70 years of in aa abandoned landscape in **Paper II**.

Remote sensing usually offers data for large areas and the problem is, that it does not necessarily provide the variables needed and scientists must look for possible correlation with available ones to derive usable results. Satellite imagery cannot provide a direct measure of forest vitality against bark beetle, but spectral indices can help to predict vulnerable forest stands as we did in **Paper III**. Remote sensing scientists can even face problems with too much data, at least too much for manual processing like visual classification. This is where computer automation helps to derive usable results, although it can lead to generalizations. Hansen et al. (2013) have used 654,178 vegetation season Landsat 7 scenes (about half of what were available) using Google Earth Engine to derive a detailed global forest map. This would not be feasible by visual interpretation, but it can also lead to problems. Their definition of forests included "all vegetation taller than 5 m in height" which according to Tropek et al. (2014) can lead to misleading interpretations, because this includes palm plantations that do not provide similar ecosystem services, as natural forests. Aguilar et al., (2016) shows that in arid ecosystems, the forest can have a lower height and still be considered forests, even if they are not present in the global map by Hansen et al. (2013). These datasets are valuable in many ways, but it is important to use them cautiously and always study the methods before making conclusions.

Spatial data including remote sensing data also face problems with spatial autocorrelation. Many statistical tests require independent samples, and therefore various methods are used to generate valid samples from remote sensing. We have used regular grid sampling and tested spatial autocorrelation using Moran I (Sokal and Oden, 1978) in **Papers I, II** and **III** to identify the best sampling distance. We have set land use type as a random effect. This helped us to identify important factors of woody species spreading into grasslands independently on former land use origin.

The true power of remote sensing data is in use with geographical information systems (GIS). In combination with spatial variables derived from field data or remote sensing, hypotheses on

a landscape or even global scale can be tested. Variety of institutions and users provide their data for free or even share it as an API so that users always get the newest data and can build applications on top of it. The most versatile data source is a digital elevation model (DEM), that can be used to derive various indexes covering hydrology, lighting, visibility, and morphometry, for example in SAGA GIS (Conrad et al., 2015). These indexes serve as a proxy for data, that is not easy to collect in the field. We had used several different indexes in **Papers I, II** and **III** and in Čuda et al. (2017) to test drivers of large-scale processes derived from a LiDAR DEM with 5 m resolution and 1 m vertical error (DMR 4G from ČÚZK, www.cuzk.cz). The most useful indexes for vegetation studies are heat load index (HLI) which describes the variation in potential solar radiation (McCune and Keon, 2002), Insolation (total, direct, diffuse; Böhner and Antonić 2009) which adds terrain features into the calculation and sums it throughout the year with respect to position of sun and can be limited to a specific time period like vegetation season, topographic Wetness Index (TWI; Beven and Kirkby 1979) used as a proxy for available water, calculated using FD8Q flow routing-algorithm as recommended by Kopecký and Čížková (2010) for vegetation studies, Topographic Position Index (TPI; Guisan et al. (1999) using several distances (50, 100, 250 and 500) defining local terrain features against their neighbourhood as well as Terrain ruggedness index (Riley et al., 1999) as a measure of topographic heterogeneity. For forest-related studies, we also use morphometric protection index, equivalent to the positive openness described in Yokoyama et al. (2002), and similar to the distance-limited Topex (Pyatt et al., 1969) widely used in windthrow risk prediction and modeling (Hanewinkel et al., 2011, 2004; Quine and White, 1992; Scott and Mitchell, 2005).

For cross-border and global studies, these can be derived from ASTER Global Digital Elevation Model V002 (METI/NASA, 2011) as we have done in **Paper I**, or from SRTM, TANDEM-X or derived models. The choice of the model influences the results, and it is therefore crucial to select the best one for each particular study (Moudrý et al., 2018). DEM derived variables are also used for species distribution modeling, for example when studying plant invasions. The areas threatened by invasion can be predicted based on knowledge of the ecology of the species, or we can test hypotheses about these using the DEM derived variables as we have done in Čuda et al. (2017). We have also used digital elevation model in combination with digital surface model produced from UAV imagery to obtain height model of vegetation to filter out trees when classifying invasive species of herbs and to filter out fields when classifying invasive trees in **Papers IV** and **V**. These height models can also be used to classify regeneration of spruce in disturbed forests and the amount of dead wood as we did in Röder et al. (2018).

Methods of processing

The papers that I present in this thesis cover a range of topics, but share similar methods and finding the right workflow and settings, to deliver the best data for each ecological question, was a crucial part of all the studies. The initial part of remote sensing studies involves radiometric and geometric corrections. With satellite imagery, geometric corrections are usually provided for all products and it is possible to obtain radiometrically corrected data as well, or use established algorithms like MADCAL (Canty et al., 2004) as Martin Hais did in our **Paper III.** The same is true for recent aerial imagery, which is usually orthorectified by the producer, but older images need to be orthorectified by the user, which involves geometric corrections caused by the camera optics and projection over a digital elevation model to obtain the final image. These will then be georeferenced using Ground Control Points obtained from the field or other georeferenced imagery and mosaicked together. Orthorectification and mosaicking of old aerial images was not an automatic task when I started and the data for **Paper II** was mostly prepared using a lot of manual input to identify tie points and mosaic the scanned original aerial survey photographs. But the process became easy in recent years with the advent of UAVs. The commonly used Structure from Motion method (SFM; Dandois and Ellis, 2010; Westoby et al., 2012) can match hundreds of photographs from UAV into a single image with millions of matching points as we did when preparing data for **Papers IV** and **V**. And even with default settings, this method produces usable results. In combination with onboard RTK GNSS and ground control points, the final orthoimage can have a horizontal error around several centimeters and even without using ground control points, the error is around one meter (as in **Papers IV** and **V**), which was a difficult task just few years ago. In **Paper II**, we have used several manually added matching points for each old image and the final horizontal error was around 1 m depending on the quality of the imagery.

The next step after creating the orthomosaic is usually classification. This can be supervised or unsupervised based on the amount of input information. I have used only supervised classification in all the studies based on training samples from the field. Regardless of the level of supervision, there are two main approaches to the classification used in remote sensing. Pixel-based approach uses only spectral information of every single pixel to determine its class, whereas the object-based classification approach (Blaschke, 2010; Blaschke et al., 2014; Hay et al., 2003) merges neighboring pixels using segmentation techniques such as multiresolution segmentation (Baatz and Schäpe, 2000) into objects and classifies the whole resulting objects based not only on brightness, but also on spatial structure, heterogeneity and context information. This is especially useful, if the classification target is covered by several pixels and has distinct shape like flowering *Heracleum mantegazzianum*

on UAV imagery in **Paper V**. It is also useful for quick classification of large structures like trees and shrubs among grasslands on aerial imagery like I did in **Paper II**, where a single bright pixel among a tree canopy was usually not a grassland. This method also eliminates the classical salt and pepper effect of pixel-based classification of detailed imagery. Even when target species or land cover class do not have distinct textural properties, this method can still help to classify the other classes more accurately. However, the simpler pixel-based classification is useful, especially in combination with machine learning algorithms. We also have successful results from pixel-based classification for detection of *Reynoutria sp.* on UAV data in **Paper V** using Support Vector Machines (Vapnik, 1995) and Random Forests (Breiman, 2001). Results in **Paper III** also rely on pixel-based classification, because the 30 m pixels of Landsat images already cover several trees that can differ in vitality. The quality of classification results also relies on accurate field data that need to have high spatial precision and include independent samples for verification and validation purposes.

Results

I have analyzed archival forestry maps and materials of mountain spruce forests in Šumava and Bavarian Forest and identified impacts and factors underlying landscape-scale disturbances of mountain forests in 1868-1870 **(Paper I)**. These disturbances (windthrow and subsequent bark beetle attack) substantially altered the age and species structure of the forests. I have identified a positive effect of mean forest age on disturbance severity, disturbances were also more severe on the Czech side of the border and in the northern areas. Mean elevation in a 250 m circle, and effective air flow heights from constant wind direction (Boehner and Conrad, 2008) also had a positive effect on the severity of the disturbance. This means that spruce forests in higher elevations and exposed areas are more vulnerable. The most disturbed age group was forests older than 120 years. The forests that grow after the 1868-1870 disturbances reached the same age recently and similar disturbances happened again in the area. We could now study details, that were not captured in the maps which combined windthrow and bark beetle damage. We have therefore focused on other pre-disturbance forest conditions that can be used to identify forests with a higher risk of bark beetle attack in **Paper III**. We have derived spectral trajectories of each component of Tasseled Cap linear transformation (Crist and Cicone, 1984; Kauth and Thomas, 1976) of a series of Landsat imagery and shown, that the Wetness index slope of the trajectory of images is an important variable to be considered for understanding the bark beetle infestation patterns. Its gradual decrease identifies the most vulnerable stands. At the beginning of the outbreak, edaphic conditions, heat load index and distance to wet areas influence the disturbance probability, later topographical wetness index (TWI;

Beven and Kirkby, 1979), age and degree of naturalness of the forest play a role. Distance to the nearest clear-cut area has a high effect on the disturbance probability at the beginning of the outbreak and at its end. If these trajectories and vulnerability maps were frequently provided to forest owners, much of the recent bark beetle outbreaks in the managed forests could have been prevented or at least the financial loss could have been lowered. The other possible solution based on our results from **Paper I** would be lowering the rotation age to avoid the disturbances.

Trajectories of images can also be prepared from aerial imagery. I have successfully adapted object-oriented classification method for monitoring of secondary succession on an abandoned landscape in **Paper II** using aerial imagery from every decade from 1952 to 2015. I have used median filtered images to help to segment the imagery and the brightness of the segmented objects and their texture based on Gray-Level Co-Occurrence Matrix (GLCM) features (Haralick et al., 1973) to classify woody vegetation and grasslands. The results and DEM derived variables helped me to identify factors behind the spatial pattern of succession on a landscape scale. The most important factor was the distance to nearest tree or shrub at the beginning of the modeled decade, which together with elevation and total insolation during vegetation season had a negative impact on succession. The density of trees and shrubs in the vicinity (15 × 15 m) and the broader neighborhood (100 × 100 m), slope and TWI had a positive effect on succession towards a forest. Which means that most of the persisting grasslands are in dry, mostly flat areas in higher elevations, with high insolation and further away from forests and shrubs. These results confirm the general pattern of secondary succession in an abandoned landscape, but thanks to the series of images offer deeper insight into the process.

Some changes in the landscape are even faster, and these can be monitored using UAV imagery. In **Papers IV** and **V**, the results are methodological and cover detection of three invasive species using a novel approach based on custom-made UAV. I have designed an optimal workflow for field data collection using a combination of aerial imagery, UAV imagery and classified imagery in Collector for ArcGIS (**Paper IV**). This data is used for training, and validation purposes. We have identified the best time and type of data to distinguish each species and the best classification method. For *Robinia pseudoacacia* the best acquisition time is after flowering, and the classification relies on near-infrared data using a supervised pixel-based classification using Support Vector Machines (SVM; Vapnik, 1995) algorithms (**Paper IV**). I have identified, that the best time for classification of *Reynoutria sp.* in a typical riparian habitat is in November after its leaves turn to red and the leaves of the surrounding trees had fallen already. If the area is without trees, the best time for detection is in the peak of vegetation season, when *Reynoutria sp.* is again highly distinguishable in the near infrared spectrum (**Paper V**). The best classification results in both acquisition times use supervised

pixel-based approach and again a SVM classifier, good results are also produced using a simple Maximum Likelihood classification. These methodological results can also serve as a basis for deeper ecological studies, for example, if the high reflectance of invasive species in near infrared spectrum is a general property of an invasive plant. The spatial distribution of individual classified species can also be used for species distribution modeling and general prediction of invasion risk based on DEM derived variables.

Use of presented papers on current environmental problems

The presented publications do not only solve ecological research questions and develop and improve methods used to address them, but also contribute to solving current environmental problems in the Czech Republic, from nature conservation in National Parks and protected areas to monitoring of plant invasions anywhere in the country. Our results can help local practitioners, and policymakers get the necessary data and hypotheses and support fact-based decisions. I have set up this goal at the beginning of my studies, and it is my main motivation for pursuing a research career. For this reason, I have also authored and co-authored several popularization articles and activities and study materials for schools.

Papers I and **III** deal with a hot topic of Czech nature protection: National park Šumava, namely large-scale disturbances of the spruce-dominated forests by windthrows and bark beetle infestation (*Ips typhographus*). Bark beetles had caused many large-scale disturbances in the recent decades across Europe in managed and protected forests. Moreover, they threat to make spruce plantations not economically viable in the near future concerning climate change. This is recently clearly visible in the managed forests in Northern Moravia. In **Paper I**, we have used archival forest maps for the reconstruction and analysis of large disturbances (windthrow and subsequent gradation of bark beetle) in forests of Šumava and the Bavarian Forest in 1868-1870. This served as a proof that such disturbances are well within the historical range of variability (Keane et al., 2009) and the forests were able to regenerate even in areas without intervention. We have further studied this ability in the field using repeated measurements of natural regeneration in core areas of NP Bavarian Forest and NP Šumava over the course of 10 years (Macek et al., 2017). This effort continues and serves as an example for NP Šumava, where the discussion about natural regeneration is ongoing. The recent outbreak of bark beetle was also studied in **Paper III** with focus on forest predisposition to bark beetle attack using the Landsat satellite data. The pre-disturbance spectral trajectories can serve for assessment of bark beetle infestation risk in a managed forest. We have also used cheap commercial

drones to assess the regeneration density and spatial structure in Bavarian Forest NP as a new method for monitoring of forests across the national park (Röder et al., 2018).

Paper II is focused on abandoned landscape, which gradually evolves during recent decades throughout the Czech Republic and Europe and high-income countries in general (Fridley and Wright, 2012; Queiroz et al., 2014; Wright and Fridley, 2010) in marginal or low productive areas (FAO, 2007). This is especially pronounced in the countries that belonged to the Soviet bloc, where the collapse of totalitarian regimes in the 1980's led to a considerable decrease of agricultural land (Alcantara et al., 2013; Kuemmerle et al., 2008; Prach et al., 2007). This is connected to the intensification of agriculture and urbanization. Six decades of secondary succession of abandoned landscape show that the results of this process are not unified and depend on environmental factors. The resulting landscape can still host many endangered species and intervention measures can be cheap. The military area Hradiště, where the study was done, is under contractual protection by Vojenský úřad vojenského újezdu Hradiště, which acts as a local nature protection body, since 2009. The protection relies on conventional conservation measures to keep the diversity of habitats for selected species and Special Areas of Conservation as defined in the European Union's Habitats Directive (92/43/EEC) in the non-military parts. In the parts used by the military, this protection is carried out by military training or targeted maintenance of selected habitats. Monitoring based on remote sensing data and modeling is currently not used but can help to target the specific military management efficiently.

Papers IV and **V** focused on monitoring of several invasive plant species using unmanned aerial vehicles (UAV). These results of an applied research project (TAČR TA04020455) were also used as a basis of a methodology of mapping invasive species using remote sensing certified by the Ministry of the Environment of the Czech Republic (Müllerová et al., 2017). This methodology, together with the custom build UAV for data acquisition and geoportal for data management is intended for use by nature protection authorities, local environmental groups and other researchers. Fast and efficient monitoring using UAVs is crucial for quick and targeted measures against invasive species. This method can also be used to monitor results of eradication measures, which was tested in Karlovarský kraj. The methodology is freely available and whole system is currently being offered to local nature protection authorities and action groups and is tested with MAS Labské skály for preparation of a project for elimination of *Reynoutria sp.* in Dečínsko region.

Conclusions

During my studies, remote sensing options and techniques have developed rapidly. There are vast amounts of data for free or at a reasonable price and studies are no longer limited by imagery (**Paper III**). The hardware and software advances in image processing enabled automation of many tasks that were laborious when I started working with remote sensing data in 2007. This can be best seen in UAV image processing. Hundreds of images can be automatically matched together using millions of automatically generated tie points to produce not only georeferenced orthoimage but also a detailed digital surface model. This removes the need for digital elevation model from orthoimage processing workflow but also produces new types of data for ecological studies. Advances in Real-Time Kinematic GNSS mean that even without tie points, the resulting image has only a minor error in georeferencing, making use of repeated acquisition even more straightforward and robust. This also means that phenology can be derived from several acquisitions through a single year, because the imagery from several flights can be easily overlaid. Species recognition based on imagery is still a challenging task, but phenology helps to distinguish many problematic species. We had taken advantage of this in **Papers IV** and **V** for classification of *Robinia pseudoacacia*, *Heracleum mantegazzianum,* and *Reynoutria sp.* and also *Ailanthus altissima* in Müllerová et al. (2017). Field data are still crucial for validation and interpretation, but their collection became more comfortable as well. Products like Collector for ArcGIS offer delineation of features in the field using custom UAV data or free worldwide imagery with the help of GNSS integrated into mobile phones or tablets. Custom databases and photo attachments make many laborious fieldwork tasks a thing of the past.

All the papers included in the thesis can be used for helping to solve current nature protection problems in the Czech Republic. Some in the form of a relevant argument based on significant field data, for scientific debate about the future management of National parks (**Papers I** and **III**) or about management interventions in smaller protected areas (**Paper II**), some as direct methods for nature protection practitioners (**Papers IV** and **V**).

I consider the aims of my thesis to be fulfilled, I have successfully adapted object-oriented classification method for monitoring of secondary succession on an abandoned landscape (**Paper II**) and also helped to develop a complete applied methodology for the monitoring of selected invasive species that is best described in the certified methodology of Ministry of Environment (Müllerová et al., 2017) and in **Papers IV** and **V**. I have used archival maps for our study of large-scale disturbances of mountain spruce forests in NP Šumava and Bavarian Forest in the 19th century and identified impacts and factors underlying a landscape scale disturbance of a mountain forest. I have also shown that large scale disturbances are well within historical range of variability in the area **(Paper I)**. Using

the time series of Landsat imagery to study recent bark beetle outbreaks around Březník, we have later identified indices that show the weakening of forest stands before bark beetle attack (**Paper III**). Old aerial imagery allowed me to study the course of 70 years of succession even in areas with restricted entrance and sparse field records (**Paper II**). Using DEM derived variables, I have identified several important conditions that slow or alter the course of secondary succession on an abandoned landscape. I conclude, that remote sensing data are a valuable source for monitoring of long-term vegetation dynamics on the landscape scale and related ecological studies.

References

Aguilar, F.J., Nemmaoui, A., Aguilar, M.A., Chourak, M., Zarhloule, Y., García Lorca, A.M., 2016. A quantitative assessment of forest cover change in the moulouya river watershed (Morocco) by the integration of a subpixel-based and object-based analysis of Landsat data. *Forests* 7, 1–19. doi: 10.3390/f7010023

Alcantara, C., Kuemmerle, T., Baumann, M., Bragina, E. V., Griffiths, P., Hostert, P., Knorn, J., Müller, D., Prishchepov, A. V., Schierhorn, F., Sieber, A., Radeloff, V.C., 2013. Mapping the extent of abandoned farmland in Central and Eastern Europe using MODIS time series satellite data. *Environmental Research Letters* 8. doi: 10.1088/1748-9326/8/3/035035

Baatz, M., Schäpe, A., 2000. Multiresolution segmentation— an optimization approach for high quality multiscale image segmentation, in: J., S. (Ed.), Angewandte Geographische Informationsverarbeitung XII. Beiträge Zum AGIT-Symposium Salzburg,. Herbert Wichman Verlag, Karlsruhe, pp. 12–23.

Beven, K.J., Kirkby, M.J., 1979. A physically based, variable contributing area model of basin hydrology / Un modèle à base physique de zone d'appel variable de l'hydrologie du bassin versant. *Hydrological Sciences Bulletin* 24, 43–69. doi: 10.1080/02626667909491834

Bird, a. C., Taylor, J.C., Brewer, T.R., 2000. Mapping National Park landscape from ground, air and space. *International Journal of Remote Sensing* 21, 2719–2736. doi: 10.1080/01431160050110250

Blaschke, T., 2010. Object based image analysis for remote sensing. *ISPRS Journal of Photogrammetry and Remote Sensing* 65, 2–16. doi: 10.1016/j.isprsjprs.2009.06.004

Blaschke, T., Hay, G.J., Kelly, M., Lang, S., Hofmann, P., Addink, E., Queiroz Feitosa, R., van der Meer, F., van der Werff, H., van Coillie, F., Tiede, D., 2014. Geographic Object-Based Image Analysis - Towards a new paradigm. *ISPRS Journal of Photogrammetry and Remote Sensing* 87, 180–191. doi: 10.1016/j.isprsjprs.2013.09.014

Boehner, J., Conrad, O., 2008. Effective Air Flow Heights.

Böhner, J., Antonić, O., 2009. Chapter 8 Land-Surface Parameters Specific to Topo-Climatology, in: Developments in Soil Science. Elsevier, pp. 195–226. doi: 10.1016/S0166-2481(08)00008-1

Breiman, L., 2001. Random forests. *Machine Learning* 45, 5–32. doi: 10.1023/A:1010933404324

Butler, D., 2014. Earth observation enters next phase. *Nature* 508, 160–161. doi: 10.1038/508160a

Canty, M.J., Nielsen, A.A., Schmidt, M., 2004. Automatic radiometric normalization of multitemporal satellite imagery. *Remote Sensing of Environment* 91, 441–451. doi: 10.1016/j.rse.2003.10.024

Carmel, Y., Kadmon, R., 1999. Effects of grazing and topography on long-term vegetation changes in a Mediterranean ecosystem in Israel. *Plant Ecology* 145, 243–254. doi: 10.1023/A:1009872306093

Carmel, Y., Kadmon, R., 1998. Computerized classification of Mediterranean vegetation using panchromatic aerial photographs. *Journal of Vegetation Science* 9, 445–454. doi: 10.2307/3237108

Comber, a. J., Law, a. N.R., Lishman, J.R., 2004. Application of knowledge for automated land cover change monitoring. *International Journal of Remote Sensing* 25, 3177–3192. doi: 10.1080/01431160310001657795

Conrad, O., Bechtel, B., Bock, M., Dietrich, H., Fischer, E., Gerlitz, L., Wehberg, J., Wichmann, V., Böhner, J., 2015. System for Automated Geoscientific Analyses (SAGA) v. 2.1.4. *Geoscientific Model Development* 8, 1991–2007. doi: 10.5194/gmd-8-1991-2015

Cousins, S.A.O., 2001. Analysis of land-cover transitions based on 17th and 18th century cadastral maps and aerial photographs. *Landscape Ecology* 16, 41–54.

Cousins, S.A.O., Ihse, M., 1998. A methodological study for biotope and landscape mapping based on CIR aerial photographs. *Landscape and Urban Planning* 41, 183–192. doi: 10.1016/S0169-2046(98)00057-7

Crist, E.P., Cicone, R.C., 1984. Application of the Tasseled Cap concept to simulated thematic mapper data. *Photogrammetric Engineering Remote Sensing* 50, 343–352.

Čuda, J., Rumlerová, Z., Brůna, J., Skálová, H., Pyšek, P., 2017. Floods affect the abundance of invasive Impatiens glandulifera and its spread from river corridors. *Diversity and Distributions* 23, 342–354. doi: 10.1111/ddi.12524

Dandois, J.P., Ellis, E.C., 2010. Remote sensing of vegetation structure using computer vision. *Remote Sensing* 2, 1157–1176. doi: 10.3390/rs2041157

Ellis, E.C., Goldewijk, K.K., Siebert, S., Lightman, D., Ramankutty, N., 2010. Anthropogenic transformation of the biomes, 1700 to 2000. *Global Ecology and Biogeography* 19, 589–606. doi: 10.1111/j.1466-8238.2010.00540.x

FAO, R. (Italy). A. and C.P.D., 2007. The agriculture-forest interface.

Fowler, M.J.F., Fowler, Y.M., 2005. Detection of archaeological crop marks on declassified CORONA KB-4B intelligence satellite photography of Southern England. *Archaeological Prospection* 12, 257–264. doi: 10.1002/arp.266

Fox, D., 2007. Back to the No-Analog Future? *Science* 316, 823–825. doi: 10.1126/science.316.5826.823

Fridley, J.D., Wright, J.P., 2012. Drivers of secondary succession rates across temperate latitudes of the Eastern USA: climate, soils, and species pools. *Oecologia* 168, 1069–1077. doi: 10.1007/s00442-011-2152-4

Fuchs, R., Verburg, P.H., Clevers, J.G.P.W., Herold, M., 2015. The potential of old maps and encyclopaedias for reconstructing historic European land cover/use change. *Applied Geography* 59, 43–55. doi: 10.1016/j.apgeog.2015.02.013

Godet, L., Thomas, A., 2013. Three centuries of land cover changes in the largest French Atlantic wetland provide new insights for wetland conservation. *Applied Geography* 42, 133–139. doi: 10.1016/j.apgeog.2013.05.011

Guisan, A., Weiss, S.B., Weiss, A.D., 1999. GLM versus CCA Spatial Modeling of Plant Species Distribution. *Plant Ecology* 143, 107–122. doi: 10.1023/A:1009841519580

Hais, M., Wild, J., Berec, L., Brůna, J., Kennedy, R., Braaten, J., Brož, Z., 2016. Landsat Imagery Spectral Trajectories — Important Variables for Spatially Predicting the Risks of Bark Beetle Disturbance. *Remote Sensing* 8, 1–22. doi: 10.3390/rs8080687

Hanewinkel, M., Peltola, H., Soares, P., González-Olabarria, J.R., 2011. Recent approaches to model the risk of storm and fire. *Forest Systems* 3, 30–47. doi: 10.5424/fs/201019S-9286

Hanewinkel, M., Zhou, W., Schill, C., 2004. A neural network approach to identify forest stands susceptible to wind damage. *Forest Ecology and Management* 196, 227–243. doi: 10.1016/j.foreco.2004.02.056

Hansen, M.C., Potapov, P. V, Moore, R., Hancher, M., Turubanova, S.A., Tyukavina, A., Thau, D., Stehman, S. V, Goetz, S.J., Loveland, T.R., Kommareddy, A., Egorov, A., Chini, L., Justice, C.O., Townshend, J.R.G., 2013. High-Resolution Global Maps of 21st-Century Forest Cover Change. *Science* 342, 850–853. doi: 10.1126/science.1244693

Haralick, R.M., Shanmugam, K., Dinstein, I., 1973. Textural features for image classification. *IEEE Transactions on Systems, Man and Cybernetics*. doi: 10.1109/TSMC.1973.4309314

Hay, G.J., Blaschke, T., Marceau, D.J., 2003. A comparison of three image-object methods for the multiscale analysis of landscape structure. *Science* 57, 327–345. doi: 10.1016/S0924-2716(02)00162-4

Jelínek, J., 2005. Od jihočeských pralesů k hospodářským lesům Šumavy. MZE ČR, Úsek lesního hospodářství, ÚHÚL Brandýs nad Labem.

Jelínek, J., 1988. Větrná a kůrovcová kalamita na Šumavě z let 1868 až 1878. Lesprojekt, Brandýs nad Labem.

Kauth, R.J., Thomas, G.S., 1976. The tasselled cap - A graphic description of the spectral-temporal development of agricultural crops as seen by Landsat. *Proceedings of the Symposium on Machine Processing of Remotely Sensed Data, West Lafayette, Indiana, U.S.A, 29 June-1 July 1976* 41–51.

Keane, R.E., Hessburg, P.F., Landres, P.B., Swanson, F.J., 2009. The use of historical range and variability (HRV) in landscape management. *Forest Ecology and Management* 258, 1025–1037. doi: 10.1016/j.foreco.2009.05.035

Kopecký, M., Čížková, Š., 2010. Using topographic wetness index in vegetation ecology: does the algorithm matter? *Applied Vegetation Science* 13, 450–459. doi: 10.1111/j.1654-109X.2010.01083.x

Korpela, I., 2006. Geometrically Accurate Time Series of Archived Aerial Images and Airborne Lidar Data in a Forest Environment. *Silva Fenica* 40, 109–126.

Kuemmerle, T., Hostert, P., Radeloff, V.C., van der Linden, S., Perzanowski, K., Kruhlov, I., 2008. Cross-border Comparison of Post-socialist Farmland Abandonment in the Carpathians. *Ecosystems* 11, 614–628. doi: 10.1007/s10021-008-9146-z

Lofman, S., Kouki, J., 2001. Fifty Years of Landscape Transformation in Managed Forests of Southern Finland. *Scandinavian Journal of Forest Research* 16, 44–53. doi: 10.1080/028275801300004406

Macek, M., Wild, J., Kopecký, M., Červenka, J., Svoboda, M., Zenáhlíková, J., Brůna, J., Mosandl, R., Fischer, A., 2017. Life and death of Picea abies after bark-beetle outbreak: ecological processes driving seedling recruitment. *Ecological Applications* 27, 156–167. doi: 10.1002/eap.1429

Manfreda, S., McCabe, M., Miller, P., Lucas, R., Pajuelo Madrigal, V., Mallinis, G., Ben Dor, E., Helman, D., Estes, L., Ciraolo, G., Müllerová, J., Tauro, F., de Lima, M., de Lima, J., Maltese, A., Frances, F., Caylor, K., Kohv, M., Perks, M., Ruiz-Pérez, G., Su, Z., Vico, G., Toth, B., 2018. On the Use of Unmanned Aerial Systems for Environmental Monitoring. *Remote Sensing* 10, 641. doi:

10.3390/rs10040641

McCune, B., Keon, D., 2002. Equations for potential annual direct incident radiation and heat load. *Journal of Vegetation Science* 13, 603–606. doi: 10.1111/j.1654-1103.2002.tb02087.x

METI/NASA, 2011. ASTER Global Digital Elevation Model V002.

Miller, D.R., Quine, C.P., Hadley, W., 2000. An investigation of the potential of digital photogrammetry to provide measurements of forest characteristics and abiotic damage. *Forest Ecology and Management* 135, 279–288. doi: 10.1016/S0378-1127(00)00286-3

Moudrý, V., Lecours, V., Gdulová, K., Gábor, L., Moudrá, L., Kropáček, J., Wild, J., 2018. On the use of global DEMs in ecological modelling and the accuracy of new bare-earth DEMs 383, 3–9. doi: 10.1016/j.ecolmodel.2018.05.006

Müllerová, J., Bartaloš, T., Brůna, J., Dvořák, P., Vítková, M., 2017. Metodika mapování invazních druhů pomocí dálkového průzkumu. Botanický ústav AV ČR, Průhonice. Certified by Ministry of the Environment of the Czech Republic.

Müllerová, J., Brůna, J., Dvořák, P., Bartaloš, T., Vítková, M., 2016. Does the data resolution/origin matter? Satellite, airborne and UAV imagery to tackle plant invasions, in: The International Archives of the Photogrammetry, Remote Sensing and Spatial Information Sciences. Prague, pp. 903–908. doi: 10.5194/isprsarchives-XLI-B7-903-2016

Pickett, S.T.A., 1989. Space-for-time substitution as an alternative to long-term studies, in: Long-Term Studies in Ecology. Springer, pp. 110–135.

Popkin, G., 2018. US government considers charging for popular Earth-observing data. *Nature* 556, 417–418. doi: 10.1038/d41586-018-04874-y

Prach, K., Lepš, J., Rejmánek, M., 2007. Old field succession in central Europe: local and regional patterns, in: Cramer, V.A., Hobbs, R.J. (Eds.), Old Fields: Dynamics and Restoration of Abandoned Farmland. Island Press Washington, DC, USA, pp. 180–201.

Pueyo, Y., Beguería, S., 2007. Modelling the rate of secondary succession after farmland abandonment in a Mediterranean mountain area. *Landscape and Urban Planning* 83, 245–254. doi: 10.1016/j.landurbplan.2007.04.008

Pyatt, D.G., Harrison, D., Ford, A.S., 1969. Guide to site types in forests of North and Mid - Wales. Forestry Commission, United Kingdom, London.

Queiroz, C., Beilin, R., Folke, C., Lindborg, R., 2014. Farmland abandonment: Threat or opportunity for biodiversity conservation? A global review. *Frontiers in Ecology and the Environment* 12, 288–296. doi: 10.1890/120348

Quine, C., White, I., 1992. Revised windiness scores for the windthrow hazard classification: the revised scoring method. *Research Information Note-Forestry ….*

Riley, S.J., DeGloria, S.D., Elliot, R., 1999. A Terrain Ruggedness Index that Qauntifies Topographic Heterogeneity. *Intermountain Journal of Sciences*. doi: citeulike-article-id:8858430

Rocchini, D., Perry, G.L.W., Salerno, M., Maccherini, S., Chiarucci, A., 2006. Landscape change and the dynamics of open formations in a natural reserve. *Landscape and Urban Planning* 77, 167–177. doi: 10.1016/j.landurbplan.2005.02.008

Röder, M., Latifi, H., Hill, S., Wild, J., Svoboda, M., Brůna, J., Macek, M., Nováková, M.H., Gülch, E., Heurich, M., 2018. Application of optical unmanned aerial vehicle-based imagery for the inventory of natural regeneration and standing deadwood in post-disturbed spruce forests. *International Journal of Remote Sensing* 00, 1–22. doi: 10.1080/01431161.2018.1441568

Scott, R.E., Mitchell, S.J., 2005. Empirical modelling of windthrow risk in partially harvested stands

using tree, neighbourhood, and stand attributes. *Forest Ecology and Management* 218, 193–209. doi: 10.1016/j.foreco.2005.07.012

Skaloš, J., Weber, M., Lipský, Z., Trpáková, I., Šantrůčková, M., Uhlířová, L., Kukla, P., 2011. Using old military survey maps and orthophotograph maps to analyse long-term land cover changes - Case study (Czech Republic). *Applied Geography* 31, 426–438. doi: 10.1016/j.apgeog.2010.10.004

Sokal, R.R., Oden, N.L., 1978. Spatial autocorrelation i n biology 1 . Methodology. *Biological Journal of the Linnean society* 10, 199–228.

Tropek, R., Sedla ek, O., Beck, J., Keil, P., Musilova, Z., Imova, I., Storch, D., 2014. Comment on "High-resolution global maps of 21st-century forest cover change." *Science* 344, 981–981. doi: 10.1126/science.1248753

Turner, M.G., Ruscher, C.L., 1988. Changes in landscape patterns in Georgia, USA. *Landscape Ecology* 1, 241–251. doi: 10.1007/BF00157696

United States Geological Survey (USGS), 2008. Imagery for Everyone …. Reston, VA.

Vapnik, V., 1995. The Nature of statistical Learning Theory, Springer-Verlag New York. doi: 10.1007/978-1-4757-2440-0

Veloz, S.D., Williams, J.W., Blois, J.L., He, F., Otto-Bliesner, B., Liu, Z., 2012. No-analog climates and shifting realized niches during the late quaternary: Implications for 21st-century predictions by species distribution models. *Global Change Biology* 18, 1698–1713. doi: 10.1111/j.1365-2486.2011.02635.x

Westoby, M.J., Brasington, J., Glasser, N.F., Hambrey, M.J., Reynolds, J.M., 2012. "Structure-from-Motion" photogrammetry: A low-cost, effective tool for geoscience applications. *Geomorphology* 179, 300–314. doi: 10.1016/j.geomorph.2012.08.021

White, M., Mladenoff, D.J., 1994. Old-growth forest landscape transition from pre-European settlement to present. *Landscape Ecology* 9, 191–205. doi: 10.1007/BF00134747

Williams, J.W., Jackson, S.T., 2007. Novel climates, no-analog communities, and ecological surprises. *Frontiers in Ecology and the Environment* 5, 475–482. doi: 10.1890/070037

Woodcock, C.E., Allen, R., Anderson, M., Belward, A., Bindschadler, R., Cohen, W., Gao, F., Goward, S.N., Helder, D., Helmer, E., Nemani, R., Oreopoulos, L., Schott, J., Thenkabail, P.S., Vermote, E.F., Vogelmann, J., Wulder, M.A., Wynne, R., 2008. Free Access to Landsat Imagery. *Science* 320, 1011a–1011a. doi: 10.1126/science.320.5879.1011a

Wright, J.P., Fridley, J.D., 2010. Biogeographic synthesis of secondary succession rates in eastern North America. *Journal of Biogeography* 37, 1584–1596. doi: 10.1111/j.1365-2699.2010.02298.x

Wulder, M.A., Masek, J.G., Cohen, W.B., Loveland, T.R., Woodcock, C.E., 2012. Opening the archive: How free data has enabled the science and monitoring promise of Landsat. *Remote Sensing of Environment* 122, 2–10. doi: 10.1016/j.rse.2012.01.010

Yokoyama, R., Shlrasawa, M., Pike, R.J., 2002. Visualizing Topography by Openness : A New Application of Image Processing to Digital Elevation Models. *Photogrammetric Engineering & Remote Sensing* 68, 257–265.

Zhu, Z., Woodcock, C.E., 2014. Continuous change detection and classification of land cover using all available Landsat data. *Remote Sensing of Environment* 144, 152–171. doi: 10.1016/j.rse.2014.01.011

Attached publications

Paper I

Brůna, J., Wild, J., Svoboda, M., Heurich, M., Müllerová, J. (2013) Impacts and underlying factors of landscape-scale, historical disturbance of mountain forest identified using archival documents. *Forest Ecology and Management* 305:294-306. doi: 10.1016/j.foreco.2013.06.017

Paper II

Brůna, J., Vojta, J. (manuscript) Landscape-scale forest succession on abandoned agricultural land is controlled by terrain topography, distance to seed source and previous land use

Paper III

Hais, M.; Wild, J.; Berec, L.; Brůna, J.; Kennedy, R.; Braaten, J.; Brož, Z. (2016) Landsat Imagery Spectral Trajectories — Important Variables for Spatially Predicting the Risks of Bark Beetle Disturbance. *Remote Sensing* 8: 1–22. doi: 10.3390/rs8080687

Paper IV

Müllerová, J., Bartaloš, T., Brůna, J., Dvořák, P., Vítková, M. (2017) Unmanned aircraft in nature conservation: an example from plant invasions. *International Journal of Remote Sensing* 38(8-10):2177-2198. doi: 10.1080/01431161.2016.1275059

Paper V

Müllerová, J., Brůna, J., Bartaloš, T., Dvořák, P., Vítková, M., Pyšek, P. (2017) Timing is important: unmanned aircraft versus satellite imagery in plant invasion monitoring. *Frontiers in Plant Science* 8 (May):1-13. doi: 10.3389/fpls.2017.00887

Paper I



Brůna, J., Wild, J., Svoboda, M., Heurich, M., Müllerová, J. (2013)

Impacts and underlying factors of landscape-scale, historical disturbance of mountain forest identified using archival documents

Forest Ecology and Management 305:294-306.

doi:10.1016/j.foreco.2013.06.017

Forest Ecology and Management 305 (2013) 294–306

Contents lists available at SciVerse ScienceDirect

Forest Ecology and Management

journal homepage: www.elsevier.com/locate/foreco

Full length article

Impacts and underlying factors of landscape-scale, historical disturbance of mountain forest identified using archival documents

J. Brůna [a,e,*], J. Wild [a,c], M. Svoboda [b], M. Heurich [d], J. Müllerová [a]

[a] Institute of Botany, Academy of Sciences of the Czech Republic, CZ-252 43 Průhonice, Czech Republic
[b] Czech University of Life Sciences Prague, Faculty of Forestry and Wood Sciences, Kamýcká 129, Praha 6, Suchdol 16 521, Czech Republic
[c] Czech University of Life Sciences Prague, Faculty of Environmental Sciences, Kamýcká 129, Praha 6, Suchdol 16 521, Czech Republic
[d] Nationalpark Bayerischer Wald, Freyunger Straße 2, 94481 Grafenau, Germany
[e] Institute of Environmental Studies, Faculty of Science, Charles University in Prague, Benátska 2, 128 44 Prague 2, Czech Republic

ARTICLE INFO

Article history:
Received 26 February 2013
Received in revised form 4 June 2013
Accepted 10 June 2013

Keywords:
Mountain forests
Disturbance
Historical maps
Historical range of variability
Bark beetle outbreak
Windthrow

ABSTRACT

Large areas of temperate mountain Norway spruce (*Picea abies*) forests in Central Europe have been disturbed by windstorms and subsequent bark beetle (*Ips typographus*) outbreaks in recent years. The impact of these events has been severe, with millions of canopy trees dying in nature reserves, where salvage logging was not conducted. The occurrence of these windstorms has raised the question of whether such events were within the historical range of variability (HRV) of forest dynamics in Central Europe, where disturbances were traditionally perceived as non-natural and without strong relevance for forest development. To answer this question, we analyzed the available historical forest management maps documenting large-scale disturbance resulting from windthrow events in the years 1868–1870 in spruce- and beech- (*Fagus sylvatica*) dominated forests in the Bohemian Forest region (Šumava Mts., Czech Republic and Bayerischer Wald, Germany). We created a cross-boundary forest database covering 54 974 ha and containing information about tree species composition and age, and the severity of the 1868–1870 disturbance, considering the cumulative effect of the windthrow, subsequent bark beetle outbreak, and salvage logging. The age structure of the forests before the disturbances was unbalanced, with stands of 80–120 years underrepresented, and covering only 9% of the area, and stands older than 120 years, historically classified as old growth, covering 26% of the area. Within the decade that included the windstorms and their aftermath, 40% of the stands in the mountain range were at least partly disturbed, with significant effect on the oldest stands. To identify important factors responsible for the severity of disturbance, we constructed regression models relating severity to two groups of explanatory variables: forest stand characteristics and environmental attributes (mainly topographic factors). Overall, stand age was identified as the most important driver of disturbance severity across the landscape, with the oldest trees most susceptible. The high importance of age for disturbance severity showed the role of forest age structure in determining the scale of disturbances resulting from windstorms and associated bark beetle outbreaks. Nevertheless, despite the documented occurrence of frequent large disturbances during the two centuries that preceded the 1868–1870 events, old growth accounted for 26% of the area, making it clear that both large scale disturbance and old-growth forest are within the HRV of mountain spruce forest dynamics in Central Europe.

© 2013 Elsevier B.V. All rights reserved.

1. Introduction

Large areas of temperate Norway spruce (*Picea abies*) forests in mountain areas of Central Europe have recently been disturbed by several major windstorms: Vivian and Wiebke in 1990, Lothar in 1999, and Kyrill in 2007. Because windthrow in spruce stands usually triggers bark beetle (*Ips typographus*) outbreaks (Fischer et al., 2002; Wermelinger, 2004; Økland and Berryman, 2004), the wind-damaged forest areas subsequently suffered bark beetle infestations. These infestations resulted in thousands of hectares of canopy trees dying in nature reserves, in which sanitary logging was not performed (Lausch et al., 2011). Until recently, such large disturbances were not thought to be a natural part of mountain spruce forest dynamics in Central Europe (Splechtna et al., 2005). These events raised two basic questions: (1) whether these large disturbances were within the historical range of variability (HRV) of forest dynamics in Central Europe; and (2) what future effects these disturbances will have on forests. Knowledge about HRV

* Corresponding author. Address: Institute of Botany of the ASCR, Zámek 1, CZ-252 43 Průhonice, Czech Republic. Tel.: +420 271 015 207; fax: +420 271 015 105.
E-mail address: josef.bruna@gmail.com (J. Brůna).

0378-1127/$ - see front matter © 2013 Elsevier B.V. All rights reserved.
http://dx.doi.org/10.1016/j.foreco.2013.06.017

could help us better understand the long-term dynamics of these mountain forests and therefore shape current management and nature protection strategies in the area (Landres et al., 1999; Keane et al., 2009).

Various kinds of disturbances, including stand-replacing events operating at the landscape scale, are among the main natural forces shaping forest structure and dynamics around the world (Pickett and White, 1985; Frelich, 2002; Gromtsev, 2002; Turner, 2010). Although severe wind disturbances are considered to be the natural, and even dominant driver of some temperate forest dynamics in North America (Canham and Loucks, 1984; Frelich and Lorimer, 1991), their natural role in temperate forests of Europe is still relatively unknown (Wolf et al., 2004; Nagel and Diaci, 2006; Nagel et al., 2006; Zielonka et al., 2010; Panayotov et al., 2011). They have also been revealed to be an important, although not dominant, feature of the disturbance regime of boreal coniferous forests (Ulanova, 2000; Rich et al., 2007).

In Europe, over the period 1950–2000, storms caused more than 50% of the damage attributed to all disturbance factors, with most of the storm damage reported from mountain areas of Sub-Atlantic and Central Europe (Schelhaas et al., 2003). Despite such a large amount of forest affected by wind disturbance, this phenomenon, along with other large-scale stand-replacing disturbances such as fire and insect outbreaks, was long thought of as non-natural in Central Europe and without strong relevance for forest development (Clark and Merkt, 1989; Ellenberg, 1996). In Europe, forest dynamics for a long time have been shaped largely by human activities (Glatzel, 1999). Therefore, the many large-scale disturbances as well as the overall increase in disturbance frequency over the last century have been ascribed mainly to management-driven changes in forest species composition and structure (Seidl et al., 2011). Additionally, Central European traditional forestry schools have emphasized the influence of site-specific conditions on vegetation patterns. Thus, small-scale gap dynamics were long thought to be the only type of disturbance influencing forest structure, with large-scale or intensive events not considered to be a natural part of forest dynamics (Falinski and Falinska, 1986; Korpel', 1995; Splechtna et al., 2005). Although large-scale disturbances eventually came to be accepted as part of the natural dynamics of various forest types in this region (Heurich and Jehl, 2000; Kulakowski and Bebi, 2004; Svoboda and Pouska, 2008; Svoboda et al., 2010; Panayotov et al., 2011), we still largely lack understanding of natural disturbance dynamics in the Central European context. In particular, we lack the knowledge of the interactions between disturbances and particular forest state and environmental factors necessary to validly assess HRV. Indeed, the effects of a storm event may vary greatly across the landscape and depend on the interaction of wind characteristics and environmental conditions that include forest species composition (Papaik and Canham, 2006), spatial/age structure, soil condition, and land surface parameters (Ruel, 2000; Achim et al., 2005; Scott and Mitchell, 2005).

The paucity of knowledge of long-term natural landscape dynamics could be addressed by space-for-time substitution (Hessburg et al., 1999), modeling (Seidl et al., 2010) or the use of archives. However, the use of space-for-time substitution is limited both by the extent of natural forest in a given region and by the variability of environmental conditions across large areas (Keane et al., 2009). Models also face obstacles, as they are difficult to parameterize precisely, and require spatially explicit data for initialization and validation. Thus, the most valuable source of information on disturbance regimes can be found in natural and documentary archives (Swetnam et al., 1999). Natural archives such as tree rings (Zielonka et al., 2010; Hadley and Knapp, 2011; Svoboda et al., 2012; Čada et al., 2013) and pollen records (Nielsen and Odgaard, 2005, 2010; Hernández et al., 2011) enable relatively precise assessment of past disturbance regimes, although obtaining landscape-scale results requires intensive, time-demanding field sampling and laboratory analyses.

In areas long used by humans, historical maps and records offer comprehensive sources of information on forest development and human impacts at the landscape scale (Brůna et al., 2010). Modern forestry in Central Europe, based on the German tradition, has employed thorough maps (Fernow, 1911) and accompanying written documents (Pretzsch, 2009) that include detailed information allowing retrospective examination of woodland development over the last ca. 200 years (Axelsson et al., 2002; Wulf et al., 2009; Šebková et al., 2011; Mikusinska et al., 2012). Despite the recognized importance of historical maps as a source of spatially explicit data on forest structure and species composition, however, they have only rarely been used for information on historical disturbances (Keane et al., 2009).

Here we employ available historical sources of information on forest management and disturbance to assess the landscape-level effects of late 19th century, severe, large-scale disturbance events on Norway spruce-, beech- (*Fagus sylvatica*), and fir- (*Abies alba*) dominated forest (Heurich and Englmaier, 2010) of a Central European mountain region. The high representation of old-growth forest in the study area that was present prior to a series of severe disturbances in 1868–1870, as documented in the archives, enabled us to gain a better understanding of landscape-scale disturbance dynamics and the factors that influence disturbance severity in both natural and managed forests.

Our particular goals are to: (i) assess age structure and species composition at the landscape scale, using available historical data from before 1868 on about 54 000 ha of forest; (ii) analyze the impacts on the forests stands of the 1868–1870 windstorms, subsequent bark beetle outbreak and salvage logging, in terms of area and type of stands affected by disturbance; and (iii) identify the factors that affected the spatial distribution and severity of disturbance, and use them for modeling disturbance at the landscape scale.

2. Materials and methods

2.1. Site and historical archive descriptions

The Bohemian Forest region (Fig. 1) comprises a 190 km long, heavily forested mountain range on the borders of Germany (Bayerischer Wald), Austria (Böhmer Wald) and the Czech Republic (Šumava Mts.), with heights of 600–1450 m a.s.l. and a northwest/southeast orientation. Geologically, this range is among the oldest in Central Europe, with typical relict plateaus having elevations higher than 1000 m a.s.l. The lower elevations in this area would naturally be covered by mixed montane forest of beech, fir and Norway spruce, which could be placed mainly in two phytosociological associations: *Luzulo-Fagetum* at lower elevations, and *Calamagrostio villosae-Fagetum* at middle and higher elevations (Neuhäuslová, 2001; Fischer et al., 2013). However, the mixed montane forests have largely been replaced by Norway spruce plantations, especially on the northeast, Czech side of the mountain range. The highest elevations are covered by pure Norway spruce woodland (*Calamagrostio villosae-Picetum*), with Norway spruce also dominating waterlogged areas that feature sphagnum-rich (*Sphagno-Picetum*) and moss-rich (*Bazzanio-Picetum*) phytosociological associations (Neuhäuslová, 2001; Fischer et al., 2013). The vegetation on south- and southwest-facing slopes includes sycamore maple (*Acer pseudoplatanus* L.), Norway maple (*Acer platanoides L.*), mountain elm (*Ulmus glabra Huds.*), large-leaved linden (*Tilia platyphyllos Scop.*), and common ash (*Fraxinus excelsior* L.) as subordinate species (Ewald et al., 2011). Two na-

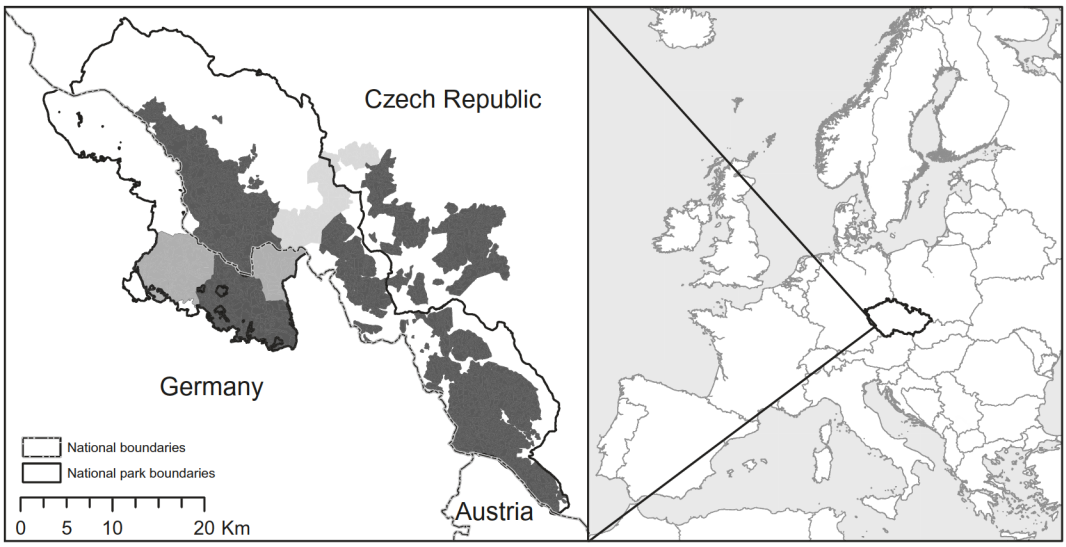


Fig. 1. Map of the area with national park borders (black lines). Area with all historical data available covers 43 247 ha (dark grey), additional 6983 ha does not contain sufficient data about age structure (grey) and 4774 ha does not contain sufficient data about disturbances in 1868–1870 (light grey). Total area with species composition data covers 54 974 ha of forests.

tional parks were established to protect this forested region: Bohemian Forest (in 1991) and Bavarian Forest (in 1970), on the Czech and German sides of the border, respectively (Fig. 1). In our study we focused mainly on the area of these two national parks.

In the 19th century, when the focal wind events of our study occurred, the area's various landowners were all using similar silvicultural practices derived from the then common Central European/German approach to forestry (Martin, 1906). These extreme wind events occurred in the winters of 1868 (December 7–8 and 24–26), 1869 (November 1–3, 14 and 15), and 1870 (October 26–27), resulting in large-scale windthrow disturbance and subsequent bark beetle outbreaks. The cumulative impact of windthrow, bark beetle outbreak, and salvage logging was well documented during the approximately 10 years that the disturbed stands were managed after the windstorms. In fact, this was the first large-scale disturbance in the area for which we have localization and disturbance severity records, as the previous events were documented only in terms of amount of timber losses (Elling et al., 1987; Jelínek, 1988).

The historical forest maps used in this study include information about the borders, dominant age class, and species composition (in terms of presence of important tree species, but not prevalence) of each stand. The positional accuracy of the old forestry maps is very high, since they were created using sophisticated cadaster mapping methods (Kačmar et al. 2013), and most of the stand borders are still used in present forest management maps. For the Czech part, they were compiled by Jelínek (2005) from multiple archives. Complementing the maps of the Czech areas were forest management books that have more detailed information about every stand. For the German part, we used forest inventory maps from 1844, 1856, and 1860 covering different parts of the area, as well as a species composition map constructed by Elling et al. (1987) based on historical data.

Importantly, both Elling et al. (1987) and Jelínek (2005) constructed maps of disturbance severity, covering approximately the decade following the 1868–1870 windstorms. The information used in these maps was originally recorded because, during this decade, stand management was dictated by disturbance impact. Therefore, these maps documented the cumulative severity of disturbance from the windthrow and subsequent beetle outbreaks and salvage logging. We presume that, due to the scale of the disturbance, most management activities (and therefore documentation) done following the 1868–1870 wind events were concentrated in or near the areas subjected to this disturbance, although this was not specifically stated in the documents.

The Czech forest management books recorded summary amounts of salvaged wood from each stand or area. Jelínek (2005) translated these salvaged wood records into disturbance severity data, classified in three roughly quantitative categories: low, consisting of damage to single trees; intermediate, indicating damage to approximately half the trees; and high, for stand-replacing events in which all canopy trees in a given stand were damaged. Jelínek (2005) also grouped the stand ages in six classes: 0–40 years, 40–80 years, 80–120 years, more than 120 years, self-regenerating logged class (R, 20% mature trees left for regeneration), and naturally sparse forest class (S). The oldest age category, encompassing stands over 120 years old, represents the definition used by historical foresters for old-growth stands, i.e., those without significant past human influence (Jelínek, 1988). We assessed the categorical accuracy of the age class designation used by Jelínek (2005) by comparing it with detailed stand information from the forest management books and maps for random locations, with reasonable results. The high accuracy was facilitated by the usage of Jelínek (2005) age classes that were broader than those in the original forest maps.

Using ArcMap 10.0 (ESRI, 2011), the historical forestry maps from both sides of the border were digitized and combined, resulting in a cross-boundary map covering 54 974 ha of the two national parks. The legend of the forest maps of both national parks was unified regarding both the disturbance severity and age structure, in both cases using the classifications developed by Jelínek (2005). Because some forest records are missing, the age structure of some parts of the Bavarian Forest NP and historical disturbance information from the Zdíkov estate (Bohemian Forest NP) remains unknown. These areas were therefore omitted from the age structure and historical analyses, respectively (Fig. 1).

2.2. Modeling the disturbance

To identify important local attributes responsible for disturbance severity, we constructed a regression model (the "all variable model") with disturbance severity as a dependent variable

and two groups of explanatory variables: forest stand characteristics and environmental, mainly topographically derived factors (all listed in Table 3). These were all assessed per point in a grid with 1.25 km spacing to minimize autocorrelation of variables used in the model. The spatial independence of explanatory variables was tested by Moran's *I* test in R 2.14.2 (R Development Core Team, 2012) as implemented by Bivand et al. (2012). The self-regenerating logged and naturally sparse forest areas, as well as areas without sufficient information on age structure or disturbances, were excluded from this analysis.

Severity of disturbance at the sampled point was calculated as the mean disturbance severity in a circle of 250 m radius, thus including the surroundings while avoiding the arbitrary nature of stand borders. This number was converted to a proportion (0–1) for use in a generalized linear regression with binomial distribution and logit link function assuming single tree damage (causing immediate or eventual tree death) to represent 10% disturbance severity, damage to half the trees to represent 50% severity, and damage to all trees to represent 100% severity.

The stand characteristics tested included age, Euclidean distance to stand edge for each different age class, and the presence/absence of each major tree species. Age was computed as the mean age class in a circle of 250 m radius (as a surrogate for forest stand), and we then calculated the difference in mean age class between the 250 m circle and a 500 m circle to yield the age difference index value. Similar index was used in Mikita et al. (2012) to identify forest edge areas susceptible to wind damage due to heights differences. We used this approach instead of stand data because there was not only variability in sizes among stands, but also in disturbance within some stands, resulting in multiple stand parts with different disturbance data.

A digital elevation model based on ASTER Global Digital Elevation Model V002 (METI/NASA, 2011) was used to calculate values of topographic variables related to wind risk and site conditions. The morphometric protection index, equivalent to the positive openness described in Yokoyama et al. (2002), and similar to the distance-limited Topex (Pyatt et al., 1969) widely used in windthrow risk prediction and modeling (Quine and White, 1998; Hanewinkel et al., 2004, 2011; Scott and Mitchell, 2005), was computed in SAGA GIS (SAGA Development Team, 2011), along with slope, aspect, and sky view factor. MAXTOPEX was calculated following the method of Mikita et al. (2012), who used it in the same area to model the recent disturbances. Other commonly used site-descriptive indexes, including SAGA wetness, solar radiation, terrain ruggedness (TRI), relative height and slope position, altitude above channel network, and effective air flow heights from eight principal directions were calculated using SAGA GIS. All stand-related variables were calculated and all DEM-related layer values and latitude and longitude were extracted using ArcMap 10.0 (ESRI, 2011). Point selection, variable testing, modeling, and validation were done using R 2.14.2 (R Development Core Team, 2012). Significant variables and all reasonable interactions for the model were selected by backward and forward selection based on the Akaike Information Criterion (AIC). To assess the usefulness of historical data for modeling the effect of disturbance, we validated the model on a set of points in the same design as the original, but shifted from it both latitudinally and longitudinally by half the distance between the points (625 m), thus covering a similar area and gradients.

3. Results

3.1. Age structure

Age structure of the 47 926 ha of forests before the 1868–1870 disturbances was unbalanced, with most stands either younger than 40 years (33%) or 40–80 years old (25%). The 80–120 year age class was present in only 10% of the area and 26% of the forest belonged to the age class comprising stands older than 120 years (Fig. 2).

The large-scale disturbances of 1868–1870 substantially altered the age structure. The older classes were subject to substantially greater disturbance, resulting in decrease of the area of forest older than 120 years (old-growth forest) by 69% and those of age 80–120 years by 55%. In the oldest age class, the windthrow

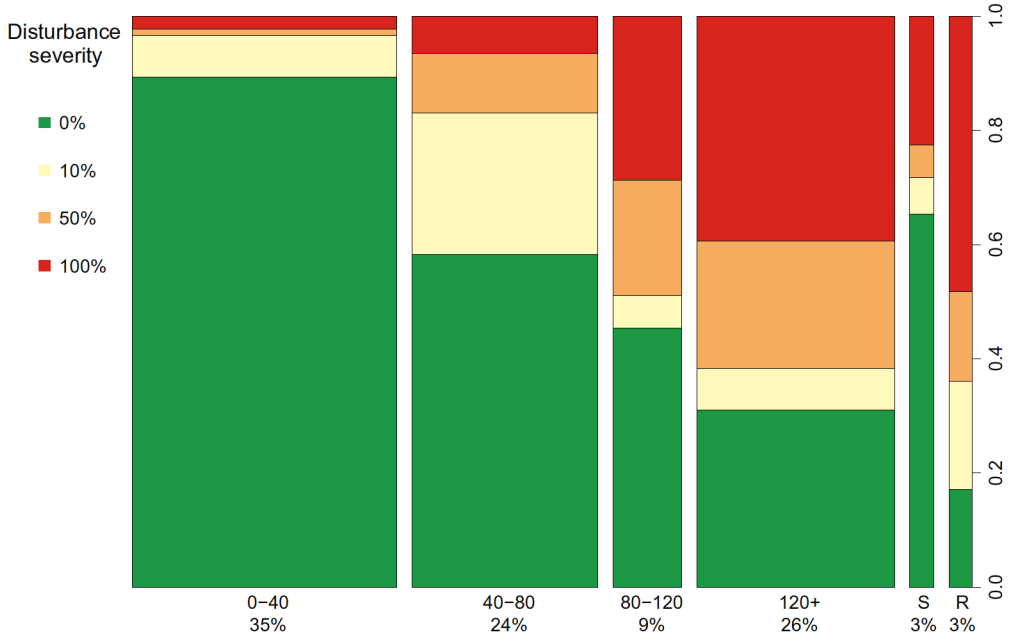


Fig. 2. Disturbance severity significantly increases in older age classes. More of the younger age stands were managed before the disturbance. Width shows proportion of total area. "S" means sparse forests and "R" means areas left intentionally for natural regeneration (20% of standing trees left after logging).

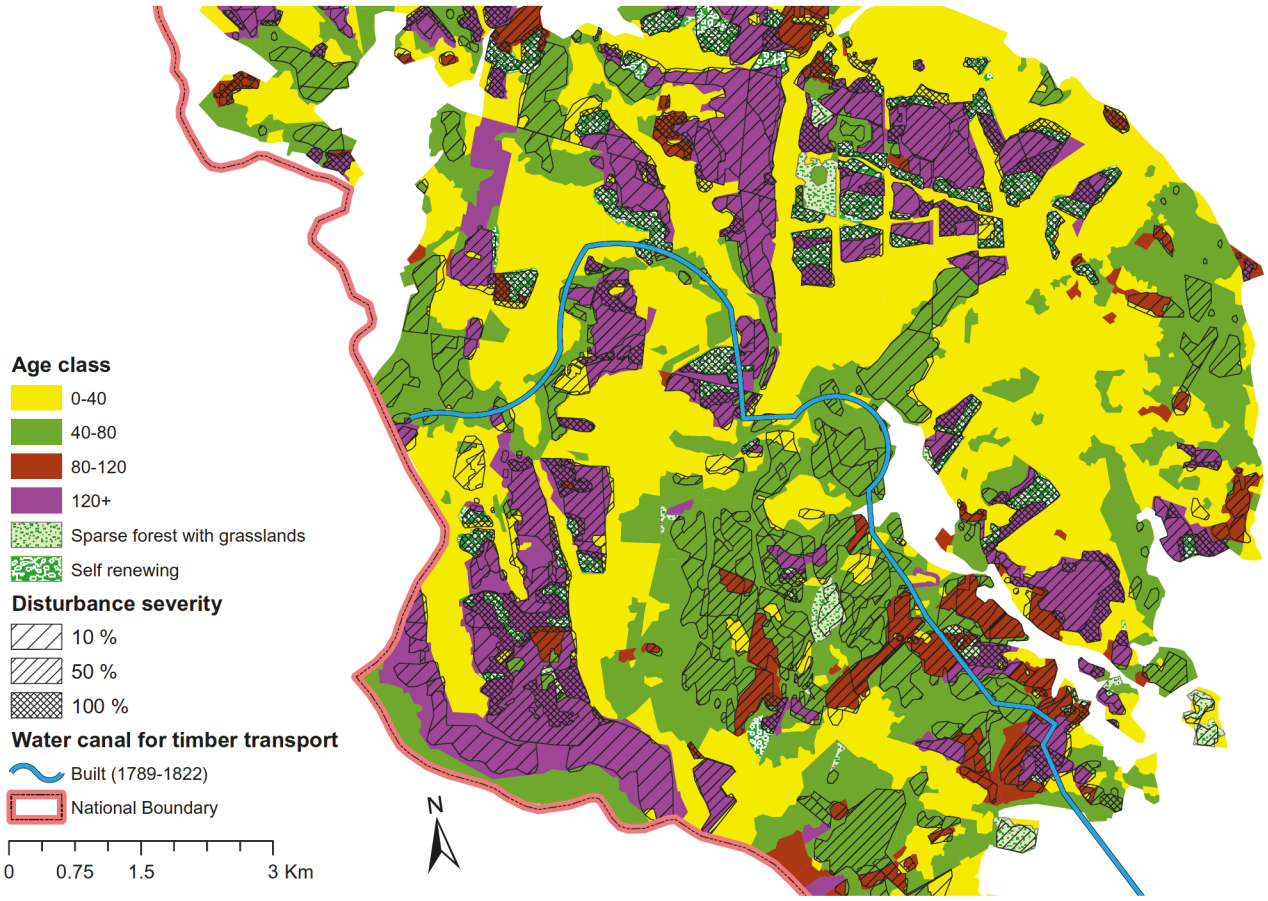


Fig. 3. Detailed map of the Trojmezná region. Almost all areas of primeval forest were disturbed to some degree, although not necessarily completely. The nearby areas were surrounded by intensively managed areas before the 1870 disturbance, partly enabled by a canal that had been constructed several decades earlier, which enabled logs to be transported from the mountains. The canal also made salvage logging possible after the 1870 disturbance, unlike for previous disturbances. Map is an overlay of data published by Jelínek (2005).

disturbance and subsequent bark beetle infestation and salvage logging resulted in the greatest proportion (41%) of stands experiencing loss of all trees, whereas in younger stands, this level of destruction was much rarer (2% for age class 0–40 years and 7% for 40–80). In the two youngest classes of stands, the most common level of disturbance was the loss of individual trees or half of the stands. Most (83%) of the forest area belonging to class R (logged with 20% of trees left for natural regeneration) was at least partly disturbed, in contrast with those of class S (naturally sparse forests), of which only 35% of their area showed disturbance.

From the analyzed area of 43 247 ha, 7725 ha of stands were completely damaged (100% of canopy removed), 4647 ha had half the canopy removed, and 5014 ha had individual trees that were damaged, resulting in 40% of the stands in the study area being at least partly disturbed within approximately a single decade. Of the oldest, unmanaged forests, only 31% were left undisturbed, meaning that the old-growth forests decreased from 26% (11 177 ha) to just 8% (3464 ha) of the analyzed area. This is most apparent in the Trojmezná region, where almost all the stands older than 80 years were disturbed to some degree (Fig. 3).

3.2. Tree species composition

Spruce was present in 90% of stands. Pure spruce stands accounted for 46% of stands, forming the most common forest type, followed by the mixture of spruce, beech and fir, which covered 34% of the area. Fir was present in 41% of the stands and beech in 37% of the stands, mainly in the southeastern part of the area (Table 1). Species composition changed along an elevation gradient (Fig. 4, Fig. 7), with higher elevations having increasing proportions of pure spruce stands and decreasing proportion of beech and fir. In pure spruce stands, the two youngest age classes prevail, whereas mixed stands had more balanced proportions of age classes dominated only slightly by the oldest one.

Pure spruce forest was the most disturbed, with 62% of its area affected by the disturbances (Table 1). Similarly, about 58% of the second most common forest type, mixed spruce, beech and fir was affected, but the proportion of stands completely destroyed was lower (21%) than in pure spruce stands (33%), and these mixed stands were more affected by single tree disturbance (19%), than were the pure spruce (11%) stands (Table 1). Disturbance severity was low in the beech-dominated and mixed spruce and beech stands, which represented a small proportion of the landscape (<5%). The species composition in the disturbed area and in the unaffected area was very similar (Fig. 4), although disturbance extent differed among species groups along the elevation gradient (Fig. 4 and Fig. 8).

3.3. Modeling the disturbances

Mean age was identified as the most important factor for disturbance severity, with a positive effect. Latitude had a positive influence, indicating more severe disturbance in northern areas. Disturbance was significantly more severe on the Czech side of the border (i.e. northeastern slopes) than the German. In the validation, the all variable model performed quite well for the Czech

Table 1
Disturbance severity distribution among species in relative procents, with tree species proportions before the disturbance, calculated using total area of stands that had the species recorded as present.

Species	Disturbance Severity				Proportion of forest stands before (%)
	0%	10%	50%	100%	
Spruce	38	11	18	33	46
Spruce + beech + fir	42	19	19	21	32
Spruce + fir	57	14	13	16	8
Spruce + beech	68	12	12	7	4
Beech + fir	57	10	14	19	2
Beech	78	17	4	1	<1
Fir	50	30	14	6	<1
Other	65	7	6	22	8
Total	44	13	17	26	100

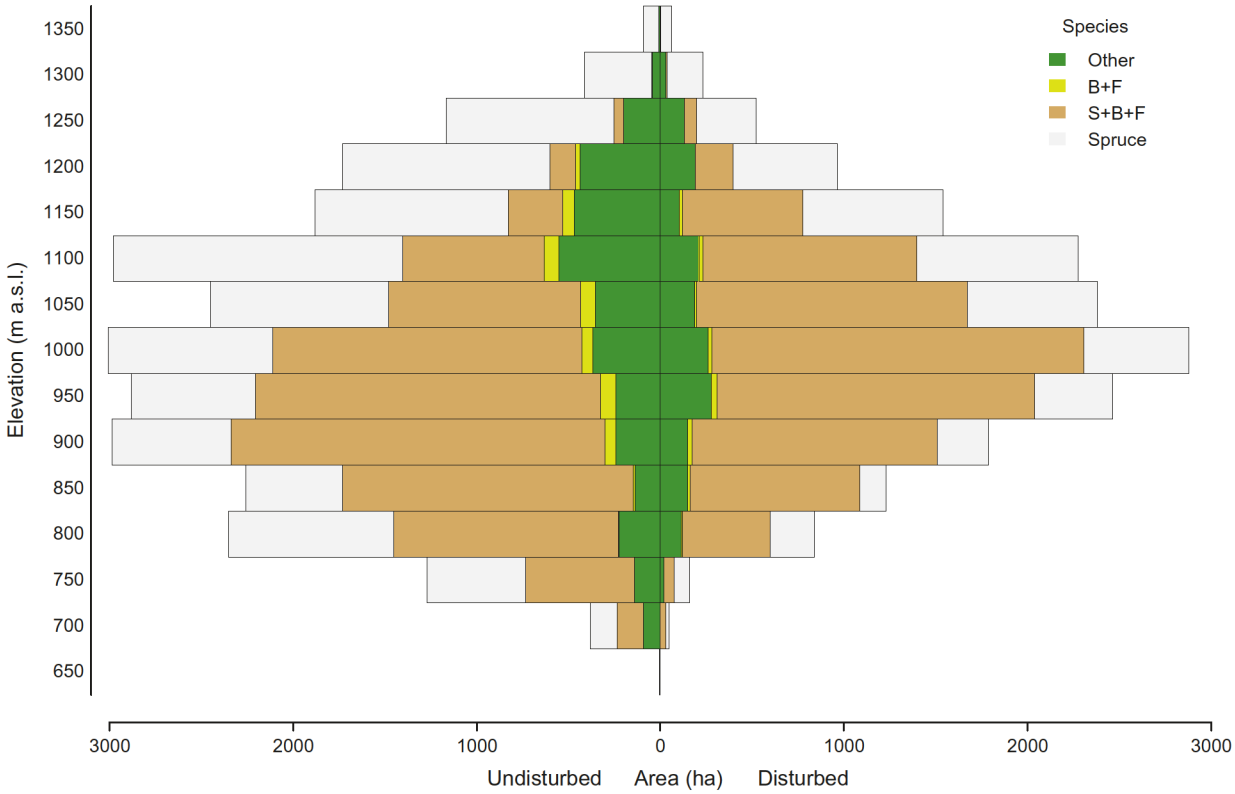


Fig. 4. Tree species composition for disturbed and undisturbed areas along the elevation gradient shows increasing proportions of spruce dominated stands and decreasing proportions of beech and fir with increasing elevation. F = fir, B = beech, S = spruce.

area, but failed to predict small-scale disturbances for the German area.

Therefore, a model with only Czech data was also developed (the "Czech territory model", Table 2), in which both mean age class and latitude were significant. There were insufficient data points to create a separate model for the German side. No topographic variable or its interaction with other potential explanatory variables was identified to be significant for the disturbances in either of the models; therefore, we created a third model without any age-related variables or country designation (the "environmental variable model") and ran the same parameter selection. This model identified mean elevation in a 250 m circle and effective air flow heights (Boehner and Conrad, 2008) from constant wind direction of 90° as the most important variables (Table 2).

Two separate models tested the responses to disturbances of the two types of stands with the most common species composition (pure spruce and mixed). In the "pure spruce stands model", age was found to be the most important factor, followed by latitude and longitude. No significant role of elevation was identified for these stands, in contrast to the "mixed stand model" (spruce, beech and fir), which responded to age, elevation, and effective air flow heights (Table 2 and Fig. 8).

Elevation was a significant explanatory variable in some of the models ("environmental variable model" and "mixed stands model"). However, the separate analysis of disturbance severity along the elevation gradient revealed that, overall, the proportion of disturbed forests increased with elevation up to 1000–1150 m and then started to decrease slightly (Fig. 5). Nevertheless, we have to consider that the area of forests at the highest elevations was much smaller than those of other elevations, and this could have distorted the results.

The spatial pattern of disturbance predicted by the all variable model for all data points was highly similar to the observed disturbance across the landscape (Fig. 6). The validation showed a close fit with this model, with a Pearson correlation coefficient of 0.723 between the predicted and observed values, indicating high predic-

Table 2
Parameters, slopes and significances of the five types of model applied. Independent variables were standardized. The "environmental variable model" did not include any age related variables. "Pure spruce model" and "mixed stands model" were used only for points on which the appropriate species were present (spruce; and spruce, beech, fir, respectively). Significance codes: '×' not tested in the analysis, '–' removed during selection, '***' < 0.001,'*' < 0.05. Variables not significant in any analyses are not included.

	All variable model		Czech territory model		Environmental variable model		Pure spruce stands model		Mixed stands model	
Mean age in 250 m circle	3.41	***	3.30	***		×	3.13	***	3.67	***
Lattitude	0.97	*	0.97	*		–	1.70	*		–
Longitude							3.19	*		–
Country (GER)	−3.11	***		×		×				
Mean elevation in 250 m circle		–		–	11.42	***		–	16.49	**
Effective air flow heights		–		–	−5.60	***		–	−8.31	**
AIC	152.87		145.35		218.47		57.51		57.52	
n	254		217		254		94		96	

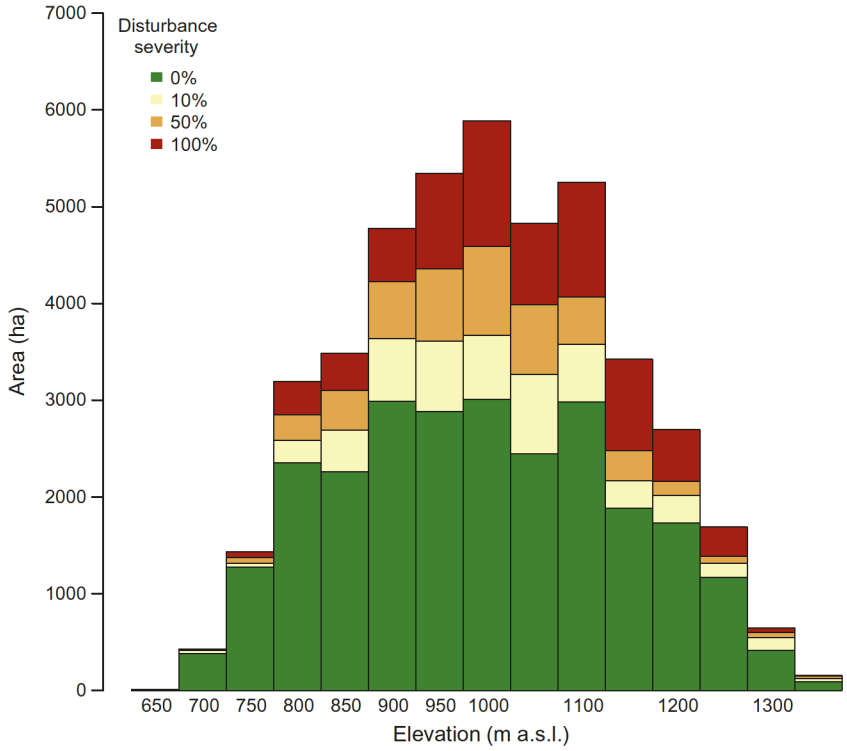


Fig. 5. Severity of disturbance along the elevation gradient (in 50 m intervals). From the relative proportions of disturbance severity categories, it can be seen that the highest severity of disturbance was between 1000 and 1150 m, the elevation range with the greatest stand area.

tive power of the model. The Czech model showed similar power, with a Pearson correlation coefficient of 0.704. The model based only on environmental variables had only a 0.373 Pearson correlation coefficient. The validity of the two models based on the most common species compositions (pure spruce and mixed stands) was not tested.

4. Discussion

4.1. Age structure and HRV

Our study showed significant changes in the age structure in the studied landscape as a result of the severe disturbance. The fact that the oldest stands experienced the highest severity disturbance (Fig. 2), leaving only 31% of their pre-disturbance extent – which had been about 26% of the area – had severe consequences for the forest on a landscape scale. This suggests that the temporal pattern of high severity disturbances probably strongly influences the proportions of forest in late successional stages.

Moreover, there is evidence of numerous previous large-scale, high-severity windstorms damaging forests in the region (Elling et al. 1987; Zatloukal 1998 and Brázdil et al. 2004), including major windstorms in 1710, 1740, 1778, 1810s, 1820s, and 1830s, most of them followed by bark beetle outbreaks. Historical documents state that the windstorms of 1710, 1740, and the 1830s disturbed large areas of forest, which was confirmed by dendrochronological analyses from two localities in the area, Trojmezná and Jezerní Hora (Svoboda et al., 2012; Čada et al., 2013). However, the precise geographical extent of the disturbance caused by any of these events is not known.

Despite the documented earlier frequent occurrence of large disturbances, the oldest class at the onset of the 1868–1870 event covered 26% of the forest area. However, if such disturbances were frequent enough, the forest would rarely naturally reach the oldest stage and so-called old-growth character.

Taken together, the high representation of old-growth forest prior to the 1868–1870 disturbance and the presence (at the highest elevations) of early successional stages that resulted from

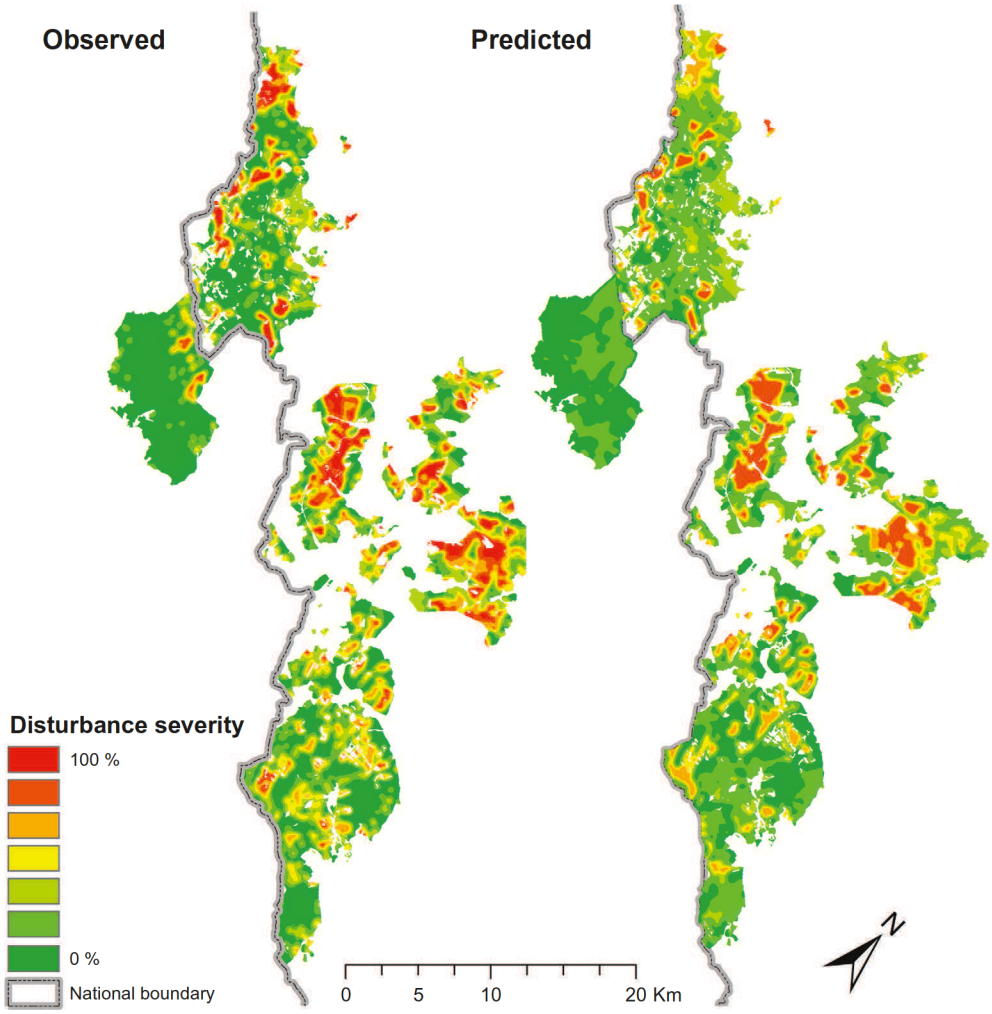


Fig. 6. Visual validation of the all variable model. Observed disturbance severity (left) and predicted disturbance severity (right) show similar patterns, although the observed is more detailed and has greater contrasts.

earlier disturbances indicate that both stand-replacing disturbances and old-growth belong to the HRV of mountain Norway spruce- and beech-dominated forests. Thus, the forest could be characterized as a landscape mosaic of old-growth and earlier successional stands.

We must consider to what extent the forest dynamics reflected management activities conducted before the study period. Up until the very late 18th century, there had been no intensive logging activities in the region, due to its low population and relative inaccessibility. Indeed, in the second half of the 18th century, this area represented one of the largest remnants of natural forest in Central Europe (Wild et al., 2004). However, canals for timber transport were built from just before the end of the 18th century until the first half of the 19th century, and they facilitated more intensive forestry logging operations by enabling logs transport from the mountains. This resulted in many new forest edges in previously homogenous areas, leaving old stands isolated and sensitive to disturbance (Fig. 3). Together with the occurrence of earlier severe disturbances (Brázdil et al., 2004), this influenced the age structure before the studied large-scale disturbance of 1868–1870. Indeed, in 1868, immediately prior to the studied disturbance, some forests had already been logged, and in combination with previous disturbances, this could have caused the relatively low representation of the 80–120 year class. However, many stands were managed for the first time only after the studied 1868–1870 disturbances (and not necessarily intensively), and therefore we could still consider this area to have been an especially large exception to the intensively managed Central European forest landscape (Glatzel, 1999), suitable for calibration of the HRV concept.

4.2. Tree species composition

Both of the most prevalent forest types – pure spruce and mixed forest stands – were similarly disturbed (62% versus 58% of affected stands, respectively), and species composition in the undisturbed and disturbed stands was very similar, suggesting the disturbance was evenly distributed among forest types. These findings could indicate that tree species composition was probably not a major driver of the disturbance. On the other hand, using the modeling approach, we identified some differences between the two major forest types in their responses to environmental variables. Lack of quantitative data on species composition (as only tree species presence was recorded on historical maps) and low representation of other than dominant forest types in the landscape, however, prevented more detailed analyses of relationships between tree species and disturbance effects.

Given that the disturbance severity was high in pure spruce stands and in mixed spruce, beech and fir stands but low in mixed beech-spruce and pure beech stands, we could expect that there should have been a shift towards beech, but no such sign was

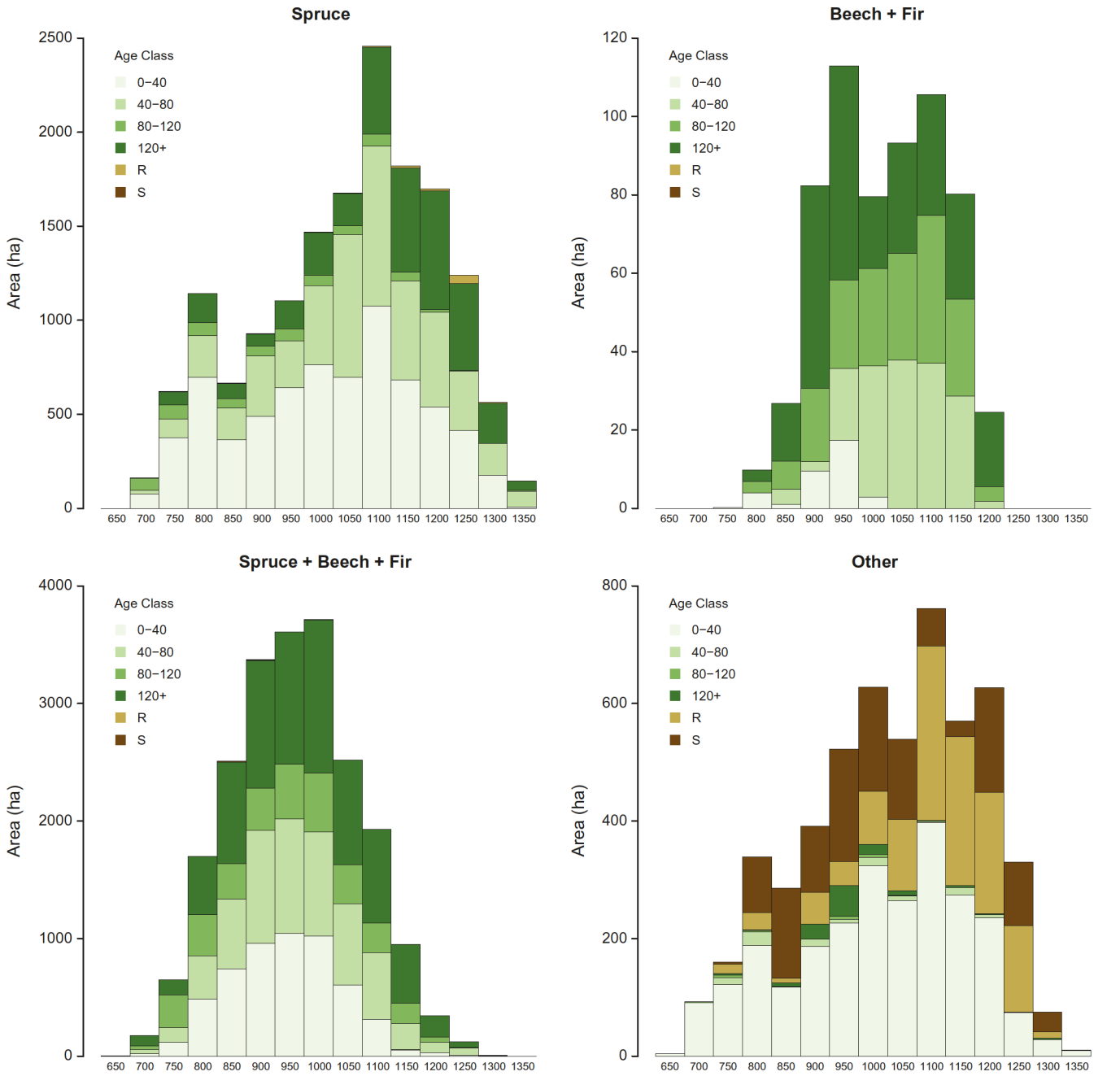


Fig. 7. Age class distribution along elevation gradient (in 50 m intervals) for different species compositions before the 1868–1870 disturbances. Most old-growth (120+) spruce forests were present in elevations higher than 1100 m a.s.l. whereas old-growth spruce, beech and fir mixed forests were more evenly distributed along the elevation gradient.

detected. This could be attributed to the fact that stands which included beech without spruce only accounted for a small proportion of the landscape. The lower amount of completely damaged canopy cover in mixed spruce, beech and fir forests was likely due to mechanical damage to young broad-leaved trees from falling spruce trees (Jelínek, 1988). Subsequent bark beetle outbreaks increased the number of spruce trees killed, while sparing beech and fir, which helps explain the disparity in disturbance severity between the pure spruce and other stand types. Elevation could also underlie this disparity, since pure spruce stands were concentrated mostly at higher elevations (Fig. 4). The greater proportion of young trees in the pure spruce stands than in mixed stands (balanced age classes, slightly dominated by the oldest one), suggests the start of a gradual shift towards pure spruce stands. This would have resulted from previous management and disturbances.

4.3. Modeling the disturbance

The strong effect of age on disturbance severity suggests an important influence of age structure on the scale of such disturbances. Particularly noteworthy, even the unmanaged oldest stands were unable to withstand the extreme winds and subsequent bark beetle outbreak. This finding is important for current management, since many of the stands have already reached the oldest age class. In fact, recent large-scale windthrow events and bark beetle outbreaks might have been direct consequences of

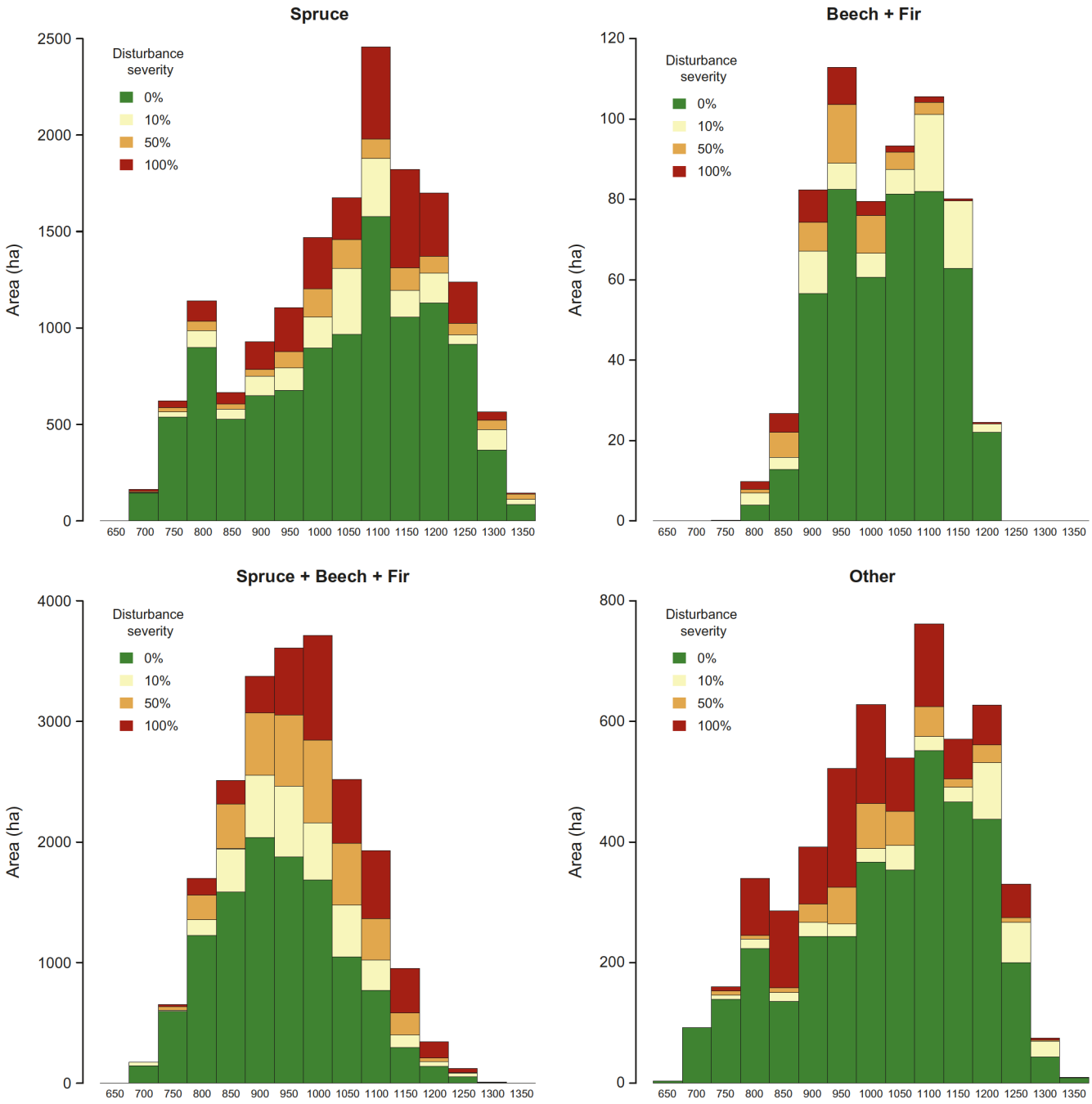


Fig. 8. Disturbance severity along elevation gradient (in 50 m intervals) for different species compositions. Largest areas of spruce forests were disturbed in 1000–1250 m a.s.l. opposing the spruce, beech and fir mixed forests that were mostly disturbed in 850–1100 m a.s.l.

the 1868–1870 disturbance, because at the onset of the recent disturbances (end of 20th century), huge areas were covered with approximately 130-year-old even-aged stands. Similarly, the 1870 disturbance might have been enabled by naturally developed even-aged stands grown after the disturbances of 1710, 1740, or 1778.

Our modeling revealed trends involving elevation effects that invite inquiry into the underlying mechanisms. In particular, although in the model omitting forest stand characteristics (the environmental variable model), both elevation and effective air flow heights were identified as important, they had low predictive power. Additionally, although our analysis of the effect of elevation showed that forests in higher areas were more threatened by disturbances (Fig. 6), as would be expected from higher wind speeds (Malberg, 2007), the highest elevation stands were less disturbed. The finding of decreased disturbance at these elevations could reflect distortion by the presence of only a rather small area of forests in these high elevations, but there could be some other underlying causes. One possibility is that different structure of these stands due to more frequent winds enabled greater tolerance of high winds (Meguro and Miyawaki, 1994). An alternative explanation would be the relatively high proportion of young stands that were remaining in high elevation areas after previous disturbances between the years 1833 and 1840, as documented by Čada et al. (2013) and Svoboda et al. (2012). However, our data did not support this explanation on the landscape scale, as the effects of

Table 3
All explanatory variables used in modeling the disturbance. Those significant in any model are marked bold.

Stand-related, based on historical data:	Topography-related (based on ASTER 2 METI/NASA, 2011):
Mean forest age in 250 m circle, distance to stand with specific age class, age difference of 250 m and 500 m circle, age difference to surrounding stands, presence of spruce, fir, beech and combination, length of stand border, stand area	**Elevation in 250 m circle, slope, aspect, latitude, longitude, country,** morphometric protection index, sky view factor, MAXTOPEX, SAGA wetness index, solar radiation, terrain ruggedness index, relative heights, slope positions, altitude above channel network, **effective air flow heights** from eight principal directions, windward effect, leeward effect, wind effect, sky view factor

elevation and age were significant only for mixed stands. Differences among locations in wind speeds or post-disturbance management practices might explain the highly significant effects of country and latitude.

The lack of significance of topographic variables in the all variable model was unexpected both because some are believed to be important in determining windthrow risk (Mitchell et al., 2008), and even more so because such disturbance risk factors as elevation, MAXTOPEX, and distance to forest edge showed explanatory power in previous modeling of the 2007 Kyrill windthrow in the same area (Mikita et al., 2012). Moreover, distance-limited topex (Quine and White, 1998; Hanewinkel et al., 2004, 2011; Scott and Mitchell, 2005), as well as slope and aspect (Hanewinkel et al., 2004; Mitchell et al., 2008) have been successfully applied in many other areas.

In our study, the lack of significance of these variables was probably due to the large influence of age. Thus, in the environmental variable model, which excluded age-related variables, we identified elevation and effective air flow heights from the east (Boehner and Conrad, 2008) as having some influence on the spatial distribution of disturbance severity, but their predictive power was low. It might also be due to the fact that the position of initial windthrow sites is unknown and was obscured by subsequent bark beetle outbreaks, windthrow events, and management activities. Indeed, for windthrow events of magnitude similar to that examined in our study, 50% of the total disturbance has been attributed to bark beetle damage (Forster et al., 2003). This likely explains why elevation was significant for the mixed stands model, as such stands were less affected by the bark beetle. Moreover, without the salvage logging, the effect of the beetle outbreak might have been greater, but there is no evidence available to examine this possibility, as our data do not let us distinguish among the disturbance components caused by direct windthrow damage, subsequent beetle damage, and salvage logging.

Similarly, the repetitive nature of the windthrow events, in combination with the timing of their recording, may have obscured effects of forest edges, tested via the age difference index. Windthrow events occurred at the beginning of every winter from 1868 through 1870, gradually extending the affected area, with the forest status not recorded between the individual events. Thus, only their cumulative effect is known. Of course, we are also prevented from identifying the influence of bark beetle on the stability of surviving stands due to the summary nature of the data. It should be noted that although we could not distinguish between the damage due directly to wind action, and that of bark beetle infestations and associated salvage logging (and in some ways the effects of these different phenomena might have obscured each other), it is entirely legitimate to consider them in combination, as on the landscape scale they often occur together.

4.4. Use of historical forest management maps

In our study, the historical maps were proven to be useful for assessing the historical range of variability. Their most important benefit is the spatially explicit nature of the data, which allows relating forest species and age structure to disturbance severity as well as environmental and topographic factors. However, their use does have some shortcomings. First, although the data on species presence and stand age are often included in map legends or easily extracted from attached written documents, the data on disturbance or management activities – as was the case in our study – require compilation and interpretation of documents from multiple, different documentary archives, which are available for only very few regions. Second, translation of written documents into maps is time-consuming, subjective work, and its results have to be taken with caution. Additionally, the mapmaking conventions in terms of colors used, age classes, and various markings can differ among countries and even among landowners, complicating the building of seamless maps – especially in cross-border areas such as are common in Central Europe. Furthermore, the information contained in historical documents can be incomplete and therefore restrict its susceptibility to particular analyses. For example, in the maps that we used, only summary disturbance evidence had been recorded during large-scale events, obscuring the individual proportions of stand damage attributable to the wind itself, bark beetle outbreaks, and salvage logging. Despite the challenges and limitations, however, such maps represent a valuable source of data for gaining insight into recent processes and identifying forests' historical range of variability.

5. Conclusions

The use of maps and other archival documents can help reveal an area's historical disturbance regime, its underlying factors, and long-term consequences. Here these sources provided significant insights into the disturbance regime of Central European mountain forests. In particular, we found that forest age was an important factor for disturbance severity, and thus its structure could influence the spatial scale of disturbances. Moreover, we found a large proportion of the forest was old-growth forest, and that it was heavily affected by the large-scale disturbance that occurred within our study period. Thus, the occurrence of both large-scale disturbance and old-growth forest are within the landscape-scale historical range of variability for this region, as also indicated by local stand-scale dendroecological studies from the area. This insight and the identification of factors influencing disturbance susceptibility can help shape management efforts.

A shortcoming of the historical data was that it did not allow us to distinguish the proportions of total disturbance due to windthrow, the ensuing bark beetle outbreak, and salvage logging. However, because the latter two typically follow windthrow events, the damage assessment represents a reasonable appraisal of the actual total impacts of such severe disturbances on the landscape scale.

Acknowledgements

The work was supported by GACR 504/10/0843, and is part of long-term research development Project No. RVO 67985939. The work would be impossible without the extensive archive work of Josef Jelínek. We would like to thank Zdeňka Konopová for

digitalization of part of the data sources and Jonathan Rosenthal for valuable comments and corrections to this text.

References

Achim, A., Ruel, J.-C., Gardiner, B.A., Laflamme, G., Meunier, S., 2005. Modelling the vulnerability of balsam fir forests to wind damage. For. Ecol. Manage. 204, 37–52.

Axelsson, A., Östlund, L., Hellberg, E., 2002. Changes in mixed deciduous forests of boreal Sweden 1866–1999 based on interpretation of historical records. Landscape Ecol. 17, 403–418.

Bivand, R., Altman, M., Anselin, L., Assunção, R., Berke, O., Andrew, B., Blanchet, G., Blankmeyer, E., Carvalho, M., Christensen, B., Chun, Y., Dormann, C., Dray, S., Halbersma, R., Krainski, E., Legendre, P., Lewin-Koh, N., Li, H., Ma, J., Millo, G., Mueller, W., Ono, H., Peres-Neto, P., Piras, G., Reder, M., Tiefelsdorf, M., Yu., D., 2012. spdep: Spatial dependence: weighting schemes, statistics and models.

Boehner, J., Conrad, O., 2008. Effective Air Flow Heights. SAGA.

Brázdil, R., Dobrovolný, P., Štekl, J., Kotyza, O., Valášek, H., Jež, J., 2004. History of Weather and Climate in the Czech Lands VI: Strong Winds. Masaryk University, Brno.

Brůna, V., Křováková, K., Nedbal, V., 2010. Historical landscape structure in the spring area of the Blanice River, Southern Bohemia – an example of the importance of old maps. Acta Geodaet Geophys Hung 45, 48–55.

Čada, V., Svoboda, M., Janda, P., 2013. Dendrochronological reconstruction of the disturbance history and past development of the mountain Norway spruce in the Bohemian Forest, central Europe. For. Ecol. Manage. 213, 59–68.

Canham, C., Loucks, O., 1984. Catastrophic windthrow in the presettlement forests of Wisconsin. Ecology 65, 803–809.

Clark, J., Merkt, J., 1989. Post-glacial fire, vegetation, and human history on the northern alpine forelands, south-western Germany. J. Ecol. 77, 897–925.

Ellenberg, H., 1996. Vegetation Mitteleuropas mit den Alpen in ökologischer, dynamischer und historischer Sicht, Ulmer. Ulmer, Stuttgart, Stuttgart.

Elling, W., Bauer, E., Klemm, G., Koch, H., 1987. Klima und Böden, 2nd ed. Bayerisches Staatsministerium für Ernährung, Landwirtschaft und Forsten.

ESRI 2011. ArcGIS Desktop: Release 10.0 Redlands, CA: Environmental Systems Research Institute.

Ewald, J., Jehl, H., Braun, L., Lohberger, E., 2011. Die Vegetation des Nationalparks Bayerischer Wald als Ausdruck von Standort und Walddynamik. Tuexenia, pp. 9–38.

Falinski, J., Falinska, K., 1986. Vegetation dynamics in temperate lowland primeval forests: ecological studies in Bialowieza Forest. Springer.

Fernow, B.E., 1911. A brief history of forestry: in Europe, the United States and other countries. Toronto : University Press; Cambridge, Mass.

Fischer, A., Lindner, M., Abs, C., Lasch, P., 2002. Vegetation dynamics in central european forest ecosystems (near-natural as well as managed) after storm events. Folia Geobot. 37, 17–32.

Fischer, H.S., Winter, S., Lohberger, E., Jehl, H., Fischer, A., 2013. Improving transboundary maps of potential natural vegetation using statistical modeling based on environmental predictors. Folia Geobot. 48, 115–135.

Forster, B., Meier, F., Gall, R., Zahn, C., 2003. Erfahrungen im Umgang mit Buchdrucker-Massenvermehrungen (*Ips typographus* L.) nach Sturmereignissen in der Schweiz. Schweiz Z Forstwes 154, 431–436.

Frelich, L.E., 2002. Forest Dynamics and Disturbance Regimes: Studies from Temperate Evergreen-Deciduous Forests, Agriculture. Cambridge University Press.

Frelich, L.E., Lorimer, C.G., 1991. Natural disturbance regimes in hemlock-hardwood forests of the upper great lakes region. Ecol. Monogr. 61, 145.

Glatzel, G., 1999. Historic forest use and its possible implications to recently accelerated tree growth in Central Europe. In: Causes and Consequences of Accelerated Tree Growth in Europe. EFI Proceedings No 27, pp. 65–74.

Gromtsev, A., 2002. Natural disturbance dynamics in the boreal forests of European Russia: a review. Silva Fenn. 36, 41–55.

Hadley, K.S., Knapp, P.A., 2011. Detection of high-wind events using tree-ring data. Can. J. For. Res. 41, 1121–1129.

Hanewinkel, M., Zhou, W., Schill, C., 2004. A neural network approach to identify forest stands susceptible to wind damage. For. Ecol. Manage. 196, 227–243.

Hanewinkel, M., Peltola, H., Soares, P., González-Olabarria, J.R., 2011. Recent approaches to model the risk of storm and fire. For. Syst. 3, 30–47.

Hernández, L., Rubiales, J.M., Morales-Molino, C., Romero, F., Sanz, C., Gómez Manzaneque, F., 2011. Reconstructing forest history from archaeological data: a case study in the Duero basin assessing the origin of controversial forests and the loss of tree populations of great biogeographical interest. For. Ecol. Manage. 261, 1178–1187.

Hessburg, P.F., Smith, B.G., Salter, R.B., 1999. Detecting change in forest spatial patterns from reference conditions. Ecol. Appl. 9, 1232–1252.

Heurich, M., Englmaier, K.H., 2010. The development of tree species composition in the Rachel – Lusen region of the Bavarian Forest National Park. Silva Gabreta 16, 165–186.

Heurich, M., Jehl, H., 2000. Waldentwicklung im Bergwald nach Windwurf und Borkenkäferbefall, Wissenschaftliche Schriftenreihe der Nationalparkverwaltung Bayerischer Wald. Grafenau, Band, p. 14.

Jelínek, J., 1988. Větrná a kůrovcová kalamita na Šumavě z let 1868 až 1878. Lesprojekt, Brandýs nad Labem.

Jelínek, J., 2005. Od jihočeských pralesů k hospodářským lesům Šumavy. MZE ČR, Úsek lesního hospodářství, ÚHÚL Brandýs nad Labem.

Kačmar, M., Wild, J., Moravcová, M., Konopová, Z., Zajíčková, L. (2013): Geodatenbank über die historische Entwicklung der Waldbestände im Nationalpark Böhmische Schweiz, In: Csaplovics, E., Seiler, U., Wild, J. (eds.): Historische Waldentwicklung in der Sächsisch-Böhmische Schweiz / Historický vývoj lesa v Českosaskm Švýcarsku, Schriftenreihe Fernerkundung und Angewandte Geoinformatik – Bd.10, Rhombos Verlag.

Keane, R.E., Hessburg, P.F., Landres, P.B., Swanson, F.J., 2009. The use of historical range and variability (HRV) in landscape management. For. Ecol. Manage. 258, 1025–1037.

Korpel', Š., 1995. The Virgin Forests of the Western Carpathians. Gustav Fischer Verlag, Stuttgart.

Kulakowski, D., Bebi, P., 2004. Range of variability of unmanaged subalpine forests. Forum für Wissen, pp. 47–54.

Landres, P.B., Morgan, P., Swanson, F.J., 1999. Overview of the use of natural variability concepts in managing ecological systems. Ecol. Appl. 9, 1179–1188.

Lausch, A., Fahse, L., Heurich, M., 2011. Factors affecting the spatio-temporal dispersion of *Ips typographus* (L.) in Bavarian Forest National Park: a long-term quantitative landscape-level analysis. For. Ecol. Manage. 261, 233–245.

Malberg, H., 2007. Meteorologie und Klimatologie: Eine Einführung. Springer DE.

Martin, H., 1906. Die Forsteinrichtung. Ein Grundriss zu Vorlesungen und ein Leitfaden für Praktiker, second ed. Julius Springer, Berlin.

Meguro, S., Miyawaki, A., 1994. A study of the relationship between mechanical characteristics and the coastal vegetation among several broad-leaf trees in Miura Peninsula in Japan. Vegetatio 112, 101–111.

METI/NASA, 2011. ASTER Global Digital Elevation Model V002.

Mikita, T., Klimánek, M., Kolejka, J., 2012. Usage of multidimensional statistic methods with MAXTOPEX factor for Windthrow risk assessment. Allg. For. Jagdztg 183, 63–74.

Mikusinska, A., Zawadzka, B., Samojlik, T., Jędrzejewska, B., Mikusiński, G., 2012. Quantifying landscape change during the last two centuries in Białowieża Primeval Forest. Appl. Veg. Sci., 16.

Mitchell, S.J., Lanquaye-Opoku, N., Modzelewski, H., Shen, Y., Stull, R., Jackson, P., Murphy, B., Ruel, J.-C., 2008. Comparison of wind speeds obtained using numerical weather prediction models and topographic exposure indices for predicting windthrow in mountainous terrain. For. Ecol. Manage. 254, 193–204.

Nagel, T.A., Diaci, J., 2006. Intermediate wind disturbance in an old-growth beech-fir forest in southeastern Slovenia. Can. J. For. Res. 36, 629–638.

Nagel, T.A., Svoboda, M., Diaci, J., 2006. Regeneration patterns after intermediate wind disturbance in an old-growth Fagus–Abies forest in southeastern Slovenia. For. Ecol. Manage. 226, 268–278.

Neuhäuslová, Z. (Ed.), 2001. The Map of Potential Natural Vegetation of the Šumava National Park. Explanatory text, Silva Gabreta, Suppl. 1/2001.

Nielsen, A.B., Odgaard, B.V., 2005. Reconstructing land cover from pollen assemblages from small lakes in Denmark. Rev. Palaeobot. Palynol. 133, 1–21.

Nielsen, A.B., Odgaard, B.V., 2010. Quantitative landscape dynamics in Denmark through the last three millennia based on the landscape reconstruction algorithm approach. Veg. Hist. Archaeobot. 19, 375–387.

Økland, B., Berryman, A., 2004. Resource dynamic plays a key role in regional fluctuations of the spruce bark beetles *Ips typographus*. Agric. For. Entomol. 6, 141–146.

Panayotov, M., Kulakowski, D., Laranjeiro Dos Santos, L., Bebi, P., 2011. Wind disturbances shape old Norway spruce-dominated forest in Bulgaria. For. Ecol. Manage. 262, 470–481.

Papaik, M.J., Canham, C.D., 2006. Species resistance and community response to wind disturbance regimes in northern temperate forests. J. Ecol. 94, 1011–1026.

Pickett, S., White, P., 1985. Patch dynamics: a synthesis, pp. 371–384.

Pretzsch, H., 2009. Forest Dynamics, Growth and Yield, Stand. Springer Berlin Heidelberg, Berlin, Heidelberg.

Pyatt, D.G., Harrison, D., Ford, A.S., 1969. Guide to site types in forests of North and Mid – Wales. Forestry Commission, United Kingdom, London.

Quine, C.P., White, I.M.S., 1998. The potential of distance-limited topex in the prediction of site windiness. Forestry 71, 325–332.

R Development Core Team, 2012. R: a language and environment for statistical computing.

Rich, R.L., Frelich, L.E., Reich, P.B., 2007. Wind-throw mortality in the southern boreal forest: effects of species, diameter and stand age. J. Ecol. 95, 1261–1273.

Ruel, J.-C., 2000. Factors influencing windthrow in balsam fir forests: from landscape studies to individual tree studies. For. Ecol. Manage. 135, 169–178.

SAGA Development Team, 2011. System for Automated Geoscientific Analyses (SAGA GIS).

Schelhaas, M.J., Nabuurs, G.J., Schuck, A., 2003. Natural disturbances in the European forests in the 19th and 20th centuries. Glob. Change Biol. 9, 1620–1633.

Scott, R.E., Mitchell, S.J., 2005. Empirical modelling of windthrow risk in partially harvested stands using tree, neighbourhood, and stand attributes. For. Ecol. Manage. 218, 193–209.

Šebková, B., Šamonil, P., Janík, D., Adam, D., Král, K., Vrška, T., Hort, L., Unar, P., 2011. Spatial and volume patterns of an unmanaged submontane mixed forest in Central Europe: 160 years of spontaneous dynamics. For. Ecol. Manage. 262, 873–885.

Seidl, R., Fernandes, P.M., Fonseca, T.F., Gillet, F., Jönsson, A.M., Merganičová, K., Netherer, S., Arpaci, A., Bontemps, J.-D., Bugmann, H., 2010. Modelling natural disturbances in forest ecosystems: a review. Ecol. Model. 222, 903–924.

Seidl, R., Schelhaas, M.-J., Lexer, M.J., 2011. Unraveling the drivers of intensifying forest disturbance regimes in Europe. Glob. Change Biol. 17, 2842–2852.
Splechtna, B.E., Gratzer, G., Black, B.A., 2005. Disturbance history of a European old-growth mixed-species forest – a spatial dendro-ecological analysis. J. Veg. Sci. 16, 511–522.
Svoboda, M., Pouska, V., 2008. Structure of a Central-European mountain spruce old-growth forest with respect to historical development. For. Ecol. Manage. 255, 2177–2188.
Svoboda, M., Fraver, S., Janda, P., Bače, R., Zenáhlíková, J., 2010. Natural development and regeneration of a Central European montane spruce forest. For. Ecol. Manage. 260, 707–714.
Svoboda, M., Janda, P., Nagel, T.a., Fraver, S., Rejzek, J., Bače, R., 2012. Disturbance history of an old-growth sub-alpine *Picea abies* stand in the Bohemian Forest, Czech Republic. J. Veg. Sci. 23, 86–97.
Swetnam, T.W., Allen, C.D., Betancourt, J.L., 1999. Applied historical ecology: using the past to manage for the future. Ecol. Appl. 9, 1189–1206.
Turner, M.G., 2010. Disturbance and landscape dynamics in a changing world. Ecology 91, 2833–2849.
Ulanova, N.G., 2000. The effects of windthrow on forests at different spatial scales: a review. For. Ecol. Manage. 135, 155–167.
Wermelinger, B., 2004. Ecology and management of the spruce bark beetle Ips typographus – a review of recent research. For. Ecol. Manage. 202, 67–82.
Wild, J., Neuhäuslová, Z., Sofron, J., 2004. Changes of plant species composition in the Šumava spruce forests, SW Bohemia, since the 1970s. For. Ecol. Manage. 187, 117–132.
Wolf, A., Møller, P.F., Bradshaw, R.H.W., Bigler, J., 2004. Storm damage and long-term mortality in a semi-natural, temperate deciduous forest. For. Ecol. Manage. 188, 197–210.
Wulf, M., Sommer, M., Schmidt, R., 2009. Forest cover changes in the Prignitz region (NE Germany) between 1790 and 1960 in relation to soils and other driving forces. Landscape Ecol. 25, 299–313.
Yokoyama, R., Shlrasawa, M., Pike, R.J., 2002. Visualizing topography by openness : a new application of image processing to digital elevation models. Photogramm. Eng. Remot. Sens. 68, 257–265.
Zatloukal, V., 1998. Historické a současné příčiny kůrovcové kalamity v Národním parku Šumava. Silva Gabreta 2, 327–357.
Zielonka, T., Holeksa, J., Fleischer, P., Kapusta, P., 2010. A tree-ring reconstruction of wind disturbances in a forest of the Slovakian Tatra Mountains, Western Carpathians. J. Veg. Sci. 21, 31–42.

Paper II



Brůna, J., Vojta, J. (manuscript)

Landscape-scale forest succession on abandoned agricultural land is controlled by terrain topography, distance to seed source and previous land use

Landscape-scale forest succession on abandoned agricultural land is controlled by terrain topography, distance to seed source and previous land use

Shortened title: Forest succession on abandoned agricultural land

Authors: Josef Brůna[1,2], Jaroslav Vojta[3]

Corresponding author: josef.bruna@gmail.com, Phone: +271 015 207

[1] Institute for Environmental Studies, Faculty of Science, Charles University, Benátská 2, 12801 Prague 2, Czech Republic
[2] Institute of Botany of the Czech Academy of Sciences, Zámek 1, 252 43 Průhonice, Czech Republic
[3] Department of Botany, Faculty of Science, Benátská 2, Prague, 128 43, Czech Republic

Abstract

Forest succession on abandoned agricultural land is a common trend in temperate regions. However, factors controlling the rate of succession towards forest are poorly understood, especially at the landscape scale. Here we used time series of aerial photography to explore the rate of forest succession and its driving forces in a landscape completely abandoned 70 years ago in the western part of the Czech Republic. The former rural landscape of arable fields, pastures, meadows and few forest patches changed into a mosaic of shrubs, forests, and grasslands. To explore factors controlling this change during each decade, we tested variables derived from digital elevation model, historical cadastral maps, distance to forest patches and their densities. Distance to closest forest patch in the previous decade was the main driving factor of succession with a negative effect, together with elevation and total insolation during vegetation season. Density of surrounding forest in the previous decade, slope and soil wetness index had a positive effect on succession rate. This means that most of the persisting grasslands are in dry areas in higher elevations, mostly flat with high insolation and further away from forests. Interestingly, the influence of terrain topography on forest succession gradually declined through time and during the last decades, the succession is no longer limited by environmental factors. In contrast, type of agricultural land use 70 years ago still has a persistent effect on forest succession. This shows long-lasting legacies of previous land use even at the landscape scale.

Keywords: secondary succession, abandoned landscape, land cover, aerial imagery, post-agricultural forest, terrain topography

Highlights:

- The density of forest, slope and soil wetness had a positive effect on succession rate towards the forest.
- Grasslands persist in dry areas in higher elevations, with high insolation and flat surface.
- Succession is no longer limited by environmental factors, whose influence declined recently.

Author contributions:

JB: performed research, contributed new methods, analyzed data and lead the writing of the paper

JV: conceived the study, obtained the data and co-wrote the paper

1. Introduction

Spreading of forests and shrubs in an abandoned landscape is a common trend in many European (FAO, 2007) and high-income countries in general (Fridley and Wright, 2012; Queiroz et al., 2014; Wright and Fridley, 2010). This is especially pronounced in the countries that belonged to the Soviet bloc, where the collapse of totalitarian regimes in the 1980's led to a considerable decrease of agricultural land (Alcantara et al., 2013; Kuemmerle et al., 2008; Prach et al., 2007).

Such parts of landscape create an opportunity for regeneration of native ecosystems and rewilding (Navarro and Pereira, 2012). However, shrubs are usually perceived as a threat to biodiversity (Poschlod and WallisDeVries, 2002; Ratajczak et al., 2012; Stoate et al., 2009) because they act as direct competitors against herbaceous species and grasses (Rejmanek and Rosen, 1992). Therefore, restoration and management of grasslands often aim to eradicate shrubs (Michielsen et al., 2017a) and the European Union agricultural policy in synergy with national subsidiary programs motivates landowners to do so (Angileri et al., 2011; Michielsen et al., 2017b). Detailed knowledge about succession on these sites is therefore seen as crucial for nature conservation.

The expected final stage of succession in a temperate climate of central Europe is a forest, except in extreme habitats (Ellenberg, 1988). However, the rate of secondary succession towards this climax state and even the climax itself varies across the landscape. Succession on mesic sites in the Czech Republic leads to forests, whereas on dry sites towards a bushy savanna-like state where grasses and dry conditions prevent the establishment of woody species (Prach et al., 2014, 2007). Generally, the secondary succession in The Czech Republic reaches species composition of potential natural vegetation in 180 years and 250 years when considering cover data (Prach et al., 2016).

There are other factors influencing this process such as grazing of wild (Horčičková et al., 2018) or domestic animals (Carmel and Kadmon, 1999), soil and climate (Wright and Fridley, 2010), species pools (Fridley and Wright, 2012) and other environmental conditions which influence the speed, direction and end of secondary succession (Odum, 1969).

Studies of secondary succession in an abandoned land are usually restricted to one land use type, smaller areas, partly managed, had been observed only at the beginning and end or using space for time substitution. It is therefore difficult to infer natural course of succession and its differences on a landscape scale. This type of data is hard to find, especially in the cultural landscape of central Europe. We have observed spatial differences in the speed and direction of secondary succession in an abandoned landscape in an unused part of a military area in the Czech Republic since 1952. Using this long-term, landscape-scale data, we aim to identify possible reasons behind these spatial differences. To achieve this aim, in an area, where old records about vegetation were not available, we have used aerial survey photography, which contains a vast amount of data about landscape changes over time. Black and white aerial photography is available in many countries of Europe (Cousins and Ihse, 1998) and USA (Turner and Ruscher, 1988) since 1930's and was successfully used for similar purposes in boreal (Cousins, 2001) and Mediterranean areas (Carmel and Kadmon, 1999, 1998; Pueyo and Beguería, 2007; Rocchini et al., 2006).

Differences in succession rate and speed were previously attributed to local moisture (Prach et al., 2014), elevation (Jelínek, 1981), former land use (Kopecký and Vojta, 2009), seed distribution (Pueyo and Alados, 2007), available light (Kobe et al., 1995a) or slope (Carmel and Kadmon, 1999)

Modern processing and classification techniques including object-oriented classification can derive even more data from this imagery. We have classified old and recent aerial photography to monitor and model woody species encroachment in decadal timestep and tested environmental factors derived from detailed digital elevation model (DEM), former land use and spatial indices based on forest density and distance to forests.

2. Data and modelling

2.1. Area of interest

The study site is a part of a military area Hradiště (331.61 km^2) in Doupovské hory Mountains near Karlovy Vary in a western part of Czech Republic. It is 2 × 2.5 km large and management is restricted since 1953 when the military area was established. This part serves as a buffer zone, entrance is prohibited, but there is no active military training in the area (Vojta et al., 2007). Interventions are limited only to several places used for hunting. These were excluded from all analyses, except for calculating the density of forest in the neighborhood.

The former rural landscape of fields, meadows and few forests had gradually changed into a mosaic of shrubs, forests, and few grassland patches. The axis of the area is the main gravel road through former village Tocov, which is still used for transport to the military area. The study area is hilly, with elevation ranging from 400 m to 800 m a s. l. There are two central valleys in the east-west direction, each with its stream. North and east borders of the area are formed by ascending slopes.

The potential natural vegetation in the area would be a mesic beech forest (Neuhäuslová et al., 1997). The main tree species in the new forests are mainly native broadleaved species *Fraxinus excelsior, Betula pendula*, *Acer pseudoplatanus,* as well as *Carpinus betulus, Ulmus glabra, Acer campestre and Quercus petraea* (Zajíčková, 2009). *Crataegus sp.* and *Rosa sp.* dominate the shrubs and *Prunus spinosa*, *Fraxinus excelsior*, *Corylus avellana*, *Populus tremula and Salix caprea, Sorbus aucuparia, Sambucus racemosa* in the areas above 750 m a.s.l. (Jelínek, 1981). Conifers are mostly limited to managed forests and are represented by *Picea abies* and *Larix decidua*. Former villages are still full of old fruit trees (*Prunus avium*, *Pyrus* sp. and *Malus sp.*) and were colonized mostly by *Fraxinus excelsior and Acer psedoplatanus* (Vojta, 2007).

2.2. Aerial imagery and processing

We have selected old aerial images acquired within vegetation season for each decade from the abandonment in 1952 until 2015 and used them as a primary source of information about land cover changes in the area. Due to inconsistencies in acquisition years and dates of the images, the resulting time steps range from 8 to 13 years. The sources of imagery and its properties are summarized in Table 1. We have orthorectified the old survey photographs in PCI Geomatica 10 Orthoengine (PCI Geomatics, 2008) using current imagery for georeferencing, similarly to (Sluiter and de Jong, 2007) and mosaicked the individual images in ERDAS Imagine 8.7 (Leica Geosystems GIS & Mapping, 2004) to produce spectrally homogenous mosaic from several overlapping images with different brightness caused by the development process of the old photographs. The imagery from 2005 and 2015 was already orthorectified by the producer, and we only converted it to grayscale and resampled to 0.5 m to ensure similar data for classification.

2.3. Classification

We have done a semi-automated object-oriented classification (OBIA) (Blaschke, 2010) of all the orthoimages using eCognition Developer 7 (Definiens, 2007) distinguishing two final categories: grasslands and trees or shrubs since it was hard to distinguish the latter two on older images.

We have added median filtered copies of the imagery to suppress inhomogeneity in heterogeneous tree canopies following the method described by Halounová (2004). The images were initially segmented into objects using multiresolution segmentation (Baatz and Schäpe, 2000) and these objects were classified using brightness and texture features based on GLCM functions (Haralick et al., 1973) following the method of Pillai et al. (2005). The features used for classification were the

same for all images, but the thresholds varied, based on brightness and contrast of individual imagery.

We have generalized the resulting classifications into a 5 m pixel grid for the model, to match the resolution of the DEM and to minimize the effect of spatial errors of georeferenced old photographs. During the study period, natural return to grassland from the forest stage is improbable, except for gap formations in older forests which is rare here. Most such occurrences are a result of classification error, the spatial error of the imagery or game management, which is the only significant human intervention and we have excluded them from all analyses, except for calculating the density of surrounding trees and shrubs.

Table 1 Aerial imagery used in the study and its properties and processing required to obtain comparable product for each decade.

Year	Date	Number of images	Processing	Type	Quality	Source
1952	July 22	3	Orthorectification, Mosaicking	Black and white aerial survey photographs	Scanned to achieve approx. 0.5 m	Military archive in Dobruška
1962	April 22	6				
1971	October 7	5				
1984	June 20	2				
1992	May 18	2				
2005	May 26	1	Resampling and conversion to black and white	RGB orthoimage	0.5 m	Czech Office for Surveying, Mapping, and Cadaster
2015	July 4	1	Resampling and conversion to black and white	RGB orthoimage	0.25 m	

2.4. Variables used

We have used two groups of variables to explain observed changes of land cover – topographical to test environmental drivers and spatial to test the effect of spatial configuration of surrounding vegetation and distances to seed source and former village.

We have derived topographic variables from a LiDAR DEM with 5 m resolution and 1 m vertical error (DMR 4G from ČÚZK, www.cuzk.cz). We have used SAGA GIS (Conrad et al., 2015) to calculate elevation, slope, Northerness (cos(aspect)), Insolation though vegetation season (total, direct, diffuse; Böhner and Antonić 2009) and Topographic Position Index (TPI; Guisan et al. (1999) using on several distances (50, 100, 250 and 500) defining local terrain features as well as Terrain ruggedness index (Riley et al., 1999) as a measure of topographic heterogeneity. Topographic Wetness Index (TWI; Beven and Kirkby 1979) was calculated using FD8Q flow routing-algorithm as recommended by Kopecký and Čížková (2010).

We have derived spatial information about trees and shrubs from the classified layers from each decade in the form of distance to trees and shrubs and densities in different vicinities. We have tested the correlation of these and selected the least correlated pair a 15 × 15 m close neighborhood and 100 × 100 m broader neighborhood. We have also calculated the distance to former buildings

based on a vectorized layer of buildings from 1952 imagery using Euclidean distance tool in ArcMap 10.4 (ESRI, 2016).
We have used the cadastral map from 1950 to extract information about the former land use (ČÚZK). There were 10 classes, but only 6 had more than 1% - field, pasture, meadow, forest, village, and road. We have merged the less frequent ones with the functionally closest class type. Each cadaster unit has its identification number (ID), that was also used in the analysis.

2.5. Analysis

We have modelled binary changes of grasslands to forests between two successive classified images (decade) with generalized linear models with mixed effects and binomial data distribution using logit transformation (*glmer*) using *lme4* (Bates et al., 2015) package in R (R Core Team, 2017). This type of models allow specification of known random variability in different levels and therefore can be used to analyze data that are not totally independent (Šmilauer, 2007). The correct settings of the random variability can reduce the effect of pseudo-replications (Crawley, 2007).
For this purpose, we set land use type as a random effect with a nested cadaster unit ID number. This helped us to identify important factors of woody species spreading into grasslands independently on former land use origin. We did not test land use in any models, because of the substantial differences in the prevalence of each type. The ID was used so that the weight of several points from the same cadaster unit (e.g., a field) is lowered.
We made several sets of the models to compare the effects of spatial variables, environmental variables, and their combinations. We standardized all numerical variables using scale function in R (R Core Team, 2017) that divides the centered values of the column by its standard deviation. Moreover, we have tested correlations between all variables and selected ecologically more meaningful variable from each correlated pair with a correlation coefficient higher than 0.5. For each decade, only remaining grassland pixels were selected for the model and from them, a regular grid-based selection was made to obtain approx. 5000 to 15000 points.
To compare the model predictions with the reality, we have used the realized proportion of change from grassland to the forest in the modelled decade to select this proportion of pixels with highest model results and set those as modelled change for model results evaluation. We have used it to calculate Cohens Kappa (Cohen, 1960) to compare individual models in each decade and also between decades since this kind of comparison does not depend on the realized change so that we can compare results between decades with different amount of change. Although it does not necessarily produce the highest possible kappa, we find it more meaningful to use the realized proportions for this use and less problematic than other threshold identification methods for kappa statistic such as AUC (Lobo et al., 2008), that can influence the resulting kappa (Allouche et al., 2006).
We have compared all combinations of explanatory variables within the models of the same type (spatial, environmental and mixed) using AIC (Burnham and Anderson, 2003). We have iteratively tested the best combinations of predictors, and if the majority of predictors were not significant in all modelled decades, the model was eliminated, and comparison of AIC was made again. If the difference in AIC was smaller than 2, the simpler model was kept.

3. Results

The monitored change over 60 years of abandonment showed a rapid succession of the whole landscape and a change from predominantly grassland to forests dominated landscape already in 1970's. However, many small and mid-sized grasslands persist, mostly on flat parts and on top of the hills.

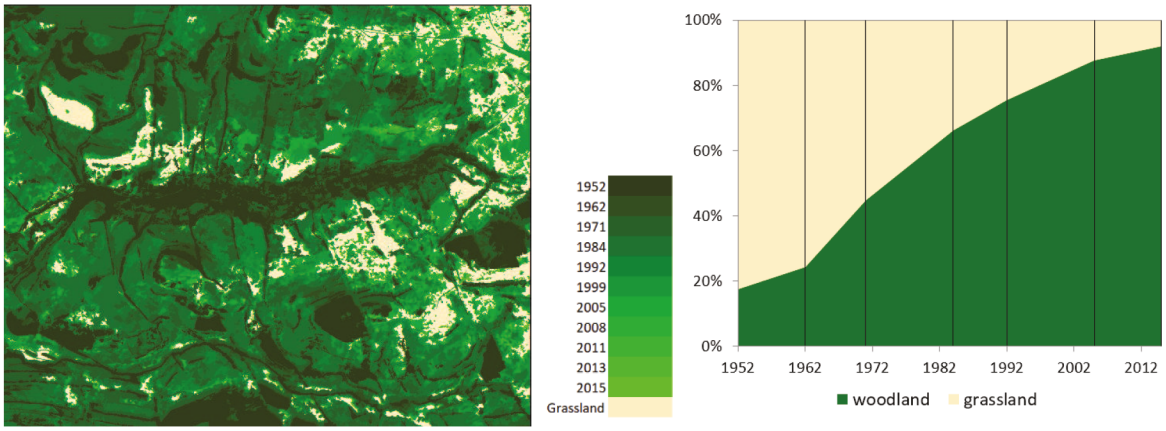


Figure 1 Trees and shrubs encroachment in the study area over the 60 years period on a map and a graph with land cover proportions.

There are still differences in forest cover on each main land use types, even 60 years from abandonment. The land use type most resistant to succession is meadows. However, meadows were rare in comparison to arable fields in the 1950's (10% vs. 66%), so the most grasslands today occur on former fields, and grasslands on former meadows are the second most prevalent type today (Tab. 2). Even the cadaster units in the forest land use type were not fully forested in 1952, but they are almost entirely covered by trees today as well as former villages and roads.

Table 2 Proportions of forest and grassland at the beginning of the study period in 1952 and 2015.

Land use type 1952		Relative to land use type 1952		Relative to the total area 1952		Relative to land use type 2015		Relative to the total area 2015	
	Proportion	grassland	forest	grassland	forest	grassland	forest	grassland	forest
roads	4%	68%	32%	3%	1%	4%	96%	0%	4%
meadow	10%	86%	14%	9%	1%	16%	84%	2%	8%
pasture	11%	67%	33%	7%	4%	4%	96%	0%	11%
field	66%	91%	9%	60%	6%	6%	94%	4%	62%
forest	4%	31%	69%	1%	3%	1%	99%	0%	4%
village	4%	39%	61%	2%	3%	0%	100%	0%	4%
Sum	100%			82%	18%			6%	94%

Models identified driving factors of secondary succession in an abandoned landscape in places with various land use origin. The most important factor was the distance to nearest tree or shrub at the beginning of the modelled decade, which together with elevation and total insolation during vegetation season had a negative impact on succession. This is consistent with our observations. The density of trees and shrubs in the vicinity (15 × 15 m) and the broader neighborhood (100 × 100 m), slope and TWI had a positive effect on succession towards a forest (Fig 2). Which means that most of the persisting grasslands are in dry areas in higher elevations, mostly flat with high insolation and further away from forests and shrubs. During the last decade, the succession seems to be no longer limited by environmental factors like elevation, slope of TWI and is driven mostly by spatial variables

like distance to the nearest tree or shrub and their densities in the neghbourhood (Fig. 2). Areas most suitable for the spread of woody species already changed to the forest, and remaining openness provide more homogeneous environmental space to reveal significant predictors.

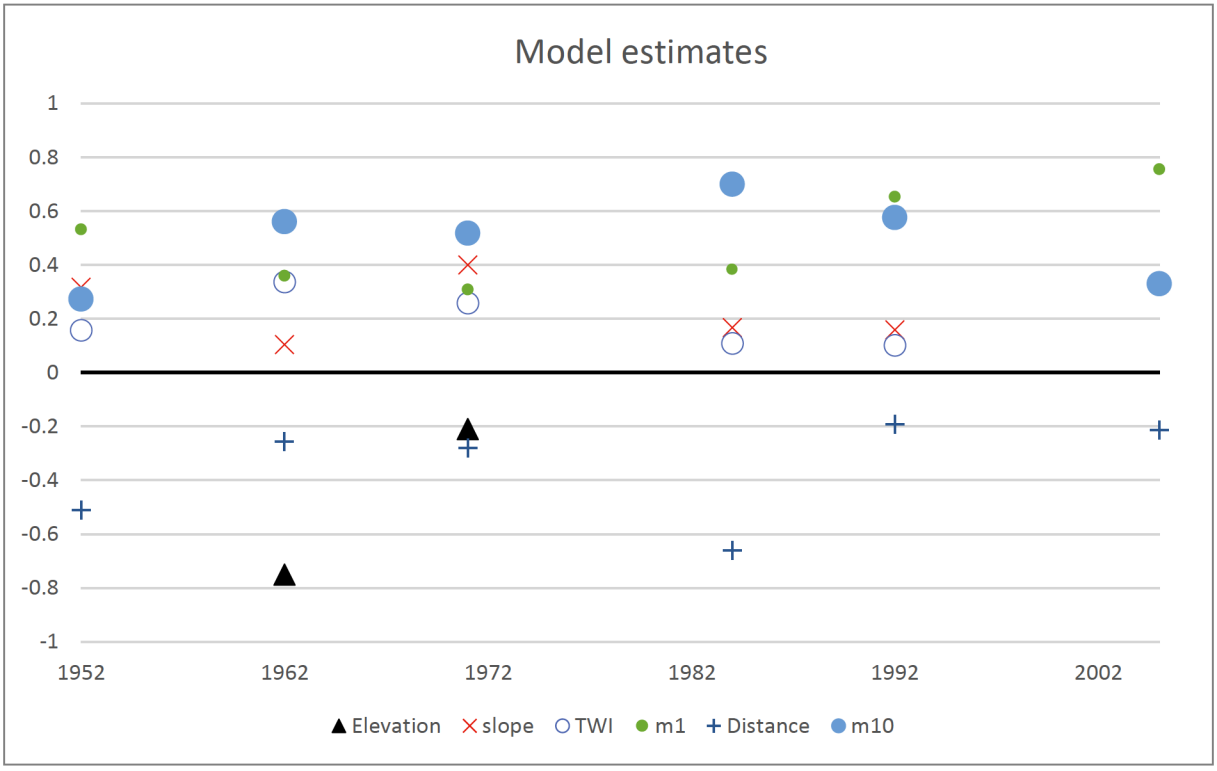


Figure 2 The role of each predictor in mixed models over time derived from model estimates using standardized data for each decade. Variables m1 and m10 are densities of forests in the immediate (15 m) and wider (100 m) neighborhood of the modelled pixel.

Models based only on spatial information (distances, densities) had a very good prediction with kappa mostly >50% (Tab 3). Distance to the former buildings was not significant during the last decade.

Table 3 Models for each decade based only on spatial information and the quality of their predictions (Kappa). Lu52r is land use type before the abandonment, lu52id is a cadaster unit ID, dist_bld is distance to former buildings, dist is distance to trees or shrubs at the beginning of the modelled decade, and m1 and m10 are densities of trees and shrubs in the immediate (15 m) and wider (100 m) neighborhood of the modelled pixel. Threshold marks the lowest probability, where the model result was considered as forest.

Start year	Model formula: change~	Kappa	Observations	Threshold
1952	dist + m1 + m10 + dist_bld + (1 | lu52r/lu52id)	41.0 %	9422	0.313
1962	dist + m1 + m10 + dist_bld + (1 | lu52r/lu52id)	51.6 %	15402	0.549
1971	dist + m1 + m10 + dist_bld + (1 | lu52r/lu52id)	56.8 %	11232	0.704
1984	dist + m1 + m10 + dist_bld + (1 | lu52r/lu52id)	53.6 %	14538	0.584
1992	dist + m1 + m10 + dist_bld + (1 | lu52r/lu52id)	51.6 %	10038	0.748
2005	dist + m1 + m10 + (1 | lu52r/lu52id)	49.1 %	4928	0.687

Models based only on factors derived from digital elevation model lead to somewhat poorer predictions with lower Kappa values (Tab 4), but their variables were almost always significant, except for total insolation, which was not significant in 1971-1984 -1992.

Table 4 Models for each decade based only on DEM derived variables and the quality of their predictions (Kappa). Lu52r is land use type before the abandonment, lu52id is a cadaster unit ID, TWI is Topographic wetness index. Threshold marks the lowest probability, where the model result was considered as forest. In 1971 and 1984 total insolation was not significant and was removed from the model.

Start year	Formula	Kappa	Observations	Threshold
1952	elevation + slope + TWI + tot_insol + (1 | lu52r/lu52id)	34.8%	9422	0.28
1962	elevation + slope + TWI + tot_insol + (1 | lu52r/lu52id)	49.8%	15402	0.55
1971	elevation + slope + TWI + (1 | lu52r/lu52id)	53.8%	11232	0.72
1984	elevation + slope + TWI + (1 | lu52r/lu52id)	46.7%	14538	0.58
1992	elevation + slope + TWI + tot_insol + (1 | lu52r/lu52id)	46.3%	10038	0.76
2005	elevation + slope + TWI + tot_insol + (1 | lu52r/lu52id)	38.7%	4928	0.68

The best prediction was almost always from a model combing spatial and environmental data (mixed, Tab. 5). The exceptions were 1971-1984 where the difference is 0.1% and in 2005-2015, where no environmental variables were significant, and only spatial variables were significant. This also confirms that the model selection method was robust enough and proves the importance of spatial information for studies of vegetation change on a landscape scale and a noticeable influence of former land use, even after 60 years without management.

Table 5 Models for each decade based on spatial information and DEM derived variables and their predictions based on a realized percentage of change using Kappa statistic. Lu52r is land use type before the abandonment, lu52id is a cadaster unit ID. Threshold marks the lowest probability, where the model result was considered as forest. Dist is the distance to trees or shrubs at the beginning of the modelled decade, and m1 and m10 are densities of trees and shrubs in the immediate (15 m) and wider (100 m) neighborhood of the modelled pixel.

Start year	Formula	Kappa	Obser-vations	Threshold
1952	elevation + slope + TWI+ m1 + dist + m10 + (1 | lu52r/lu52id)	41.9%	9422	0.31
1962	elevation + slope + TWI+ m1 + dist + m10 + (1 | lu52r/lu52id)	52.3%	15402	0.55
1971	elevation + slope + TWI+ m1 + dist + m10 + (1 | lu52r/lu52id)	57.3%	11232	0.70
1984	elevation + slope + TWI+ m1 + dist + m10 + (1 | lu52r/lu52id)	53.5%	14538	0.59
1992	elevation + slope + TWI+ m1 + dist + m10 + (1 | lu52r/lu52id)	51.7%	10038	0.75
2005	m1 + dist + m10 + (1 | lu52r/lu52id)	49.1%	4928	0.69

4. Discussion

Old aerial images allowed us to study a remote area that had not been monitored for many decades by any fieldwork. Even after six decades of succession, there are still many open grasslands, which is consistent with results of Sluiter and de Jong (2007) who also found that many sites did not advance to the final stage of succession during 55 years of their study, but contradicts the results of Prach et al., (2014), that concluded that in most cases woodland established after 20 years. At the same time, Prach et al. (2014) attribute this differences in local moisture conditions and that dry and wet conditions lead to open habitats, and mesic conditions lead to woodland.

Forest succession on a landscape scale is limited by spatial factors. The distance to forests affects succession also in other regions, mainly through seed availability limitation (Cook et al., 2005; Duncan and Duncan, 2000; Pueyo and Alados, 2007). It was identified as the second most important

environmental predictor of the course of succession, after age, in a review by Prach and Řehounková (2006). The spread of woody vegetation was quick despite the suspected propagule availability limitation. This is due to the zoochorous spread of *Crataegus*, the main pioneer species in the area, that can disperse over long distances and quickly occupy large areas (Carlo et al., 2013).

The positive effect of density of forest in the neighborhood changes can be explained by the amount of available light in the surrounding grasslands (Kobe et al., 1995b), or by mycorrhizal infection (Dickie et al., 2007), enabling establishment and growth of tree and shrub species. At the same time, these seedlings are limited by competition in the grasslands (de Blois et al., 2004; Dickie et al., 2007) or litter (Facelli and Pickett, 1991). It is also consistent with standard seed distribution curves confirmed on site by Zajíčková (2009) and elsewhere (Pueyo and Alados, 2007) who also note, that fragmentation slows down spreading. This would also explain the increase in the rate of trees and shrubs spread once the dominant type of land cover changed from grasslands to trees and shrubs after 1971.

Osbornová et al. (1990) found the decline of *Crataegus sp.* after 45 to 60 years of secondary succession on abandoned fields which triggers an increase in light and faster growth of *Sambucus nigra* and *Fraxinus excelsior* that were beneath its canopy and were not competing with other species. A similar exchange of dominants is also visible in the study area, where *Fraxinus excelsior* and some other late successional species are increasing in quantity. However, we were not able to test this observation from the aerial images.

Generally, the spatial variables alone performed better for prediction of trees and shrubs spread than environmental variables derived from DEM alone, but environmental variables still explained some variability unexplained by spatial variables. The remaining grasslands occupy dry places as shown in other studies (Cramer and Hobbs, 2007; Osbornová et al., 1990; Prach et al., 2014, 2007), but did not persist on wet places, as Prach et al. (2014) found.

It may also be attributed to the stability of grasslands associated with bare bedrock (Cousins, 2001), although bedrock is rarely exposed in the study area, there are grasslands with shallower soils. The role of elevation and slope is also consistent with other studies on similar areas (Jelínek, 1981). The seed sources may be limited in higher areas (Dostalova, 2008). Steeper areas were generally used for pastures and might already contain enough seedling in the time of abandonment. Similarly, Carmel and Kadmon (1999) identified slope as the main driver for woody species spread in Israel. They also identify modified aspect, but this was not significant in our area.

There is also a significant influence of wild animals (deer, sika deer, and wild boar) examined in different research in the same area (Horčičková, 2010; Horčičková et al., 2018) and elsewhere (Sluiter and de Jong, 2007). Herbivores help to keep the present grasslands open and graze on tree and shrubs saplings.

Prevailing influence of former land use even after 70 years can be explained by different competition conditions for later successional species on different former land use types (Kopecký and Vojta, 2009). Kopecký and Vojta (2009) also mention a change in C, N, and C: N ratio in the soil as one of the reasons for long-term effects of land use. In earlier successional stages, small scattered shrubs in pastures can serve as perching sites for birds and significantly enhance the dispersion of *Crataegus* (Carlo et al. 2013). Vojta and Kopecký (2006) found that individual tree species differ between former land use types, *Crataegus* shrubs with *Acer campestre* grow typically on former field and pastures, whereas *Fraxinus excelsior* and *Acer pseudoplatanus* thrive in former villages. Adding information about species would improve the model, but it was not possible to differentiate them from the old aerial images.

The general increase of Kappa statistic of models through the decades is consistent with (Sluiter and de Jong, 2007) who argue, that it is due to lack of understanding of the pattern of initial secondary succession stage.

The fast succession toward forested landscape after abandonment effectively restored forest environment on former agricultural land (Vojta, 2007; Vojta and Drhovská, 2012). However, the communities of forest plants remain unsaturated (Vojta and Drhovská, 2012). On the other hand, open habitat specialists were still frequently recorded (Kopecký and Vojta, 2009) because of numerous gaps in shrub canopies and possibly surviving populations in sub-optimal conditions (extinction debt, Tilman et al., 1994). Our results cannot be directly used for evaluating the current status of either of these group of species in the study area. However, we can expect that the succession will lead to further improvement of forest environment in the long-term perspective and to further loss of habitats suitable for non-forest species. The current environment with very heterogeneous light conditions will disappear or will be restricted to driest places (Prach et al., 2007). The mosaic habitats with both woody vegetation patches and open areas supports the coexistence of both shade tolerant and light-demanding species (Best, 1998; Einarsson and Milberg, 1999; Škornik et al., 2008) and are recognized as a unusually species-rich systems that can develop even on former agricultural land (Forejt et al., 2017). Considering the positive feedback between the woody vegetation cover and further succession, the restoration and management of mosaic landscape in the study area will be soon very complicated and would require the introduction of managed grazing of domestic or wild animals and other measures in order to regulate the density of shrubs (Dostálek and Frantík, 2008; Elias and Tischew, 2016; Laborde and Thompson, 2013).

5. Conclusions

Simple extrapolation suggests that the complete loss of open landscape will happen in the near future, but our analysis shows many factors are slowing or blocking this process. This leads us to believe that there will always be some open areas and the identified factors can help to predict changes on a landscape scale and plan management practices in similar areas to protect diversity and reduce costs of management interventions. Whether it will be enough for light-demanding species survival remains to be seen and tested by other methods. However, it is evident that better understanding of the dynamics and speed of succession is crucial for conservation of the reaming grasslands and protection of its species.

6. Acknowledgments

We would like to thank Martin Kopecký and Lucie Drhovská for the vectorization of the land cover map from 1952 and Eva Horčičková for countless field experience and useful comments and discussions during the preparation of the manuscript. The study was mostly financed by Grant Agency of Charles University Grant No. 20310 and was supported by long-term research development project of The Institute of Botany No. RVO 67985939.

References:

Alcantara, C., Kuemmerle, T., Baumann, M., Bragina, E. V., Griffiths, P., Hostert, P., Knorn, J., Müller, D., Prishchepov, A. V., Schierhorn, F., Sieber, A., Radeloff, V.C., 2013. Mapping the extent of abandoned farmland in Central and Eastern Europe using MODIS time series satellite data. *Environmental Research Letters* 8. doi: 10.1088/1748-9326/8/3/035035

Allouche, O., Tsoar, A., Kadmon, R., 2006. Assessing the accuracy of species distribution models: Prevalence, kappa and the true skill statistic (TSS). *Journal of Applied Ecology* 43, 1223–1232.

doi: 10.1111/j.1365-2664.2006.01214.x

Angileri, V., Loudjani, P., Serafini, F., 2011. GAEC implementation in the EU: situation and perspectives. *Italian Journal of Agronomy* 6, 2. doi: 10.4081/ija.2011.6.s1.e2

Baatz, M., Schäpe, A., 2000. Multiresolution segmentation— an optimization approach for high quality multiscale image segmentation, in: J., S. (Ed.), Angewandte Geographische Informationsverarbeitung XII. Beiträge Zum AGIT-Symposium Salzburg,. Herbert Wichman Verlag, Karlsruhe, pp. 12–23.

Bates, D., Mächler, M., Bolker, B., Walker, S., 2015. Fitting Linear Mixed-Effects Models Using {lme4}. *Journal of Statistical Software* 67, 1–48. doi: 10.18637/jss.v067.i01

Best, J.A., 1998. Persistent outcomes of coppice grazing in Rockingham Forest, Northamptonshire, UK, in: Kirby, K.W. (Ed.), The Ecological History of European Forests. CAB International, pp. 63–72.

Beven, K.J., Kirkby, M.J., 1979. A physically based, variable contributing area model of basin hydrology / Un modèle à base physique de zone d'appel variable de l'hydrologie du bassin versant. *Hydrological Sciences Bulletin* 24, 43–69. doi: 10.1080/02626667909491834

Blaschke, T., 2010. Object based image analysis for remote sensing. *ISPRS Journal of Photogrammetry and Remote Sensing* 65, 2–16. doi: 10.1016/j.isprsjprs.2009.06.004

Böhner, J., Antonić, O., 2009. Chapter 8 Land-Surface Parameters Specific to Topo-Climatology, in: Developments in Soil Science. Elsevier, pp. 195–226. doi: 10.1016/S0166-2481(08)00008-1

Burnham, K.P., Anderson, D.R., 2003. Model selection and multimodel inference: a practical information-theoretic approach. Springer Science & Business Media.

Carlo, T.A., García, D., Martínez, D., Gleditsch, J.M., Morales, J.M., 2013. Where do seeds go when they go far? Distance and directionality of avian seed dispersal in heterogeneous landscapes. *Ecology* 94, 301–307. doi: 10.1890/12-0913.1

Carmel, Y., Kadmon, R., 1999. Effects of grazing and topography on long-term vegetation changes in a Mediterranean ecosystem in Israel. *Plant Ecology* 145, 243–254. doi: 10.1023/A:1009872306093

Carmel, Y., Kadmon, R., 1998. Computerized classification of Mediterranean vegetation using panchromatic aerial photographs. *Journal of Vegetation Science* 9, 445–454. doi: 10.2307/3237108

Cohen, J., 1960. A coefficient of agreement for nominal scales. *Educational and Psychological Measurement* 20, 37–46. doi: 10.1177/001316446002000104

Conrad, O., Bechtel, B., Bock, M., Dietrich, H., Fischer, E., Gerlitz, L., Wehberg, J., Wichmann, V., Böhner, J., 2015. System for Automated Geoscientific Analyses (SAGA) v. 2.1.4. *Geoscientific Model Development* 8, 1991–2007. doi: 10.5194/gmd-8-1991-2015

Cook, W.M., Yao, J., Foster, B.L., Holt, R.D., Patrick, L.B., 2005. Secondary succession in an experimentally fragmented landscape: community patterns across space and time. *Ecology* 86, 1267–1279.

Cousins, S.A.O., 2001. Analysis of land-cover transitions based on 17th and 18th century cadastral maps and aerial photographs. *Landscape Ecology* 16, 41–54.

Cousins, S.A.O., Ihse, M., 1998. A methodological study for biotope and landscape mapping based on CIR aerial photographs. *Landscape and Urban Planning* 41, 183–192. doi: 10.1016/S0169-2046(98)00057-7

Cramer, V.A., Hobbs, R.J., 2007. Old Fields: Dynamics and Restoration of Abandned Farmland, Uma ética para quantos? doi: 10.1007/s13398-014-0173-7.2

Crawley, M.J., 2007. The R book. John Wiley & Sons Ltd, Chichester, UK.

de Blois, S., Brisson, J., Bouchard, A., 2004. Herbaceous Covers to Control Tree Invasion in Rights-of-Way: Ecological Concepts and Applications. *Environmental Management* 33, 606–619. doi:

10.1007/s00267-004-0039-4

Definiens, A., 2007. Definiens Developer 7.

Dickie, I.A., Schnitzer, S.A., Reich, P.B., Hobbie, S.E., 2007. Is oak establishment in old-fields and savanna openings context dependent? *Journal of Ecology* 95, 309–320. doi: 10.1111/j.1365-2745.2006.01202.x

Dostálek, J., Frantík, T., 2008. Dry grassland plant diversity conservation using low-intensity sheep and goat grazing management: case study in Prague (Czech Republic). *Biodiversity and Conservation* 17, 1439–1454. doi: 10.1007/s10531-008-9352-1

Dostalova, A., 2008. Tree seedlings: how do they establish in spontaneously developed forests? A study from a mountainous area in the Czech Republic. *Biodiversity and Conservation* 18, 1671–1684. doi: 10.1007/s10531-008-9549-3

Duncan, R.S., Duncan, V.E., 2000. Forest Succession and Distance from Forest Edge in an Afro-Tropical Grassland1. *Biotropica* 32, 33–41. doi: 10.1111/j.1744-7429.2000.tb00445.x

Einarsson, A., Milberg, P., 1999. Species richness and distribution in relation to light in wooded meadows and pastures in southern Sweden. *Annales Botanici Fennici* 36, 99–107.

Elias, D., Tischew, S., 2016. Goat pasturing—A biological solution to counteract shrub encroachment on abandoned dry grasslands in Central Europe? *Agriculture, Ecosystems & Environment*, Grazing in {European} open landscapes: how to reconcile sustainable land management and biodiversity conservation? 234, 98–106. doi: 10.1016/j.agee.2016.02.023

Ellenberg, H., 1988. Vegetation ecology of central Europe. Cambridge University Press.

ESRI, I., 2016. ArcMap 10.4.

Facelli, J.M., Pickett, S.T.A., 1991. Plant litter: light interception and effects on an old field planta community. *Ecology* 72, 1024–1031. doi: 10.2307/1940602

FAO, R. (Italy). A. and C.P.D., 2007. The agriculture-forest interface.

Forejt, M., Skalos, J., Pereponova, A., Plieninger, T., Vojta, J., Šantrůčková, M., 2017. Changes and continuity of wood-pastures in the lowland landscape in Czechia. *Applied Geography* 79, 235–244. doi: 10.1016/j.apgeog.2016.12.016

Fridley, J.D., Wright, J.P., 2012. Drivers of secondary succession rates across temperate latitudes of the Eastern USA: climate, soils, and species pools. *Oecologia* 168, 1069–1077. doi: 10.1007/s00442-011-2152-4

Guisan, A., Weiss, S.B., Weiss, A.D., 1999. GLM versus CCA Spatial Modeling of Plant Species Distribution. *Plant Ecology* 143, 107–122. doi: 10.1023/A:1009841519580

Halounová, L., 2004. The automatic classification of b&w photos. *The International Archives of the Photogrammetry, Remote Sensing and Spatial Information Sciences 34, Part 3* 34, 455–460.

Haralick, R.M., Shanmugam, K., Dinstein, I., 1973. Textural features for image classification. *IEEE Transactions on Systems, Man and Cybernetics*. doi: 10.1109/TSMC.1973.4309314

Horčičková, E., 2010. Study of disturbances caused by wild boar (Sus scrofa) and their impact on vegetation of semi-dry grasslands with use of experimental method. Depon. in Knihovna Ústavu pro životní prostředí PřF UK, Praha.

Horčičková, E., Brůna, J., Vojta, J., 2018. Wild boar (Sus scrofa) increases species diversity of semi-dry grassland: Field experiment with simulated soil disturbances. *in progress*.

Jelínek, F., 1981. Sukcese a struktura vegetace na úhorech Doupovských hor. Disertační práce. Depon. in Knihovna katedry botaniky PřF UK, Praha.

Kobe, R.K., Pacala, S.W., Silander, J. a, Canham, C.D., 1995a. Juvenile Tree Survivorship as a Component of Shade Tolerance. *Ecological Applications* 5, 517–532. doi: 10.2307/1942040

Kobe, R.K., Pacala, S.W., Silander, J. a, Canham, C.D., 1995b. Juvenile Tree Survivorship as a Component of Shade Tolerance. *Ecological Applications* 5, 517–532. doi: 10.2307/1942040

Kopecký, M., Čížková, Š., 2010. Using topographic wetness index in vegetation ecology: does the algorithm matter? *Applied Vegetation Science* 13, 450–459. doi: 10.1111/j.1654-109X.2010.01083.x

Kopecký, M., Vojta, J., 2009. Land use legacies in post-agricultural forests in the Doupovské Mountains, Czech Republic. *Applied Vegetation Science* 12, 251–260. doi: 10.1111/j.1654-109X.2009.01023.x

Kuemmerle, T., Hostert, P., Radeloff, V.C., van der Linden, S., Perzanowski, K., Kruhlov, I., 2008. Cross-border Comparison of Post-socialist Farmland Abandonment in the Carpathians. *Ecosystems* 11, 614–628. doi: 10.1007/s10021-008-9146-z

Laborde, J., Thompson, K., 2013. Colonization of limestone grasslands by woody plants: the role of seed limitation and herbivory by vertebrates. *Journal of Vegetation Science* 24, 307–319. doi: 10.1111/j.1654-1103.2012.01463.x

Leica Geosystems GIS & Mapping, L., 2004. ERDAS Imagine 8.7.

Lobo, J.M., Jiménez-valverde, A., Real, R., 2008. AUC: A misleading measure of the performance of predictive distribution models. *Global Ecology and Biogeography* 17, 145–151. doi: 10.1111/j.1466-8238.2007.00358.x

Michielsen, M., Szemák, L., Fenesi, A., Nijs, I., Ruprecht, E., 2017a. Resprouting of woody species encroaching temperate European grasslands after cutting and burning. *Applied Vegetation Science* 20, 388–396. doi: 10.1111/avsc.12300

Michielsen, M., Szemák, L., Fenesi, A., Nijs, I., Ruprecht, E., 2017b. Resprouting of woody species encroaching temperate European grasslands after cutting and burning. *Applied Vegetation Science* 20, 388–396. doi: 10.1111/avsc.12300

Navarro, L.M., Pereira, H.M., 2012. Rewilding Abandoned Landscapes in Europe. *Ecosystems* 900–912. doi: 10.1007/s10021-012-9558-7

Neuhäuslová, Z., Moravec, J., Chytrý, M., Sádlo, J., Rybníček, K., Kolbek, J., Jirásek, K., 1997. Map of potential natural vegetation of the Czech Republic 1: 500 000. *Institute of Botany, Academy of Sciences of Czech Republic, Průhonice*.

Odum, E.P., 1969. The strategy of Ecosystem Development. *Science* 164, 262–270.

Osbornová, J., Kovárová, M., Leps, J., Prach, K., 1990. Succession in Abandoned Fields. Springer Netherlands, Dordrecht. doi: 10.1007/978-94-009-2444-4

PCI Geomatics, I., 2008. PCI Geomatica 10.0.3 - Orthoengine.

Pillai, R.B., Weisberg, P.J., Lingua, E., 2005. Object-oriented classification of repeat aerial photography for quantifying woodland expansion in central Nevada, in: 20th Biennial Workshop on Aerial Photography, Videography, and High Resolution Digital Imagery for Resource Assessment. Weslaco, Texas, pp. 2–6.

Poschlod, P., WallisDeVries, M.F., 2002. The historical and socioeconomic perspective of calcareous grasslands—lessons from the distant and recent past. *Biological Conservation* 104, 361–376. doi: 10.1016/S0006-3207(01)00201-4

Prach, K., Lepš, J., Rejmánek, M., 2007. Old field succession in central Europe: local and regional patterns, in: Cramer, V.A., Hobbs, R.J. (Eds.), Old Fields: Dynamics and Restoration of Abandoned Farmland. Island Press Washington, DC, USA, pp. 180–201.

Prach, K., Řehounková, K., 2006. Vegetation succession over broad geographical scales: Which factors determine the patterns? *Preslia*.

Prach, K., Řehounková, K., Lencová, K., Jírová, A., Konvalinková, P., Mudrák, O., Študent, V., Vaněček, Z., Tichý, L., Petřík, P., Šmilauer, P., Pyšek, P., 2014. Vegetation succession in restoration of disturbed sites in Central Europe: The direction of succession and species richness across 19 seres. *Applied Vegetation Science* 17, 193–200. doi: 10.1111/avsc.12064

Prach, K., Tichý, L., Lencová, K., Adámek, M., Koutecký, T., Sádlo, J., Bartošová, A., Novák, J., Kovář, P.,

Jírová, A., Šmilauer, P., Řehounková, K., 2016. Does succession run towards potential natural vegetation? An analysis across seres. *Journal of Vegetation Science* 27, 515–523. doi: 10.1111/jvs.12383

Pueyo, Y., Alados, C.L., 2007. Effects of fragmentation, abiotic factors and land use on vegetation recovery in a semi-arid Mediterranean area. *Basic and Applied Ecology* 8, 158–170. doi: 10.1016/j.baae.2006.03.009

Pueyo, Y., Beguería, S., 2007. Modelling the rate of secondary succession after farmland abandonment in a Mediterranean mountain area. *Landscape and Urban Planning* 83, 245–254. doi: 10.1016/j.landurbplan.2007.04.008

Queiroz, C., Beilin, R., Folke, C., Lindborg, R., 2014. Farmland abandonment: Threat or opportunity for biodiversity conservation? A global review. *Frontiers in Ecology and the Environment* 12, 288–296. doi: 10.1890/120348

R Core Team, 2017. R: A Language and Environment for Statistical Computing.

Ratajczak, Z., Nippert, J.B., Collins, S.L., 2012. Woody encroachment decreases diversity across North American grasslands and savannas. *Ecology* 93, 697–703. doi: 10.1890/11-1199.1

Rejmanek, M., Rosen, E., 1992. Influence of colonizing shrubs on species-area relationships in alvar plant communities. *Journal of Vegetation Science* 3, 625–630.

Riley, S.J., DeGloria, S.D., Elliot, R., 1999. A Terrain Ruggedness Index that Qauntifies Topographic Heterogeneity. *Intermountain Journal of Sciences*. doi: citeulike-article-id:8858430

Rocchini, D., Perry, G.L.W., Salerno, M., Maccherini, S., Chiarucci, A., 2006. Landscape change and the dynamics of open formations in a natural reserve. *Landscape and Urban Planning* 77, 167–177. doi: 10.1016/j.landurbplan.2005.02.008

Škornik, S., Šajna, N., Kramberger, B., Kaligarič, S., Kaligarič, M., 2008. Last Remnants of Riparian Wooded Meadows along the Middle Drava River (Slovenia): Species Composition Is a Response to Light Conditions and Management. *Folia Geobotanica* 43, 431–445. doi: 10.1007/s12224-008-9024-7

Sluiter, R., de Jong, S.M., 2007. Spatial patterns of Mediterranean land abandonment and related land cover transitions. *Landscape Ecology* 22, 559–576. doi: 10.1007/s10980-006-9049-3

Šmilauer, P., 2007. Moderní regresní metody 1998–2007.

Stoate, C., Báldi, A., Beja, P., Boatman, N.D., Herzon, I., van Doorn, A., de Snoo, G.R., Rakosy, L., Ramwell, C., 2009. Ecological impacts of early 21st century agricultural change in Europe – A review. *Journal of Environmental Management* 91, 22–46. doi: 10.1016/j.jenvman.2009.07.005

Tilman, D., May, R.M., Lehman, C.L., Nowak, M.A., 1994. Habitat destruction and the extinction debt. *Nature* 371, 65–66. doi: 10.1038/371065a0

Turner, M.G., Ruscher, C.L., 1988. Changes in landscape patterns in Georgia, USA. *Landscape Ecology* 1, 241–251. doi: 10.1007/BF00157696

Vojta, J., 2007. Relative importance of historical and natural factors influencing vegetation of secondary forests in abandoned villages. *Preslia (Prague)* 223–244.

Vojta, J., Drhovská, L., 2012. Are abandoned wooded pastures suitable refugia for forest species? *Journal of Vegetation Science* 23, 880–891. doi: 10.1111/j.1654-1103.2012.01399.x

Vojta, J., Kopecký, M., 2006. Vegetace sekundárních lesů a křovin Doupovských hor. *Zprávy Čes. Bot. Společ.* 21, 209–225.

Wright, J.P., Fridley, J.D., 2010. Biogeographic synthesis of secondary succession rates in eastern North America. *Journal of Biogeography* 37, 1584–1596. doi: 10.1111/j.1365-2699.2010.02298.x

Zajíčková, L., 2009. Factors influencing woody species distribution in an abandoned landscape. Charles University In Prague.

Paper III



Hais, M.; Wild, J.; Berec, L.; Brůna, J.; Kennedy, R.; Braaten, J.; Brož, Z. (2016)

Landsat Imagery Spectral Trajectories — Important Variables for Spatially Predicting the Risks of Bark Beetle Disturbance

Remote Sensing 8: 1–22.

doi:10.3390/rs8080687

remote sensing

MDPI

Article

Landsat Imagery Spectral Trajectories—Important Variables for Spatially Predicting the Risks of Bark Beetle Disturbance

Martin Hais [1,*], Jan Wild [2,3], Luděk Berec [4], Josef Brůna [2,5], Robert Kennedy [6], Justin Braaten [7] and Zdeněk Brož [1]

1 Department of Ecosystem Biology, Faculty of Science, University of South Bohemia, Branišovská 31, České Budějovice 37005, Czech Republic; lairelosse@seznam.cz
2 Institute of Botany, The Czech Academy of Sciences, Průhonice 25243, Czech Republic; jan.wild@ibot.cas.cz (J.W.); josef.bruna@ibot.cas.cz (J.B.)
3 Faculty of Environmental Sciences, Czech University of Life Sciences Prague, Kamýcká 129, Praha 6—Suchdol 16521, Czech Republic
4 Department of Ecology, Institute of Entomology, Biology Centre CAS, Branišovská 31, České Budějovice 37005, Czech Republic; berec@entu.cas.cz
5 Institute for Environmental Studies, Faculty of Science, Charles University in Prague, Benátská 2, 12801 Prague 2, Czech Republic
6 College of Earth, Ocean, and Atmospheric Sciences, Oregon State University, 114 Wilkinson Hall, Corvallis, OR 97331, USA; rkennedy@coas.oregonstate.edu
7 Department of Forest Ecosystems and Society, Oregon State University, 321 Richardson Hall, Corvallis, OR 97331, USA; justin.braaten@oregonstate.edu
* Correspondence: martin.hais@seznam.cz; Tel.: +420-3-8777-2310

Academic Editors: Angela Lausch, Marco Heurich, Randolph H. Wynne and Prasad S. Thenkabail
Received: 30 May 2016; Accepted: 16 August 2016; Published: 22 August 2016

Abstract: Tree mortality caused by bark beetle infestation has significant effects on the ecology and value of both natural and commercial forests. Therefore, prediction of bark beetle infestations is critical in forest management. Existing predictive models, however, rarely consider the influence of long-term stressors on forest susceptibility to bark beetle infestation. In this study we introduce pre-disturbance spectral trajectories from Landsat Thematic Mapper (TM) imagery as an indicator of long-term stress into models of bark beetle infestation together with commonly used environmental predictors. Observations for this study come from forests in the central part of the Šumava Mountains, in the border region between the Czech Republic and Germany, Central Europe. The areas of bark beetle-infested forest were delineated from aerial photographs taken in 1991 and in every year from 1994 to 2000. The environmental predictors represent forest stand attributes (e.g., tree density and distance to the infested forest from previous year) and common abiotic factors, such as topography, climate, geology, and soil. Pre-disturbance spectral trajectories were defined by the linear regression slope of Tasseled Cap components (Wetness, Brightness and Greenness) calculated from a time series of 16 Landsat TM images across years from 1984 until one year before the bark beetle infestation. Using logistic regression and multimodel inference, we calculated predictive models separately for each single year from 1994 to 2000 to account for a possible shift in importance of individual predictors during disturbance. Inclusion of two pre-disturbance spectral trajectories (Wetness slope and Brightness slope) significantly improved predictive ability of bark beetle infestation models. Wetness slope had the greatest predictive power, even relative to environmental predictors, and was relatively stable in its power over the years. Brightness slope improved the model only in the middle of the disturbance period (1996). Importantly, these pre-disturbance predictors were not correlated with other predictors, and therefore bring additional explanatory power to the model. Generally, the predictive power of most fitted model decreases as time progresses and models describing the initial phase of bark beetle outbreaks appear more reliable for conducting near-future predictions.

The pre-disturbance spectral trajectories are valuable not only for assessing the risk of bark beetle infestation, but also for detection of long-term gradual changes even in non-forest ecosystems.

Keywords: forest disturbance; spectral trajectories; bark beetle; Landsat

1. Introduction

Forest disturbances caused by wind, fire and insects are prominent forces controlling forest ecosystem dynamics across the world [1]. Insect forest disturbances represent slower events relative to wind and fire, but have strong effects because of irreversible defoliation and subsequent dieback of mature trees [2]. Bark beetles are among the most common insect disturbance agents in temperate coniferous forests, affecting tens of millions of hectares in recent decades [3,4]. Moreover, the affected forest area is predicted to double in the next two decades because of climate change and cultivation of large areas of coniferous plantations outside their natural distribution [5]. Even though bark beetle disturbances are a part of the natural dynamics of coniferous forest [6–8] they also represent a significant threat for timber production and certain forest-provided ecosystem services [9]. Therefore, the need for both detection and prediction of bark beetle infestation is increasing.

Bark beetle outbreaks are commonly detected from satellite imagery using spectral indices, which are primarily based on differences and/or ratios between multiple spectral bands [10]. While the first studies of bark beetle infestation used changes in red and near-infrared (NIR) bands (i.e., normalized difference vegetation index (NDVI)), indices based on NIR and shortwave infrared (SWIR) have become the standard, mostly because of their greater sensitivity to forest canopy defoliation caused by bark beetle infestation [11]. The widely used Tasseled Cap (TC) linear transformation has three components: Brightness, Greenness, and Wetness [12,13]. Among these three components, Wetness is often used to identify bark beetle forest disturbances. It is a combination of all Landsat TM or Enhanced Thematic Mapper Plus (ETM+) spectral bands except the thermal band, with the greatest weight given to the SWIR channel (e.g., [14]).

While the use of remote sensing for detection of bark beetle infestation is well established, its application for prediction or risk assessment is rather rare [15–17]. Empirical bark beetle risk-assessment models commonly use environmental predictors including topography, climate, or soil types [18–20]. While these environmental predictors are important for bark beetle population dynamics and tree vitality, the forest stand attributes like structure, composition and spatial configuration have at least the same importance; however, they differ at various phases of infestation [16,21,22].

Information on tree vigor, which is the crucial factor shaping the risk of infestation, is usually missing in the standard forest inventory data. Earth observation imagery, specifically from the Landsat sensor family, can fill this lack of information by providing data on tree vitality and forest health status [23]. When analyzed as a time series, Landsat can provide information regarding pre-disturbance change events (e.g., windstorm) or gradual changes in forest vitality (e.g., soil depletion or air pollution), which increase the stand's vulnerability to bark beetle infestation [24–27]. Besides the tree to stand-level factors, the risk of bark beetle infestation is increased by large-scale drivers, which include climatic variables and/or landscape connectivity [28]. Most of these latter changes are well reflected in spectral indices and can be documented using multi-temporal remote sensing [29]. Free access to the Landsat data archive by the US Geological Survey (USGS) in 2008 accelerated the use of these data for multi-temporal change detection [30]. Subsequently, temporal segmentation algorithms and spectral trajectory processing tools like LandTrendr [31] and TimeSync [32] were developed to extract the main features (e.g., greatest disturbance segment, segment duration, and magnitude) from spectral time series trajectories. These approaches have enabled a wide use of Landsat data for broad scale ecosystem studies [33]. The use of spectral trajectories based on Landsat imagery helped to describe forest disturbance history since 1972 [34], encouraging forest recovery [35], and

detecting bark beetle-affected forest stands more precisely [36]. The following studies distinguished different defoliator and bark beetle effects [37], duration and severity of insect disturbances [38], and large-scale drivers of primary forest disturbance events [39]. A similar trajectory-based approach could be used to detect less pronounced pre-disturbance forest state changes which predispose the forest to disturbances [40].

We hypothesize that gradual changes in forest vitality significantly increase forest vulnerability to bark beetle infestation. Therefore our primary objective is to determine if pre-disturbance spectral trajectories are useful predictors of bark beetle infestation. In particular, we examine how explanatory and predictive power of models that include pre-disturbance spectral trajectories change relative to models in which these variables are excluded. For this purpose, we combine pre-disturbance predictors with environmental predictors in a logistic regression model combined with multimodel inference using several sets of models to assess the importance of pre-disturbance spectral trajectories.

2. Data and Methods

2.1. Study Area

The study area (1376 ha, centroid N 48°57.78435′, E 13°28.33847′) is located in the central part of the Šumava Mountains, in the border region between the Czech Republic and Germany, Central Europe (Figure 1). It is part of the Šumava National Park (Czech Republic) and is adjacent to the Bavarian Forest National Park (Germany). The dominant natural vegetation unit is Norway spruce forest (*Picea abies* L. Karst.) [41,42]. Where the area is not covered by forest, mostly peats and mountain meadows occur. The relief of the study area is created by a peneplain with numerous local hills. The elevation ranges from 700 m to 1453 m with an average elevation of 1093 m.

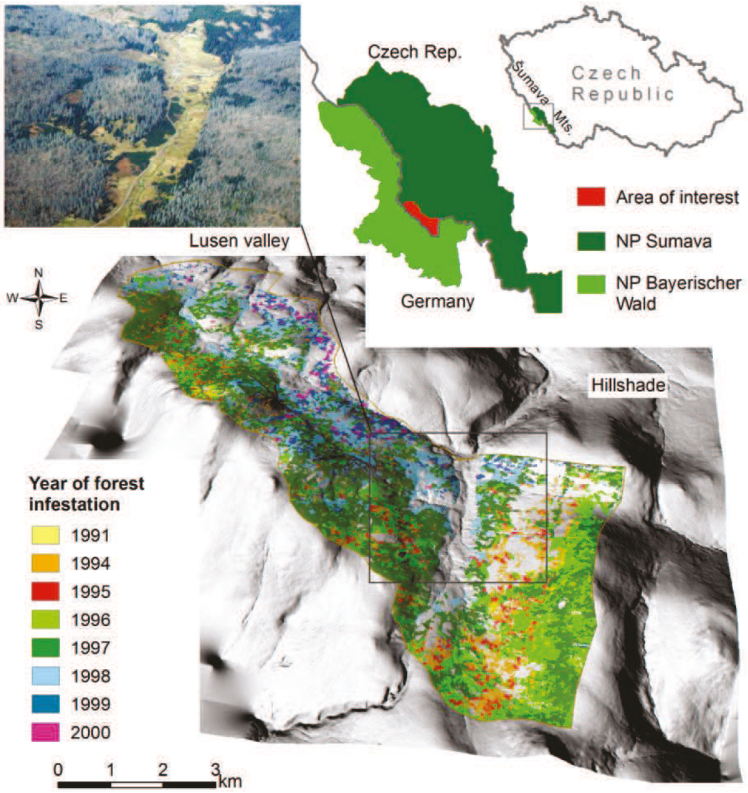


Figure 1. Study area located in the Šumava Mountains, Czech Republic–Germany border region.

Over the last 25 years, several outbreak waves of the European spruce bark beetle (*Ips typographus* L.) have caused extensive spruce forest dieback in this area. The outbreak originated in wind-fallen

trees (173 ha) in 1983 and 1984, following two windstorms in the western part of the Bavarian Forest National Park. These fallen and heavily damaged trees provided suitable conditions for the start of the outbreak [43,44]. At the beginning of the 1990s the first infested trees occurred in the Czech region. Because of the subsequent bark beetle dispersal, the Šumava NP administration applied two management approaches to the infested forests in 1995: (1) a small portion of the stands in the core zone was left unmanaged (more than 2.000 ha); and (2) the stands in the surrounding buffer zone were cut to prevent the spread of bark beetles. We analyzed the area in the unmanaged zone where we expect a dominant role of natural predictors of tree infestation. The bark beetle infestation accelerated between 1995 and 1997 when the largest area in the central part of Šumava Mountains was affected [45]. By the end of the year 2000, most of the spruce stands lost all canopy trees and only small patches of living trees persisted, mostly near peat bogs or at forest edges. After the main dieback in the study area the forest regenerated successfully towards a natural mountain spruce forest [46,47].

2.2. Aerial and Satellite Data

Groups of trees infested by bark beetle (grey-attack stage) were delineated from ortho-rectified aerial photographs, which were acquired in 1991 and every year for the period 1994–2000. The smallest polygon was defined as a group of five adjacent dead trees (0.03 ha). Simultaneously, living spruce forest, clear-cuts and non-forest areas (meadows, peat-bogs) were also delineated. To avoid their influence on values of mixed pixels, we excluded all pixels up to 100 m to clear-cuts and non-forest areas. The resulting land cover polygon layers were transformed to UTM Zone 33 North coordinate system and overlaid on a 30 m $\times$ 30 m grid to make them compatible with Landsat imagery. Pixels were defined as declined when the dieback was higher than 50% of its area. We used 16 Landsat TM images from 1984 to 1999 (Table 1). For some years (1988, 1994), multiple images were used to cover no data areas because of clouds and their shadows. To avoid phenological differences among the images, only data acquired during the high summer season were used (nominally July and August with an exception in 1999). The imagery was obtained from the USGS data archive (glovis.usgs.gov). All images were radiometrically normalized to a common image (acquired on 4 August 1990) using the MADCAL approach of Canty et al. [48], following Schroeder et al. [49].

Table 1. List of Landsat TM5 images (path 192, row 25).

Acquisition Date
3 August 1984
9 August 1986
11 July 1987
6 August 1988
5 July 1988
8 July 1989
4 August 1990
7 August 1991
9 August 1992
31 August 1994
14 July 1994
30 July 1994
1 July 1995
7 August 1997
10 August 1998
14 September 1999

2.3. Spectral Trajectories

Based on the study of Hais et al. [40], which shows the potential of spectral trajectories to describe forest vigor decline before bark beetle infestation, we used this approach to test the significance of these predictors for modelling bark beetle infestation risk. The abovementioned approach uses linear

regression to fit multi-temporal spectral data. In our study, we consider all three TC components (Wetness, Brightness and Greenness), though mainly Wetness and Brightness have been shown as the appropriate multi-spectral vegetation indices to describe forest structure [50] and forest health in relation to insect disturbance [14,51–53]. To obtain the pre-disturbance spectral trajectories, we calculated the linear regression slope of each TC component from 1984 to one year before the year for which the model was calibrated. The slope was calculated for each 30 m × 30 m pixel except those already infested in previous years. Slopes for non-affected stands were calculated from the same years as the affected ones in the one-year model. An example of Wetness slope is shown in Figure 2. These slopes, which represent historical stand condition (e.g., stress, stability, growth), were included as a model predictor together with commonly used environmental predictors in models of bark beetle infestation risk.

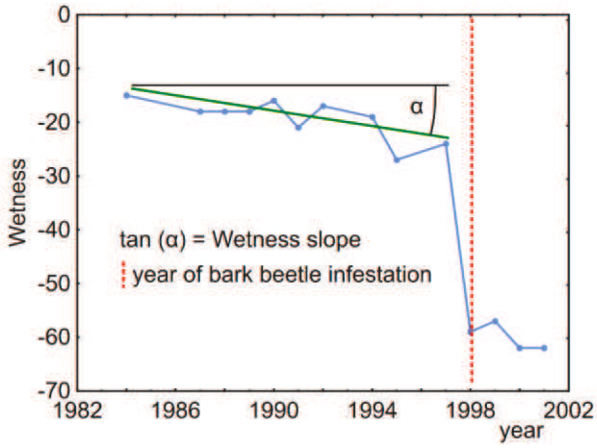


Figure 2. Spectral trajectory of Wetness TC component in a given pixel calculated as the slope of linear regression of Wetness for consecutive years from 1984 to one year before the year for which the model was calibrated. Slope was calculated for both infested and non-infested pixels; the infested one is shown as an example.

2.4. Environmental Predictors of Bark Beetle Infestation

Despite a large amount of environmental predictors tested for the risk of bark beetle infestation [19,21], we selected representatives of each group (see Table 2) to cover all types of possible influences. Forest stand susceptibility to bark beetle infestation is determined by forest condition itself or abiotic environmental factors, which in turn influence forest vigor. One of the most significant forest attributes for bark beetle dispersal is distance to the nearest infested forest [21]. Despite just 100 m buffer zones of forest in each year, it is still possible to test the distance to the nearest declined forest inside these buffer zones. In addition, we tested the direction to the nearest declined forest in the previous year. The direction azimuth value was transformed to eight 45° wide classes (N, NE, E, ES, S, SW, W and NW). Distance to the nearest clear-cut area and distance to the nearest natural forest edge were taken as a static variable from aerial photograph acquired in 1991. We hypothesize that the clear-cut edges might ease the entry of bark beetles into the stand while the natural forest edges represent a physical barrier for the beetles. Moreover, the trees in forest edge adjacent to clear-cut may suffer from water stress due to higher amount of solar radiation [20,54]. The degree of forest "naturalness" was calculated as a difference between current forest inventory and potential natural tree species composition [55], derived from modified Czech typological maps (natural forest types [56]), which followed a similar concept as potential natural vegetation [57]. Stand age represents an important attribute and we used age of dominant (>50%) tree layer because bark beetles preferentially attack trees older than 60 years [44]. If any tree layer does not reach 50%, we calculated age as a mean value from the first and second dominant tree layer age. Similarly, the dominant tree layer was used for

determining the tree density. In fact, there was mostly one dominant tree layer and one small layer of young trees. Soil is characterized by edaphic category, using the Czech typological system. It combines soil texture, nutrient richness and soil moisture [58]. The age, tree density and edaphic category are from the Forest Management Institute (FMI) database (www.uhul.cz). The geology parameters are from Czech Geological Survey maps (www.geology.cz). We calculated the distance to two merged geological classes (7th moor, peat and 8th sediment), because we anticipated that the distance to these geology classes reflect wet or aquatic conditions or water supply. Altitude and other topographic variables were derived from a digital elevation model (DEM) with high spatial resolution (5 m) and vertical error of 1 m (DMR 4G from ČÚZK, www.cuzk.cz). We have used the heat load index (HLI) which describes the variation in potential solar radiation and increasing temperature on SW slopes [59], and the area solar radiation (ASR12), which is a cumulative value of potential solar radiation for entire year (watt hours per square meter—Wh/m^2) with maximum value on south slopes. Topographical wetness index (TWI), reflecting potential wetness was calculated using SAGA GIS 2.1.0. We expect that water availability may positively influence the tree resistance against the bark beetle infestation.

Table 2. List of predictors for bark beetle infestation including pre-disturbance indices describing forest susceptibility and predictors of bark beetle dispersal.

Variable Name and Description	Abbreviation	State	Units	Data Source
Forest structure				
Distance to the nearest infested forest in the previous year	Dist-source	dynamic	(m)	map of land cover
Direction to the nearest infested forest in the previous year	Dir-source	dynamic	8 classes	map of land cover
Distance to the nearest clear-cut	D-clear-cut	static	(m)	map of land cover
Distance to the natural non forested area	D-natur-edg	static	(m)	map of land cover
Degree of naturalness of forest stand	Dg-natur	static	6 classes	[55,60]
Age of dominant tree layer	Age	static	years	FMI database
Tree density of dominant tree layer	Density	static	trees no./ha	FMI database
Pedology and geology				
Edaphic category	Edaphic	static	11 classes	FMI database
Distance to wet or aquatic conditions	Geol-wet	static	(m)	Geological map
Topography and climate				
Altitude	DEM	static	(m)	DMR 4G DEM
Heat load index	HLI	static	unitless	DMR 4G DEM
Area solar radiation for entire year	ASR12	static	Wh/m^2	DMR 4G DEM
Topography wetness index	TWI	static	unitless	DMR 4G DEM
Pre-disturbance forest conditions				
Slope of Brightness index	Bright-sl	dynamic	unitless	Landsat imagery
Slope of Wetness index	Wet-sl	dynamic	unitless	Landsat imagery
Slope of Greenness index	Green-sl	dynamic	unitless	Landsat imagery

2.5. Statistical Models

Bark beetle dispersal results in gradual infestation of adjacent stands from year to year, which carries the possibility of changes in predictor significance during the outbreak period [21]. To assess predictor significance changes, we built an individual statistical model of bark beetle infestation for every year within the studied period. The model for a given year included declined and living forest

limited by the 100 m buffer zone around declined forest in the previous year because more than 90% of affected trees for every year were located in this zone. Because of gaps in data on bark beetle dispersal for 1992–1993, we used a 250 m buffer zone between the years 1991 and 1994.

To assess if pre-disturbance spectral trajectories improve the ability of a model to predict bark beetle infestation, we first composed a maximum model that contains all environmental variables plus all spectral trajectories (slopes). We used the square root transformation of the ASR12 variable to get values comparable in order to those of the other variables. To assess potential collinearity between any of the candidate predictors, we looked at the correlations between all combinations of variable pairs, as well as variance inflation factors (VIFs), calculated from the *corvif* function, which quantifies the severity of multicollinearity [61]. The highest correlation we found was between Brightness and Greenness slopes, ranging between −0.89 and −0.97 for various years. Also, Greenness slope achieved the highest VIF value every year, ranging between 80 and 130, but reaching as high as 430 in one year. A strategy to avoid multicollinearity is to remove the predictor with the highest VIF value and recalculate the VIFs, repeating this process until all VIFs are smaller than a threshold value commonly set to 3–10 [61]. Both approaches suggest removing Greenness slope from our subsequent analyses. Doing this, maximum observed correlations between any two remaining variables reach 0.6–0.7, and all VIFs are mostly below 3, with one or two VIFs reaching 3.1–3.5 in some years. Thus, except for Greenness slope, we keep all explanatory variables for the subsequent statistical modeling.

Since we fix three explanatory variables as mandatory parts of any model (DEM, Dist-source, ASR12), 12 other explanatory variables are left as candidate predictors. From the previous analyses we found that these three variables have relatively stable contribution to the models across years. While the DEM has relatively low importance, the latter two variables played dominant roles for models. Because these variables do not show any trend between the years, we decided to fix them. Using the all-subset approach, we investigate the effect of the pre-disturbance variables by running a total of $M = 2^{12} = 4096$ candidate models.

Since our response variable is binary (30 m × 30 m forest on pixel is declined or not), we use binary logistic regression for fitting a regression curve. Our data for years 1995 and 2000 suffer from the problem of complete separation, meaning that a predictor or a subset of predictors is associated with only one outcome value when the predictor is greater than a threshold. This occurs commonly in small data sets when an event is rare, and this is also the case here. To cope with this, we use the Bayesian generalized linear model approach (*bayesglm* function) implemented in the library *arm* in the statistical software R version 3.1.1 [62,63]. We used the default procedure settings, i.e., an independent Cauchy prior distribution for the model coefficients.

2.6. Multimodel Inference

Because of high uncertainty in model selection (several candidate models or even several dozens of candidate models may describe data similarly well), we used the multimodel inference method as a basis for investigating explanatory and predictive performance of the considered model variables. In this approach, inference is based not on one, but several models in the candidate set [64–66]. In particular, the Akaike information criterion (AIC) is calculated for each model in the candidate set (we actually calculate AICc, since our sample sizes are relatively small) and these models are ranked according to their Akaike weights, defined for a model i as:

$$w_i = \frac{\exp\left(-\frac{1}{2}\Delta\mathrm{AIC}\,(\text{model } i)\right)}{\sum_{k=1}^{M}\exp\left(-\frac{1}{2}\Delta\mathrm{AIC}\,(\text{model } k)\right)}$$

In this formula, ΔAIC is the difference between AIC of the model with the minimum AIC value and AIC of each respective model. The Akaike weight w_i expresses the likelihood that the model i is the best approximating model [66]. We note that AIC (and any of its variants) provides only a relative measure of how good a model is, given the data and the candidate model set.

The Akaike weights allow estimating relative importance of every predictor variable in the full model by summing the Akaike weights for each model in which an individual variable occurs [64,66]. We calculated this for all predictor variables, including with and without the pre-disturbance Wetness and Brightness slopes, allowing assessment of importance of the remote sensing predictors relative to the environmental variables. Similar to the Akaike weight, this relative importance (or predictor weight) can be interpreted as equivalent to a likelihood that the respective variable is a part of the best model [64,66].

We conducted the above-described procedure for four nested model groups. The first group consists of all *M* candidate models (full model set). The second group consists of all candidate models in which the predictor variable Brightness slope is absent and the only candidate pre-disturbance predictor is the Wetness slope (Wetness slope model set). Similarly, the third group consists of all candidate models in which the Wetness slope is absent and the only candidate pre-disturbance predictor is Brightness slope (Brightness slope model set). Our final set of models did not contain any pre-disturbance variable (plain model set). We used these four model sets to assess predictive importance of the Wetness slope and Brightness slope variables. All calculations involving multimodel inference were performed using the R package *MuMIn* [67].

2.7. Predictions

From each of the four model sets (the full, Wetness slope, Brightness slope and plain model sets), candidate models with the highest Akaike weights (with summed Akaike weight of at least 0.95) were selected. These were then used to predict probability of bark beetle attack in the years different from those for which the models were fitted. This was done to assess whether models fitted for a specific year in the outbreak cycle could be used to predict dynamics of the bark beetle attack in its other part of the cycle or how robust the fitted models are across the outbreak. These "best" model sets contained tens of candidate models, as opposed to thousands of models in the original model sets. We used models fitted for the year F (referred to as F-models) to calculate probability of bark beetle attack in the year P (referred to as P-predictions) as follows. Any F-model was used individually to calculate P-predictions, using data from the year P as its "validation" data. These individual P-predictions were then averaged, weighting specific P-predictions by the respective F-model Akaike weights [64,66].

Binary logistic regression models allow modeling binary responses (presence/absence of infestation) by linear regression via a logistic link function. As such, they can predict the probability of infestation, which can then be classified into two discrete classes choosing a probability threshold [15]. Receiver Operating Characteristics (ROC) curves are a way of evaluating such binary models, since they are threshold-independent [68,69]. The area under the ROC curve (AUC) is often taken as a typical performance measure for a binary response variable since it provides a single measure of classification accuracy [68,69]. We quantified a predictive power of our model-averaged predictions using the ROC curves and AUC values. In particular, to assess an impact of considering the pre-disturbance spectral trajectories for making predictions, we statistically tested the null hypothesis that relevant pairs of the ROC curves (e.g., when both pre-disturbance variables are used vs. only one such variable is used) are statistically insignificant. We used the R package *pROC* [70] for calculating the ROC curves, AUC values, and statistical differences between any two ROC curves.

3. Results

3.1. Pre-Disturbance Forest Condition

Both pre-disturbance predictors Wetness slope and Brightness slope show a similar spatial pattern (Figure 3). The spatial variability of both of these predictors is quite high and the slope values vary from negative to positive, with a clear spatial autocorrelation. Except for the highest Wetness slope and Brightness slope in affected stands at the beginning of the outbreak relative to latter years of infestation [40], the most obvious observation here is that the slopes of both indices vary most near

non-forested areas (Figures 3 and 4). While values of the Wetness slope decrease near clear-cuts and locally increase near natural non-forested areas, the Brightness slope values demonstrate quite opposite behavior (Figures 3 and 4). Its values increase near clear-cuts and decrease near natural non-forested areas. Still, the correlation between Wetness and Brightness slopes is not that high ($r = -0.54$). The linear regression of Wetness from 1984 to 1994 has mean values of coefficient of determination for pixels with affected forest higher ($R^2 = 0.35$; SD 0.32) than pixels with unaffected forest until 1994 ($R^2 = 0.17$; SD 0.33). Similar results show the linear regression of Brightness from 1984 to 1994 for affected forest, which has higher coefficient of determination ($R^2 = 27$; SD 0.37) than unaffected ($R^2 = 0.14$; SD 0.38). More detailed information about the linear fitting of pre-disturbance trajectories in our study area is given in [40].

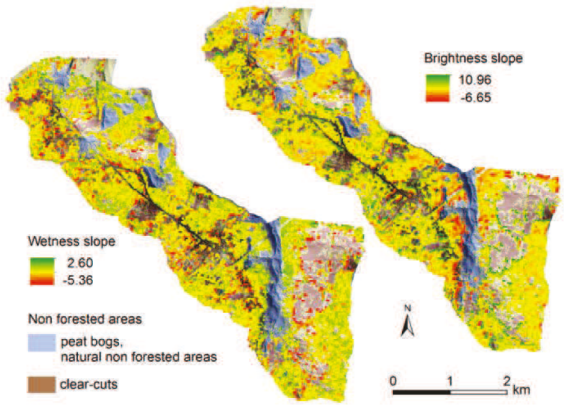


Figure 3. Spatial distribution of Wetness slope and Brightness slope values. Similar to Figure 2, the pixel values were calculated as the slope of linear regression of Wetness/Brightness for consecutive years from 1984 to one year before the year for which the model was calibrated. The maps are composed from pixels combined among all evaluated years (1994–2000) according to the year of bark beetle infestation. The lowest Wetness slope values and highest Brightness slope values are mostly adjacent to clear-cuts, while the slope values in the vicinity of natural non-forested areas show opposite behavior, especially in the Lusen valley.

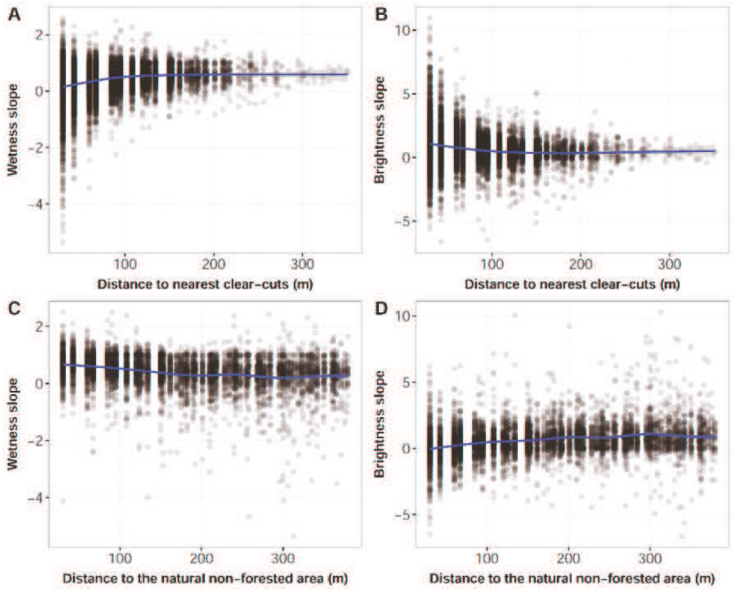


Figure 4. Wetness slope and Brightness slope values as they vary with distance to the nearest clear-cuts (**A**,**B**) and natural non-forested areas (**C**,**D**). The trend (blue line) of slope among distances is visualized using local polynomial regression (loess) ±1 standard error mean (grey area).

3.2. Predictors of Bark Beetle Infestation

Statistical modelling based on the all-subsets approach and multimodel inference suggests that when both pre-disturbance predictors are taken into account, Wetness slope is an important variable to be considered for understanding the bark beetle infestation patterns (Table 3). Conversely, the likelihood that Brightness slope is a part of the best model is often as low as 0.3 (Table 3). In addition, whereas the high importance weights of Wetness slope are relatively stable over the years (with the exception of 2000), the Brightness slope weights show an increase in the years 1994–1996 and then a steady decline to lower values ($\geq$0.28, see Table 3). The weights of other environmental predictors show relatively high variability over the years. However, similar to the pre-disturbance predictors, we recognize two basic trend-groups (Table 3). One group of predictors has a relatively high weight in the initial years of bark beetle infestation, while gradually losing weight towards the last modelled year. This group includes the edaphic category, which has high weight values until 1998 (with the exception of 1995); heat load index (HLI) and distance to wet or aquatic conditions (Geol-wet) show similar trends. The second group of predictors (TWI, AGE, and Dg-natur) reach the highest importance weights in the middle of bark beetle outbreak (1996–1997) when the largest forest areas are declined in our study area [45]. A special case of the opposite trend is represented by distance to clear-cut (D-clear-cut), which has the highest weights at the beginning and the end of the outbreak. The remaining predictors show somewhat fluctuating weights over the years.

To examine how explanatory power of models that include our two considered remote sensing variable changes relative to models in which one of these variables is excluded, we repeated the above analysis considering all environmental predictors but only with either Wetness or Brightness slope. With just Wetness slope (i.e., without Brightness slope), its importance weight and those of all environmental variables remained virtually unchanged (compare Table 3 and Table A1). On the contrary, with just Brightness slope (i.e., without Wetness slope), its importance weight increased in several years (1994, 1996), but decreased in other ones (1995, 1997; compare Table 3 and Table A2). These changes in the Brightness slope importance weights were accompanied by changes in the HLI importance weights. In particular, the HLI importance weight generally increased, with the highest increase in the years 1996 to 1998 being in the range of 10% to 20%. Similar importance weight changes were observed when the results based on the Wetness model set were compared with those based on the plain model set (high importance of Wetness slope; Table A3), and when the results based on the Brightness model set were compared with those based on the plain model set (low to medium importance of Brightness slope; Table A3).

Table 3. Predictor importance weights based on multimodel inference when both pre-disturbance indices are used as predictors. The darkest/lightest green show the highest/lowers predictor importance weights.

Year	Wet-sl	Bright-sl	Dir-Source	D-Clear-Cut	D-natur-Edge	Dg-Natur	AGE	Density	Edaphic	Geol-Wet	HLI	TWI	Legend
1994	0.93	0.38	1	1	0.96	0.53	0.65	0.36	1	0.98	1	0.62	≤0.2
1995	0.81	0.57	0.09	0.33	0.53	0.56	0.36	0.48	0.01	0.42	0.84	0.62	0.21–0.40
1996	1	0.86	0.07	0.32	1	1	0.61	0.3	1	1	0.7	1	0.41–0.60
1997	1	0.54	0.95	0.45	0.29	1	1	1	1	0.53	0.74	1	0.61–0.80
1998	1	0.27	1	0.26	1	0.3	0.3	0.37	0.99	0.29	0.54	0.61	0.81–1.00
1999	0.99	0.28	0.45	0.68	0.4	0.86	0.31	0.93	0.47	0.48	0.29	0.3	
2000	0.26	0.28	0.01	0.95	0.32	0.38	0.26	0.32	0.01	0.37	0.66	0.43	

3.3. Model Predictions

We assessed the predictive power of our fitted models by calculating the ROC curves and the corresponding AUC values for all years except the training year of the model. Regardless of the modelling scenario used, the trend is quite similar. Table 4 shows the results of models including both Wetness and Brightness slope. Generally, the predictive power of most fitted models decreases as time progresses. Further, models fitted at the beginning of bark beetle outbreak have higher predictive power than models fitted after outbreak culmination. The models describing an initial phase of bark beetle outbreaks thus appear more reliable for conducting near-future predictions. The higher predictive power of a few models for the year 2000 breaks this rule, but at the end of outbreak, reliability of models somewhat decreases because of low sample size.

Table 4. Ability of fitted full models for each individual year (rows) to predict bark beetle forest infestation in the years 1994 to 2000 (columns), except the same year for which the model was fitted, evaluated using AUC. Higher AUC values mean higher predictive power of the respective models; value 0.5 represents random prediction.

		Years of Prediction							Legend
		1994	**1995**	**1996**	**1997**	**1998**	**1999**	**2000**	
Years of Model Fit	**1994**	-	0.76	0.75	0.66	0.49	0.50	0.62	≤0.5
	1995	0.79	-	0.77	0.71	0.60	0.52	0.47	0.51–0.60
	1996	0.81	0.83	-	0.73	0.54	0.51	0.66	0.61–0.70
	1997	0.73	0.75	0.79	-	0.65	0.57	0.53	0.71–0.80
	1998	0.65	0.68	0.63	0.69	-	0.57	0.76	0.81–0.90
	1999	0.69	0.62	0.63	0.67	0.65	-	0.82	
	2000	0.70	0.66	0.63	0.67	0.65	0.65	-	

Inclusion of the pre-disturbance indices generally increases model predictive power (Table 5). Although the improvement may seem marginal, it is statistically significant in many cases (Table A4). Interestingly, an increase is generally higher with backward prediction (Table 5, values below the diagonal) than forward one (Table 5, values above the diagonal). Differences in Table 5 would not change much if we replace the plain model set with the Brightness model set. On the other hand, if we consider differences between AUC values corresponding to the full model set and the Wetness model set, they are all virtually zero and statistically insignificant. This also suggests that with respect to the model predictive power, the Wetness slope plays a more important role than the Brightness slope.

Table 5. Difference between AUC values corresponding to the full model set (with both Wetness and Brightness slopes) and the plain model set (with no remote sensing variable).

		Year of Prediction						
		1994	**1995**	**1996**	**1997**	**1998**	**1999**	**2000**
Year of Model Fit	**1994**	-	0.01	0.01	0.02	0.01	−0.01	−0.04
	1995	0.03	-	0.02	0.02	0.03	−0.01	0.01
	1996	0.04	0.01	-	0.01	0.01	0.01	−0.02
	1997	0.06	0.04	0.03	-	0.02	0.03	0.03
	1998	0.06	0.07	0.05	0.01	-	0.12	0.02
	1999	0.10	0.06	0.06	0.02	0.02	-	−0.02
	2000	0.00	0.00	0.00	0.00	0.00	0.00	-

4. Discussion

4.1. Spectral Indices Reflecting the Forest Health Change

Our results clearly demonstrate that long-term changes of TC Wetness and Brightness are related to the probability of bark beetle infestation during outbreak. This corroborates our hypothesis that bark beetles preferably affect the weakened forest stands, and that these changes in forest health or tree vigor are detectable in spectral signal change. In general the nature of spectral signal change is connected with the tree defoliation [37], chlorophyll fluorescence change and/or water content decrease in needles due to water stress [71]. This spectral change is well detected in NIR and SWIR spectral region [11]. In particular the SWIR-based indices (NDMI, Wetness, Brightness, NBR) are often used to assess change in forest health due to acid rain [72], defoliation following insect attack (e.g., [51]), or forest mortality (e.g., [73]). For this study, we selected Wetness and Brightness indices. These two indices show almost opposite behavior in reaction on forest decline [45]. In contrast, some authors have reported success using NIR-based indices. For example, Senf et al. [37] found stronger association of spruce budworm disturbance with Greenness than two other TC indices. However, the same study describes the highest sensitivity of Wetness and Brightness to mountain pine beetle disturbance. We removed Greenness early during our statistical analysis due to correlation and collinearity. Moreover, previous results from the same study area [45] support this removal, because they showed the inconsistent response of Greenness to the forest decline, when the magnitude of change was lower and the values changed with delay after forest decline. A possible reason could be the variability in understory composition; a dying canopy may uncover either soil and litter, or a green shrub/herbaceous layer. The sensitivity in spectral response to these contrasting cover types may be greater in Greenness than Wetness or Brightness and lead to inconsistent spectral-temporal trends associated with infestation-related tree mortality.

Further understanding of ecological processes underlying changes in Wetness and Brightness can be inferred from index trends we observed near forest edges. The decrease of Wetness and increase of Brightness and/or high variability of both predictors near clear-cuts may be related to water stress due to higher amount of solar radiation, particularly in southern and western forest edges [20,54]. Similar results were reported by Dantas de Paula et al. [74] in a Landsat-based study, where the tree cover variation increases towards the forest edge. The authors suggested the underlying causes for this variability to be degradation debt, hyperdynamism and environmental factors (topography, soil conditions etc.). In contrast to clear-cuts, the natural forest edges do not show obvious change of variability in the pre-disturbance indices. Nevertheless, some of these edges have higher Wetness slope values than do areas inside the forest. This effect is pronounced at the margin between forest and meadows (e.g., Lusen valley), where the high canopy closure protects the soil against drying, or denser canopies may serve as a physical defense to bark beetle infestation.

4.2. Pre-Disturbance Forest Conditions

If the trend in both indices indicates changes in forest health status or stand vigor, we should be able to describe their main causes. One of the strongest factors responsible for forest decline in Central Europe and North America in the second half of the last century was anthropogenic air pollution causing acid deposition. Even though the Šumava Mountains do not belong to the most heavily polluted areas in Czech Republic (e.g., the "black triangle" in northern Czech Republic with large historical forest decline), there is evidence from ground observations of forest decline due to air pollution in the last century [75,76]. Other retrospective methods suggest the consequences of acid deposition on forest health can be still recognized. Šantrůčková et al. [76] found a proportional relation between Δ ^{13}C in tree rings and soil acidification (pH decrease). Polák et al. [77] describe tree defoliation followed by crown regeneration using secondary shots that were detectable even after 30 years. It is therefore likely that multi-temporal imagery captures this forest health decline due to acid deposition, which is in concordance with results reported by Rock et al. [72]. Another possible

long-term stress factor in the Šumava Mountains is stand damage due to repeated windstorms or snow [7]. The repeated windstorms may damage the tree roots and cause tree vigor decrease. Drought is another possible long-term factor [28], and its role probably increases during bark beetle infestation.

All the aforementioned factors may reflect the spatial variability resulting from climate and topography differences from local to regional scales. Even though some studies mention no significant relation between forest health and bark beetle attack (e.g., [78]), Bytnerowicz et al. [79] suggested that long-term elevated levels of atmospheric N and S depositions and elevated O^3 predispose trees to insect attacks and other stresses.

4.3. Spectral Trajectories

The use of linear regression for Wetness and Brightness fit impose simple trends over time. This assumption is consistent with results of Hais et al. [40], who reported lower Wetness slope values in the first years of the bark beetle outbreak in comparison to latter years, which were more stable. This suggests that the initial bark beetle attack occurred in the most vulnerable stands that show long-term Wetness/Brightness change before the disturbance. Nevertheless, the resulting spectral trajectory may be influenced by other factors, which can act antagonistically. While long-term stress factors decrease Wetness values (or increase Brightness) over time, canopy growth may support an opposite trend, in particular for fast-growing tree species. For example, partial forest defoliation may result in small spectral change, which is quickly followed by spectral recovery after disturbance [37,38]. Similarly, forest thinning is reflected in Wetness change [16] when the values first decrease due to lower canopy closure (and higher role of ground cover in the spectral signal), but after several years, the values increase due to faster tree growth [16]. Users should therefore be careful when using these indices in managed forests. Additionally, recent forest history often includes high magnitude changes that are not always linear in their spectral-temporal response. Because of this complexity, the non-linear fit of spectral trajectory is often needed to describe forest history for a given pixel [35]. Nevertheless, much easier interpretable linear fits are valuable for description of many long-term processes with unaltered trend like gradual systematic change in natural vegetation communities [80]. Similarly we used the linear fit to describe pre-disturbance forest condition assuming it mostly follows simple trend. However, to avoid complexity in the course of spectral-temporal response we use just forest pixels without any type of disturbance during assessed pre-disturbance time.

4.4. Risk of Bark Beetle Infestation and Model Predictions

Among all predictors used in our study, Wetness slope provided the greatest improvement of bark beetle infestation risk modelling, while Brightness slope was a significant predictor only for a few years. Moreover, Wetness slope and Brightness slope are not correlated with the environmental predictors, and thus are able to explain additional observed variability. The Landsat spatial resolution (30 m) provides a good dataset to describe the spatial variability on a stand level. Relatively low weights of importance for some environmental variables may be caused by the small dataset, especially when the spatial resolution of the data is relatively coarse and/or the predictor is categorical. This may be the case for very low weights of broad edaphic categories in models for years 1995 and 2000 (lowest number of cases), which are high in other years. This limitation has lower importance for continuous variables like pre-disturbance indices. This supports the potential of the Landsat data for local to global-level modelling in general. In agreement with Lausch et al. [21], we conclude that the importance of individual predictors changes during the bark beetle infestation. The predictors with the highest model weights (edaphic category, Geol-wet, HLI) in the first years of the bark beetle outbreak document the selective infestation of the most susceptible forest stands. The selective infestation is critical until bark beetle population size reaches the threshold where tree defense is overwhelmed [78]. After successful selective infestation, bark beetle propagation produces population sizes so great that selective behavior is an unnecessary strategy to seize trees, which shifts increased importance to other predictors. This was demonstrated in 1997, when the largest forest area was affected, and tree-related

predictors had the highest weights (age, density, DG-natur). The trees were probably more susceptible individually, reflecting stand structure and not the environment predictors as in the beginning of the bark beetle outbreak. The decrease in almost all predictor weights further into the future, shows that the high bark beetle density led to random-like infestation, where the beetles were able to overcome any tree's defense. The predictor D-clear-cut has high importance in the first and last years of bark beetle outbreak, which might be connected with low bark beetle numbers in both periods and need for selective behavior.

Predictive power of our fitted models (including all predictors) calculated using ROC curves and corresponding AUC values was quite similar. The high AUC values when data were used for fitting and also for prediction (0.76–0.91) documented reasonably good fit to the data, when assessed using AUCs. The decrease of predictive power in fitted models over the years documents not only the general decrease of fits to the distant years, but it also supports the explanation of predictor importance changes during a bark beetle outbreak [21]. Moreover, the slower decrease of predictive power (higher predictive power for distant years) for models fitted at the beginning of the bark beetle outbreak nicely corresponds with the hypothesis that at the beginning of the bark beetle outbreak beetles are more selective, while later, when beetle densities rise and/or the most susceptible stands are already destroyed, beetles need to be more opportunistic.

5. Conclusions

Using pre-disturbance slopes of Tasseled Cap components Wetness and Brightness, spectral trajectories improved our understanding and prediction of bark beetle infestation. Linear regression slopes of these two variables calculated for the time period before the disturbance significantly increase the predictive power of bark beetle infestation models from year to year and even for longer predictions. Moreover, these predictors were not correlated with environmental predictors and therefore are able to explain additional observed variability. This also suggests that long-term gradual decrease of forest vitality significantly increases forest vulnerability to bark beetle infestation. When comparing the importance weights of both pre-disturbance predictors, the Wetness slope weights are high and relatively stable over the years (with the exception of 2000), while the weights of Brightness slopes show an increase only in the middle of the bark beetle outbreak (1996) and steadily decline to low values. We distinguished two components of relationship between these two indices and tree susceptibility to bark beetle infestation. First, they reflect long-term stress factors (acid deposition, drought, snow, windstorms). The second component is their change near forest clear-cuts edges. This probably relates to higher solar radiation at open edges or other disturbances caused during the clear-cut.

We have also identified two groups of environmental factors important for prediction of bark beetle infestation risk. The first group has high importance weights in the initial years of the outbreak (edaphic category, distance to aquatic conditions, heat load index), which might be connected with high pest selectivity for the most susceptible stands. The second group of tree-related predictors has the highest weights in the middle of the outbreak, when the largest forest area was affected, and the pest numbers were highest (age of dominant tree layer, tree density of dominant tree layer, Distance to the natural non-forested area). The first can be used to identify potentially vulnerable areas, and the second for predicting bark beetle spread after the initial phase of infestation.

But forest ecosystems also face long-term, gradual changes due to hidden stress factors that contribute to their vulnerability and susceptibility to bark beetle infestation. And this is where non-correlated pre-disturbance spectral trajectories, based on Landsat data with its vast and accessible archive, can really help.

Acknowledgments: The work was supported by COST LD 15158 and was part of long-term research development project No. RVO 67985939. We thank Zdeňka Konopová for help with vectorization of land-cover units from aerial photographs, Karel Matějka for data support, Stanislav Grill for discussions focused on insect forest disturbance and four anonymous reviewers for helpful comments.

Author Contributions: Martin Hais conceived the general idea of the paper, processed satellite data, made GIS analyses and wrote the manuscript. Jan Wild authored ecological interpretation of modelling results. He wrote the manuscript and analyzed the GIS data. Luděk Berec performed the main statistical analyses and wrote the manuscript. Josef Brůna processed the GIS data and wrote the manuscript. Robert Kennedy formed the idea of pre-disturbance spectral trajectories and supervised the manuscript writing. Justin Braaten made the radiometric normalization of the Landsat imagery, wrote and corrected the manuscript. Zdeněk Brož performed the aerial images rectification, delineated the trees affected by bark beetles and calculated some of the environmental variables.

Conflicts of Interest: The authors declare no conflict of interest. The founding sponsors had no role in the design of the study; in the collection, analyses, or interpretation of data; in the writing of the manuscript, and in the decision to publish the results.

Appendix A

A1. Predictor Importance Weights

Table A1. Predictor importance weights based on multimodel inference when only the Wetness slope is used with the environmental predictors. The darkest/lightest green show the highest/lowest predictor importance weights.

Year	Wet-sl	Dir-Source	D-Clear-Cut	D-Natur-Edg	Dg-Natur	AGE	Density	Edaphic	Geol-Wet	HLI	TWI	Legend
1994	0.99	1.00	1.00	0.96	0.52	0.65	0.36	1.00	0.98	1.00	0.62	≤0.2
1995	0.68	0.09	0.33	0.52	0.56	0.36	0.48	0.01	0.39	0.84	0.65	0.21–0.40
1996	1.00	0.07	0.37	1.00	1.00	0.67	0.30	1.00	1.00	0.70	1.00	0.41–0.60
1997	1.00	0.95	0.48	0.29	1.00	1.00	1.00	1.00	0.54	0.74	1.00	0.61–0.80
1998	1.00	1.00	0.26	1.00	0.30	0.29	0.37	0.99	0.29	0.55	0.61	0.81–1.00
1999	0.99	0.45	0.68	0.34	0.86	0.31	0.94	0.47	0.48	0.29	0.30	
2000	0.26	0.01	0.95	0.32	0.38	0.26	0.32	0.01	0.37	0.67	0.44	

Table A2. Predictor importance weights based on multimodel inference when only the Brightness slope is used with the environmental predictors. The darkest/lightest green show the highest/lowers predictor importance weights.

Year	Bright-sl	Dir-Source	D-Clear-Cut	D-Natur-Edg	Dg-Natur	AGE	Density	Edaphic	Geol-Wet	HLI	TWI	Legend
1994	0.90	1.00	1.00	0.96	0.52	0.71	0.35	1.00	0.98	1.00	0.62	≤0.2
1995	0.27	0.07	0.29	0.55	0.59	0.36	0.49	0.01	0.38	0.86	0.65	0.21–0.40
1996	1.00	0.14	0.39	1.00	1.00	0.67	0.32	1.00	1.00	0.82	1.00	0.41–0.60
1997	0.33	0.99	0.36	0.29	1.00	1.00	1.00	1.00	0.69	0.94	1.00	0.61–0.80
1998	0.36	1.00	0.26	1.00	0.27	0.28	0.33	0.99	0.35	0.71	0.59	0.81–1.00
1999	0.29	0.22	0.74	0.34	0.84	0.31	0.93	0.67	0.46	0.32	0.28	
2000	0.28	0.01	0.95	0.32	0.38	0.27	0.32	0.01	0.37	0.67	0.44	

Table A3. Predictor importance weights based on multimodel inference when no pre-disturbance index is used as a predictor. The darkest/lightest green show the highest/lowest predictor importance weights.

Year	Dir-Source	D-Clear-Cut	D-Natur-Edg	Dg-Natur	AGE	Density	Edaphic	Geol-Wet	HLI	TWI	Legend
1994	1.00	1.00	0.98	0.56	0.77	0.33	1.00	0.97	1.00	0.61	≤0.2
1995	0.07	0.29	0.55	0.59	0.36	0.49	0.01	0.38	0.86	0.65	0.21–0.40
1996	0.16	0.68	1.00	1.00	0.60	0.33	1.00	1.00	0.88	1.00	0.41–0.60
1997	0.99	0.35	0.29	1.00	1.00	1.00	1.00	0.69	0.94	1.00	0.61–0.80
1998	1.00	0.26	1.00	0.27	0.28	0.32	0.99	0.35	0.72	0.59	0.81–1.00
1999	0.22	0.74	0.34	0.84	0.31	0.92	0.68	0.46	0.33	0.28	
2000	0.01	0.95	0.32	0.38	0.27	0.32	0.01	0.37	0.67	0.44	

A2. Predictive Power of the Remote Sensing Variables

Table A4. Results of comparison tests of two ROC curves, one corresponding to the full model set (with both Wetness and Brightness slopes) and the other to the plain model set (with no remote sensing variable). *p*-values are shown. The ROC curve differs significantly for most comparisons.

	1994	1995	1996	1997	1998	1999	2000
1994	-	0.09	0.00	0.00	0.00	0.00	0.00
1995	0.00	-	0.00	0.00	0.00	0.81	0.93
1996	0.00	0.31	-	0.01	0.00	0.86	0.03
1997	0.00	0.01	0.00	-	0.00	0.00	0.04
1998	0.00	0.01	0.00	0.00	-	0.04	0.46
1999	0.00	0.09	0.00	0.00	0.01	-	0.41
2000	0.00	0.59	0.02	0.42	0.49	0.36	-

References

1. Frelich, L.E. *Forest Dynamics and Disturbance Regimes*; Cambridge University Press: Cambridge, UK, 2002.
2. Waring, R.H.; Running, S.W. *Forest Ecosystems: Analysis at Multiple Scales*, 3rd ed.; Elsevier: San Diego, CA, USA, 2007.
3. Seidl, R.; Schelhaas, M.-J.; Lexer, M.J. Unraveling the drivers of intensifying forest disturbance regimes in Europe. *Glob. Chang. Biol.* **2011**, *17*, 2842–2852. [CrossRef]
4. Schelhaas, M.J.; Nabuurs, G.J.; Schuck, A. Natural disturbances in the European forests in the 19th and 20th centuries. *Glob. Chang. Biol.* **2003**, *9*, 1620–1633. [CrossRef]
5. Seidl, R.; Schelhaas, M.-J.; Rammer, W.; Verkerk, P.J. Increasing forest disturbances in Europe and their impact on carbon storage. *Nat. Clim. Chang.* **2014**, *4*, 806–810. [CrossRef] [PubMed]
6. Wild, J.; Kopecký, M.; Svoboda, M.; Zenáhlíková, J.; Edwards-Jonášová, M.; Herben, T. Spatial patterns with memory: Tree regeneration after stand-replacing disturbance in Picea abies mountain forests. *J. Veg. Sci.* **2014**, *25*, 1327–1340. [CrossRef]
7. Čada, V.; Morrissey, R.C.; Michalová, Z.; Bače, R.; Janda, P.; Svoboda, M. Frequent severe natural disturbances and non-equilibrium landscape dynamics shaped the mountain spruce forest in central Europe. *For. Ecol. Manag.* **2016**, *363*, 169–178. [CrossRef]
8. Svoboda, M.; Janda, P.; Nagel, T.A.; Fraver, S.; Rejzek, J.; Bače, R. Disturbance history of an old-growth sub-alpine Picea abies stand in the Bohemian Forest, Czech Republic. *J. Veg. Sci.* **2012**, *23*, 86–97. [CrossRef]
9. Seidl, R.; Rammer, W.; Jäger, D.; Lexer, M.J. Impact of bark beetle (*Ips typographus* L.) disturbance on timber production and carbon sequestration in different management strategies under climate change. *For. Ecol. Manag.* **2008**, *256*, 209–220. [CrossRef]
10. Lambert, N.J.; Ardo, J.; Rock, B.N.; Vogelmann, J.E. Spectral characterization and regression-based classification of forest damage in Norway spruce stands in the Czech Republic using Landsat Thematic Mapper data. *Int. J. Remote Sens.* **1995**, *16*, 1261–1287. [CrossRef]
11. Rullan-Silva, C.D.; Olthoff, A.E.; Delgado de la Mata, J.A.; Pajares-Alonso, J.A. Remote monitoring of forest insect defoliation. A review. *For. Syst.* **2013**, *22*, 377–391. [CrossRef]
12. Kauth, R.J.; Thomas, G.S. The tasselled cap—A graphic description of the spectral-temporal development of agricultural crops as seen by Landsat. In Proceedings of the Symposium Machine Processing of Remotely Sensed Data, West Lafayette, IN, USA, 29 June–1 July 1976; pp. 41–51.
13. Crist, E.P.; Cicone, R.C. Application of the Tasseled Cap concept to simulated thematic mapper data. *Photogramm. Eng. Remote Sens.* **1984**, *50*, 343–352.
14. Skakun, R.S.; Wulder, M.A.; Franklin, S.E. Sensitivity of the thematic mapper enhanced wetness difference index to detect mountain pine beetle red-attack damage. *Remote Sens. Environ.* **2003**, *86*, 433–443. [CrossRef]
15. Wulder, M.A.; White, J.C.; Bentz, B.; Alvarez, M.F.; Coops, N.C. Estimating the probability of mountain pine beetle red-attack damage. *Remote Sens. Environ.* **2006**, *101*, 150–166. [CrossRef]
16. Coops, N.C.; Waring, R.H.; Wulder, M.A.; White, J.C. Prediction and assessment of bark beetle-induced mortality of lodgepole pine using estimates of stand vigor derived from remotely sensed data. *Remote Sens. Environ.* **2009**, *113*, 1058–1066. [CrossRef]
17. Lausch, A.; Heurich, M.; Gordalla, D.; Dobner, H.-J.; Gwillym-Margianto, S.; Salbach, C. Forecasting potential bark beetle outbreaks based on spruce forest vitality using hyperspectral remote-sensing techniques at different scales. *For. Ecol. Manag.* **2013**, *308*, 76–89. [CrossRef]
18. Overbeck, M.; Schmidt, M. Modelling infestation risk of Norway spruce by *Ips typographus* (L.) in the Lower Saxon Harz Mountains (Germany). *For. Ecol. Manag.* **2012**, *266*, 115–125. [CrossRef]
19. Netherer, S.; Nopp-Mayr, U. Predisposition assessment systems (PAS) as supportive tools in forest management—Rating of site and stand-related hazards of bark beetle infestation in the High Tatra Mountains as an example for system application and verification. *For. Ecol. Manag.* **2005**, *207*, 99–107. [CrossRef]
20. Dutilleul, P.; Nef, L.; Frigon, D. Assessment of site characteristics as predictors of the vulnerability of Norway spruce (*Picea abies* Karst.) stands to attack by *Ips typographus* L. (Col., Scolytidae). *J. Appl. Entomol.* **2000**, *124*, 1–5. [CrossRef]
21. Lausch, A.; Fahse, L.; Heurich, M. Factors affecting the spatio-temporal dispersion of *Ips typographus* (L.) in Bavarian Forest National Park: A long-term quantitative landscape-level analysis. *For. Ecol. Manag.* **2011**, *261*, 233–245. [CrossRef]

22. Lausch, A.; Heurich, M.; Fahse, L. Spatio-temporal infestation patterns of *Ips typographus* (L.) in the Bavarian Forest National Park, Germany. *Ecol. Indic.* **2013**, *31*, 73–81. [CrossRef]
23. Wulder, M.A.; Franklin, S.E. *Understanding Forest Disturbance and Spatial Pattern: Remote Sensing and GIS Approaches*; CRC Press, Taylor & Francis Group: Boca Raton, FL, USA, 2007.
24. Bjørnstad, O.N.; Økland, B. Synchrony and geographical variation of the spruce bark beetle (*Ips typographus*) during a non-epidemic period. *Popul. Ecol.* **2003**, *45*, 213–219. [CrossRef]
25. Brůna, J.; Wild, J.; Svoboda, M.; Heurich, M.; Müllerová, J. Impacts and underlying factors of landscape-scale, historical disturbance of mountain forest identified using archival documents. *For. Ecol. Manag.* **2013**, *305*, 294–306. [CrossRef]
26. Aakala, T.; Kuuluvainen, T.; Wallenius, T.; Kauhanen, H. Tree mortality episodes in the intact *Picea abies*-dominated taiga in the Arkhangelsk region of northern European Russia. *J. Veg. Sci.* **2011**, *22*, 322–333. [CrossRef]
27. Schroeder, L.M.; Weslien, J.; Lindelöw, Å.; Lindhe, A. Attacks by bark- and wood-boring Coleoptera on mechanically created high stumps of Norway spruce in the two years following cutting. *For. Ecol. Manag.* **1999**, *123*, 21–30. [CrossRef]
28. Seidl, R.; Müller, J.; Hothorn, T.; Bässler, C.; Heurich, M.; Kautz, M. Small beetle, large-scale drivers: How regional and landscape factors affect outbreaks of the European spruce bark beetle. *J. Appl. Ecol.* **2015**, *53*, 530–540. [CrossRef] [PubMed]
29. Wang, J.; Sammis, T.W.; Gutschick, V.P.; Gebremichael, M.; Dennis, S.O.; Harrison, R.E. Review of satellite remote sensing use in forest health studies. *Open Geogr. J.* **2010**, *3*, 28–42. [CrossRef]
30. Wulder, M.A.; Masek, J.G.; Cohen, W.B.; Loveland, T.R.; Woodcock, C.E. Opening the archive: How free data has enabled the science and monitoring promise of Landsat. *Remote Sens. Environ.* **2012**, *122*, 2–10. [CrossRef]
31. Kennedy, R.E.; Yang, Z.; Cohen, W.B. Detecting trends in forest disturbance and recovery using yearly Landsat time series: LandTrendr—Temporal segmentation algorithms. *Remote Sens. Environ.* **2010**, *114*, 2897–2910. [CrossRef]
32. Cohen, W.B.; Yang, Z.; Kennedy, R. Detecting trends in forest disturbance and recovery using yearly Landsat time series: TimeSync—Tools for calibration and validation. *Remote Sens. Environ.* **2010**, *114*, 2911–2924. [CrossRef]
33. Kennedy, R.E.; Andréfouët, S.; Cohen, W.B.; Gómez, C.; Griffiths, P.; Hais, M.; Healey, S.P.; Helmer, E.H.; Hostert, P.; Lyons, M.B.; et al. Bringing an ecological view of change to Landsat-based remote sensing. *Front. Ecol. Environ.* **2014**, *12*, 339–346. [CrossRef]
34. Pflugmacher, D.; Cohen, W.B.; Kennedy, R.E. Using Landsat-derived disturbance history (1972–2010) to predict current forest structure. *Remote Sens. Environ.* **2012**, *122*, 146–165. [CrossRef]
35. Kennedy, R.E.; Yang, Z.; Cohen, W.B.; Pfaff, E.; Braaten, J.; Nelson, P. Spatial and temporal patterns of forest disturbance and regrowth within the area of the Northwest Forest Plan. *Remote Sens. Environ.* **2012**, *122*, 117–133. [CrossRef]
36. Meddens, A.J.H.; Hicke, J.A.; Vierling, L.A.; Hudak, A.T. Evaluating methods to detect bark beetle-caused tree mortality using single-date and multi-date Landsat imagery. *Remote Sens. Environ.* **2013**, *132*, 49–58. [CrossRef]
37. Senf, C.; Pflugmacher, D.; Wulder, M.A.; Hostert, P. Characterizing spectral–temporal patterns of defoliator and bark beetle disturbances using Landsat time series. *Remote Sens. Environ.* **2015**, *170*, 166–177. [CrossRef]
38. Meigs, G.W.; Kennedy, R.E.; Cohen, W.B. A Landsat time series approach to characterize bark beetle and defoliator impacts on tree mortality and surface fuels in conifer forests. *Remote Sens. Environ.* **2011**, *115*, 3707–3718. [CrossRef]
39. Cohen, W.B.; Yang, Z.; Stehman, S.V.; Schroeder, T.A.; Bell, D.M.; Masek, J.G.; Huang, C.; Meigs, G.W. Forest disturbance across the conterminous United States from 1985 to 2012: The emerging dominance of forest decline. *For. Ecol. Manag.* **2016**, *360*, 242–252. [CrossRef]
40. Hais, M.; Kennedy, R.; Braaten, J.; Pflugmacher, D. Landsat spectral trajectories may aid in detecting precursors to spruce bark beetle outbreak. Unpublished Manuscript. 2016.
41. Neuhäuslová, Z. (Ed.) *The Map of Potential Natural Vegetation of the Šumava National Park*; Explanatory Text; Suppl. 1/2001; Silva Gabreta: Vimperk, Czech Republic, 2001.

42. Fischer, H.S.; Winter, S.; Lohberger, E.; Jehl, H.; Fischer, A. Improving transboundary maps of potential natural vegetation using statistical modeling based on environmental predictors. *Folia Geobot.* **2013**, *48*, 115–135. [CrossRef]
43. Heurich, M.; Reinelt, A.; Fahse, L. Die buchdruckermassenvermehrung im nationalpark bayerischer wald. In *Waldentwicklung im Bergwald nach Wind, und Borkenkäferbefall*; Bayer, Staatsforstverwaltung Wiss. Reihe: Grafenau, Germany, 2001; Volume 14, pp. 9–48.
44. Skuhravý, V. *Lýkožrout Smrkový* Ips typographus *(L.) a Jeho Kalamity*; Agrospoj: Praha, Czech Republic, 2002.
45. Hais, M.; Jonášová, M.; Langhammer, J.; Kučera, T. Comparison of two types of forest disturbance using multitemporal Landsat TM/ETM+ imagery and field vegetation data. *Remote Sens. Environ.* **2009**, *113*, 835–845. [CrossRef]
46. Nováková, M.H.; Edwards-Jonášová, M. Restoration of Central-European mountain Norway spruce forest 15 years after natural and anthropogenic disturbance. *For. Ecol. Manag.* **2015**, *344*, 120–130. [CrossRef]
47. Zeppenfeld, T.; Svoboda, M.; DeRose, R.J.; Heurich, M.; Müller, J.; Čížková, P.; Starý, M.; Bače, R.; Donato, D.C. Response of mountain *Picea abies* forests to stand-replacing bark beetle outbreaks: Neighbourhood effects lead to self-replacement. *J. Appl. Ecol.* **2015**, *52*, 1402–1411. [CrossRef]
48. Canty, M.J.; Nielsen, A.A.; Schmidt, M. Automatic radiometric normalization of multitemporal satellite imagery. *Remote Sens. Environ.* **2004**, *91*, 441–451. [CrossRef]
49. Schroeder, T.A.; Cohen, W.B.; Song, C.; Canty, M.J.; Yang, Z. Radiometric correction of multi-temporal Landsat data for characterization of early successional forest patterns in western Oregon. *Remote Sens. Environ.* **2006**, *103*, 16–26. [CrossRef]
50. Cohen, W.B.; Spies, T.A.; Fiorella, M. Estimating the age and structure of forests in a multi-ownership landscape of western Oregon, U.S.A. *Int. J. Remote Sens.* **1995**, *16*, 721–746. [CrossRef]
51. Bonneau, L.R.; Shields, K.S.; Civco, D.L. Using Satellite Images to Classify and Analyze the Health of Hemlock Forests Infested by the Hemlock Woolly Adelgid. *Biol. Invasions* **1999**, *1*, 255–267. [CrossRef]
52. Wulder, M.A.; Skakun, R.S.; Kurz, W.A.; White, J.C. Estimating time since forest harvest using segmented Landsat ETM+ imagery. *Remote Sens. Environ.* **2004**, *93*, 179–187. [CrossRef]
53. Jin, S.; Sader, S.A. Comparison of time series tasseled cap wetness and the normalized difference moisture index in detecting forest disturbances. *Remote Sens. Environ.* **2005**, *94*, 364–372. [CrossRef]
54. Jakuš, R. A method for the protection of spruce stands againstIps typographus by the use of barriers of pheromone traps in north-eastern Slovakia. *Anz. Schädlingskd Pflanzenschutz Umweltschutz* **1998**, *71*, 152–158. [CrossRef]
55. Matějka, K. Forest Altitudinal Zones with Dominant Norway Spruce in the Czech Republic. Available online: http://www.infodatasys.cz/public/Lesnik21_2014km.pdf (accessed on 25 May 2016).
56. Randuška, D. Forest typology in Czechoslovakia. In *Application of Vegetation Science to Forestry. Handbook of Vegetation Science*; Jahn, G., Ed.; Dr. W. Junk Publication: The Hague, The Netherlands, 1982; Volume 12, pp. 147–178.
57. Tüxen, R. *Die Heutige Potentielle Natürliche Vegetation Als Gegenstand der Vegetationskartierung*; Zentralstelle für Vegetationskartierung: Remagen, Germany, 1956.
58. Viewegh, J.; Kusbach, A.; Mikeska, M. Czech forest ecosystem classification. *J. For. Sci.* **2003**, *49*, 85–93.
59. McCune, B.; Keon, D. Equations for potential annual direct incident radiation and heat load. *J. Veg. Sci.* **2002**, *13*, 603–606. [CrossRef]
60. Matějka, K. *Hodnocení Přirozenosti Lesů NP Šumava (Evaluation of Naturalness of Forests in the Šumava National Park)*; Report for the Ministry of Environment. Ministry of Environment: Prague, Czech Republic, 2014.
61. Zuur, A.F.; Ieno, E.N.; Elphick, C.S. A protocol for data exploration to avoid common statistical problems. *Methods Ecol. Evol.* **2010**, *1*, 3–14. [CrossRef]
62. Gelman, A.; Su, Y.-S. *Data Analysis Using Regression and Multilevel/Hierarchical Models*; Cambridge University Press: Cambridge, UK, 2015.
63. R Development Core Team. *R: A Language and Environment for Statistical Computing*; R Foundation for Statistical Computing: Vienna, Austria, 2014.
64. Burnham, K.P.; Anderson, D.R.; Huyvaert, K.P. AIC model selection and multimodel inference in behavioral ecology: Some background, observations, and comparisons. *Behav. Ecol. Sociobiol.* **2011**, *65*, 23–35. [CrossRef]
65. Grueber, C.E.; Nakagawa, S.; Laws, R.J.; Jamieson, I.G. Multimodel inference in ecology and evolution: Challenges and solutions. *J. Evol. Biol.* **2011**, *24*, 699–711. [CrossRef] [PubMed]

66. Symonds, M.R.E.; Moussalli, A. A brief guide to model selection, multimodel inference and model averaging in behavioural ecology using Akaike's information criterion. *Behav. Ecol. Sociobiol.* **2011**, *65*, 13–21. [CrossRef]
67. Bartoń, K. *MuMIn: Multi-Model Inference*; R Package Version 1.15; Bartoń: Krakow, Poland, 2016.
68. Fawcett, T. An introduction to ROC analysis. *Pattern Recognit. Lett.* **2006**, *27*, 861–874. [CrossRef]
69. Fielding, A.H.; Bell, J.F. A review of methods for the assessment of prediction errors in conservation presence/absence models. *Environ. Conserv.* **1997**, *24*, 38–49. [CrossRef]
70. Robin, X.; Turck, N.; Hainard, A.; Tiberti, N.; Lisacek, F.; Sanchez, J.-C.; Müller, M. pROC: An open-source package for R and S+ to analyze and compare ROC curves. *BMC Bioinform.* **2011**, *12*. [CrossRef] [PubMed]
71. Yoshida, Y.; Joiner, J.; Tucker, C.; Berry, J.; Lee, J.-E.; Walker, G.; Reichle, R.; Koster, R.; Lyapustin, A.; Wang, Y. The 2010 Russian drought impact on satellite measurements of solar-induced chlorophyll fluorescence: Insights from modeling and comparisons with parameters derived from satellite reflectances. *Remote Sens. Environ.* **2015**, *166*, 163–177. [CrossRef]
72. Rock, B.N.; Vogelmann, J.E.; Williams, D.L.; Vogelmann, A.F.; Hoshizaki, T. Remote Detection of forest damage. *Bioscience* **1986**, *36*, 439–445. [CrossRef]
73. Collins, J.B.; Woodcock, C.E. An assessment of several linear change detection techniques for mapping forest mortality using multitemporal Landsat TM data. *Remote Sens. Environ.* **1996**, *56*, 66–77. [CrossRef]
74. Dantas de Paula, M.; Groeneveld, J.; Huth, A. The extent of edge effects in fragmented landscapes: Insights from satellite measurements of tree cover. *Ecol. Indic.* **2016**, *69*, 196–204. [CrossRef]
75. Kopácek, J.; Veselý, J.; Stuchlík, E. Sulphur and nitrogen fluxes and budgets in the Bohemian Forest and Tatra Mountains during the Industrial Revolution (1850–2000). *Hydrol. Earth Syst. Sci.* **2001**, *5*, 391–406. [CrossRef]
76. Šantrůčková, H.; Šantrůček, J.; Šetlík, J.; Svoboda, M.; Kopáček, J. Carbon isotopes in tree rings of Norway spruce exposed to atmospheric pollution. *Environ. Sci. Technol.* **2007**, *41*, 5778–5782. [CrossRef] [PubMed]
77. Polák, T.; Cudlín, P.; Moravec, I.; Albrechtová, J. Macroscopic indicators for the retrospective assessment of Norway spruce crown response to stress in the Krkonoše Mountains. *Trees* **2007**, *21*, 23–35. [CrossRef]
78. Wermelinger, B. Ecology and management of the spruce bark beetle Ips typographus—A review of recent research. *For. Ecol. Manag.* **2004**, *202*, 67–82. [CrossRef]
79. Bytnerowicz, A.; Badea, O.; Barbu, I.; Fleischer, P.; Frączek, W.; Gancz, V.; Godzik, B.; Grodzińska, K.; Grodzki, W.; Karnosky, D.; et al. New international long-term ecological research on air pollution effects on the Carpathian Mountain forests, Central Europe. *Environ. Int.* **2003**, *29*, 367–376. [CrossRef]
80. Vogelmann, J.E.; Xian, G.; Homer, C.; Tolk, B. Monitoring gradual ecosystem change using Landsat time series analyses: Case studies in selected forest and rangeland ecosystems. *Remote Sens. Environ.* **2012**, *122*, 92–105. [CrossRef]



© 2016 by the authors; licensee MDPI, Basel, Switzerland. This article is an open access article distributed under the terms and conditions of the Creative Commons Attribution (CC-BY) license (http://creativecommons.org/licenses/by/4.0/).

Paper IV



Müllerová, J., Bartaloš, T., Brůna, J., Dvořák, P., Vítková, M. (2017)

Unmanned aircraft in nature conservation: an example from plant invasions

International Journal of Remote Sensing 38(8-10):2177-2198.

doi: 10.1080/01431161.2016.1275059

INTERNATIONAL JOURNAL OF REMOTE SENSING, 2017
http://dx.doi.org/10.1080/01431161.2016.1275059

Taylor & Francis
Taylor & Francis Group

Unmanned aircraft in nature conservation: an example from plant invasions

Jana Müllerová[a], Tomáš Bartaloš[b], Josef Brůna[a,c], Petr Dvořák[d] and Michaela Vítková[a]

[a]Institute of Botany, The Czech Academy of Sciences, Průhonice, Czech Republic; [b]Remote Sensing Department, GISAT Ltd, Prague, Czech Republic; [c]Institute for Environmental Studies, Faculty of Science, Charles University, Prague 2, Czech Republic; [d]Brno University of Technology, Institute of Aerospace Engineering, Brno, Czech Republic

ABSTRACT

To successfully fight plant invasions, new methods enabling fast and efficient monitoring are needed, and remote sensing can make their management more efficient and less expensive. However, the data resolution, cost, and availability can be limiting. Optimal solution depends on the species characteristics, where the spectral and spatial resolution can compensate each other to some extent, and phenology plays an important role. Available high spatial resolution satellite data are sufficient for recognition of species that are distinct and either large or form uniform patches at size comparable to the data pixel size. For other species, higher spatial resolution is needed, and unmanned aircraft (UAV) provide data of extremely high spatial resolution (cm) at low cost and high flexibility. We assess its potential to map invasive black locust (BL, *Robinia pseudoaccacia*), testing imagery of different origin (satellite, UAV), spectral (multispectral, red, green, and blue (RGB) + near-infrared (NIR)) and spatial resolution, and various technical approaches to choose the best strategy for the species monitoring balancing between precision of detection and economic feasibility. Using purposely designed low-cost UAV with tailless fixed wing design for two consumer cameras (RGB and modified NIR) ensures robustness and repeatable field performance while maintaining high aerodynamic efficiency, with resulting mapping capacity over 10 km^2 per day. Several challenges exist in UAV application, such as lower spectral resolution, geometrical and radiometric distortions, and significant amount of data (necessity of automatic processing). In our study, we tested different options of UAV data processing and present comparison of resulting orthomosaic accuracies. For repeated measurements, it is extremely important to ensure spatial co-registration of pixels/objects from different phenological phases. Investment in GPS receiver in the UAV and GPS post-processing eliminated laborious collection of ground control points, while maintaining the co-registration of objects across multiple flights. In our study we provide evidence of benefit of the low cost unmanned system for species monitoring with high classification accuracies of target species from UAV orthomosaic outcompeting WorldView-2

ARTICLE HISTORY
Received 26 September 2016
Accepted 10 December 2016

CONTACT Jana Müllerová jana.mullerova@ibot.cas.cz Institute of Botany, The Czech Academy of Sciences, Zámek 1, 25243 Průhonice, Czech Republic

© 2017 Informa UK Limited, trading as Taylor & Francis Group

satellite data, and describe methodology that can be used for practical management of invasions.

1. Introduction

Plant invasions impose increasing impacts not only on biodiversity and ecosystem functioning, but also economy and human health (Pimentel, Zuniga, and Morrison 2005; Hulme et al. 2009; Ehrenfeld 2010; Pyšek and Richardson 2010). They can be fast and very dynamic, and this makes the control measures difficult especially at the later stages of invasion (Pluess et al. 2012). Eradication should therefore focus first on recently infested sites (Müllerová et al. 2005; Pluess et al. 2012). Hence, early and regular detection of the invading species and rapid management response on both local and landscape level is crucial (Rejmánek 2000; Vilà and Ibáñez 2011), and new techniques enabling timely, fast and precise monitoring are urgently needed (European Commission 2008, 2014; van Kleunen et al. 2015).

Remote sensing (RS) represents a promising option, potentially reducing the needs for extensive field campaigns and connected costs (Lawes and Wallace 2008; Buchanan et al. 2015; Marvin et al. 2016). It has been successfully applied for some invasive species (for reviews, see C. and Asner 2009; Bradley 2014; Rocchini et al. 2015), mostly for shrubs and trees (Hamada et al. 2007; Hantson et al. 2012; Somodi et al. 2012). The potential for invasive species monitoring has still not been fully exploited and detection algorithms are missing for the majority of invasive species. Our species of interest, black locust (BL, *Robinia pseudoaccacia*), an invasive North American tree widely planted in Europe for centuries, is not much exploited although it is very common in Europe. Somodi et al. (2012) explored Landsat and aerial data (red, green, blue (RGB) and RGB + near-infrared (NIR)) potential for the species detection, comparing spring and summer imagery. They determined the spring flowering as an important for the species detection. Wang et al. (2015) used combined spectral, spatial and textural information from IKONOS imagery to assess the BL health conditions. By using spectral characteristics combined with texture measures, they were able to identify the forest health and characterize the spatial structure of stressed forests.

Data of very-high spatial resolution, such as from unmanned aerial system (UAV), together with semi-automated, computer-assisted processing can enable cost-effective, fast, and frequent monitoring in case of appropriate methodological approach (Müllerová et al. 2016). For plant species detection, the proper timing of the RS data acquisition is important since some species might be better detected at certain phenological stages (Müllerová, Pergl, and Pyšek 2013). UAV can provide flexible data acquisition of very high spatial and temporal resolution data at very low costs, and is also suitable for targeted monitoring (e.g. focus on sites of high natural interest such as NATURA 2000 sites, areas prone to invasion, or those recently managed to check eradication effectivity). Amongst the main limits are reduced spectral resolution compared to the satellite imagery, and the data degradation by geometrical distortions and other inhomogeneous artefacts (Colomina and Molina 2014; Whitehead and Hugenholtz 2014). The high spatial resolution may also result in 'salt and pepper' classification in

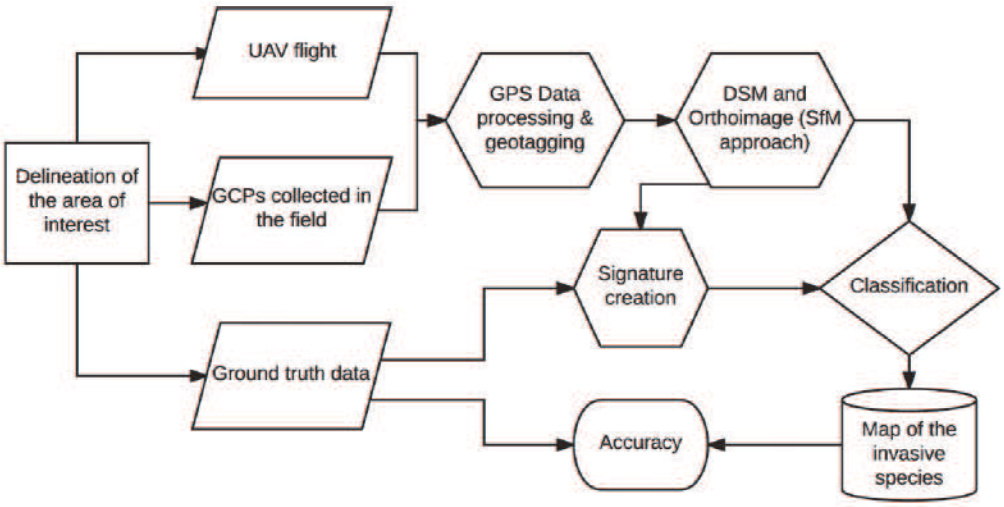


Figure 1. Flow-chart of the presented study.

case of increased within-patch variability (if image resolution does not match the resolution of the studied community texture (Zweig et al. 2015).

Unmanned platforms are being increasingly utilized in diverse scientific fields including ecology (Whitehead et al. 2014; Zweig et al. 2015). Majority of the used UAV systems are based on multicopter aerial platforms (Whitehead and Hugenholtz 2014). Since such type of platform is able to cover only limited areas due to the inherent energy demands of the rotorcraft concept, fixed wing UAVs are much better suited to the monitoring purpose, and their operational radius is restricted primarily by the legislation (most often requiring visual contact between the UAV and its operator) rather than the capability of the platform itself. This article aims at describing the cost-effective and efficient methodology of invasive plant species monitoring (one example of invasive BL) using purposely designed unmanned aerial system. Compared to the commercial products, such as Trimble/Gatewing, SenseFly eBee, Aeromapper, and others, deployment of in-house developed system brings the advantage of reduced cost, operational experience and most importantly it can be easily adapted for the required payload.

In our research, we seek for optimal low-cost solution of invasive species monitoring, applicable in both plant ecology and practical management. We describe methodology of application of UAV for such purpose, assessing to what extent it can be used to analyse plant invasions (Figure 1).

2. Methods

2.1. *The deployed unmanned system*

Development of dedicated unmanned platform optimized for invasive species monitoring forms an important part of presented low-cost invasive monitoring solution. During the development, several aerial platforms were tested (Table 1).

For the initial trials, a motorized glider concept was selected (VUT 720, Dvořák et al. 2015, Figure 2(a)) to take advantage of the low wing loading. Combined with expanded polypropylene, a durable material featuring excellent impact properties, this concept ensures safe landings even in rugged terrain. The platform is hand-

Table 1. Summary of small unmanned platforms used for invasive species monitoring in this project.

	VUT 712	VUT 713	VUT 720
Span	2.1 m	2.0 m	2.6 m
Length	0.9 m	0.7 m	1.3 m
m_{TOW}	3.1 kg	2.7 kg	2.2 kg
v_C	17 m/s	18 m/s	15 m/s
Battery	LiPo 4S 5000 mAh	LiPo 4S 5000 mAh	LiPo 3S 5000 mAh
Endurance	1 h	0.7 h	1 h
Power	650 W	300 W	360 W
Payload	0.8 kg	0.9 kg	0.3 kg
Autopilot	Pixhawk autopilot	DroPix autopilot	APM2.5+ autopilot
Camera	2× Canon S100 Stabilized	2× Sony A5100 + E20/2.8	1× Canon S100+ 1× GoPro
Based on	SkyWalker X8	RVJET	Multiplex Cularis



Figure 2. Unmanned systems used in the project – VUT 720 (a), VUT 712 (b), and VUT 713 (c).

launched with no need for additional equipment. However, VUT 720 is able to carry only one camera (Canon PowerShot S100) at a time. The requirement to produce RGB + NIR data for further classification and research meant that two consecutive flights had to be performed at each location. This procedure not only resulted in increased time spent at a single site, but also introduced significant problems during image processing, as the lighting conditions often change during consecutive flights making the radiometric corrections of the captured images more complex. Therefore, a platform providing actively stabilized mount for two Canon S100 cameras was devised – VUT 712 (Figure 2(b)). Data acquired by VUT 712 showed higher quality compared to previous datasets in terms of both radiometric consistency and georeferencing accuracy.

Our operational experience clearly shows that consumer point-and-shoot cameras such as Canon S100 are not well suited for the harsh environmental conditions of repeated mapping missions. Retractable zoom lenses of the cameras are inherently prone to (uncommanded) focal length changes, deteriorating the photogrammetric quality of acquired imagery. Dust can easily penetrate the lens during landings, resulting in jammed lens and prolonged down-times of the platform.

Deployment of dedicated multispectral cameras (such as Micasense RedEdge) or an array of industrial grade cameras with spectral filters would overcome mentioned problems; however the costs would limit operational use. As a cost-effective solution, fixed pancake lens (Sony E20/2.8) coupled to a lightweight mirrorless camera (Sony A5100) has been deployed in a new platform – VUT 713 (Figure 2(c), Table 2). To save

Table 2. Technical details of an aerial platform VUT 713.

Platform	Range video RVJET
Remote control	Graupner MC 22 s + Jeti 2,4GHz Tx Modul + JetiBox Profi
RC telemetry	Jeti Duplex Rsat2 + Mvario2EX + MT125EX
Battery	Schweighofer Modster 4S1P 5000mAh
Motor speed controller	Foxy R-65SB 65A SBEC
Motor	Dualsky XM3542EA-6 790RPM/V modified, 140 g
Propeller	Aeronaut CAM Carbon folding prop 13/6.5"
Servos	2× elevon: Hitec Mini Digital Servo HS-5245 MG
Autopilot	Drotek Dropix v2.1, 3DR PowerModule, Digital Airspeed sensor
GPS	Drotek u-blox M8 T, external magnetometer
Autopilot telemetry	SiK radio V2 433 mHz
Ground station	Panasonic Toughbook CF-19
Camera	2× Sony A5100 + E20/2.8

weight, the stabilized mount was substituted by software limited camera triggering based on UAV attitude. Our operational experience confirms the described setup as a reliable and high-performing system. Approximate costs of our solution are 1000 EUR for the unmanned system and 1600 EUR for the cameras (NIR and RGB). Men power is not considered in the calculation. To assemble the system no professional expertise is needed. Elementary technical skills and motivation are sufficient (for more information, see e.g. https://conservationdrones.org).

2.2. *Image acquisition and pre-processing*

2.2.1. *Camera selection and spectral characteristics*

For vegetation classification the NIR band is very important. As mentioned in previous chapter, a set of two consumer cameras (one standard RGB, and one modified to be sensitive in NIR band – built-in IR-cut filter removed and Hoya R72 filter added) was used instead of expensive multispectral camera (Table 3, Figure 3). Two camera types were tested during the project – Canon S100 and Sony A5100 (Table 3). The sensor of Canon S100, size of 1/1.7 in. (7.44 × 5.58 mm) resulted in comparably high levels of noise and

Table 3. Comparison of the two cameras setup used for tested unmanned platforms.

Platform	VUT 712	VUT 713	Comparison
Cameras	2× Canon S100 (VIS + NIR)	2× Sony A5100 + E20/2.8 (VIS+NIR)	
Sensor size	1/1.7 in. (7.44 mm × 5.58 mm)	APS-C (23.5 × 15.6 mm)	~9 times larger Fixed lens
Stabilization	External mechanical (two-axis simple BGC BLDC gimbal) + internal optical	N/A (autopilot does not trigger if the attitude exceeds preset limits)	OK even without stabilization
Georeferencing	• Internal GPS • Precise shutter time (CHDK script) synchro with autopilot GPS	• Autopilot DGPS – trigger log • Correction for shutter lag	Much better precision
Triggering	Intervalometer ~0.5 Hz (CHDK scripting)	Distance based – from autopilot system	Efficient – no unnecessary images; maintains overlap
Total weight	2 × 192 g + 280 g gimbal = 664 g	2 × 360 g = 720 g	Not a significant penalty

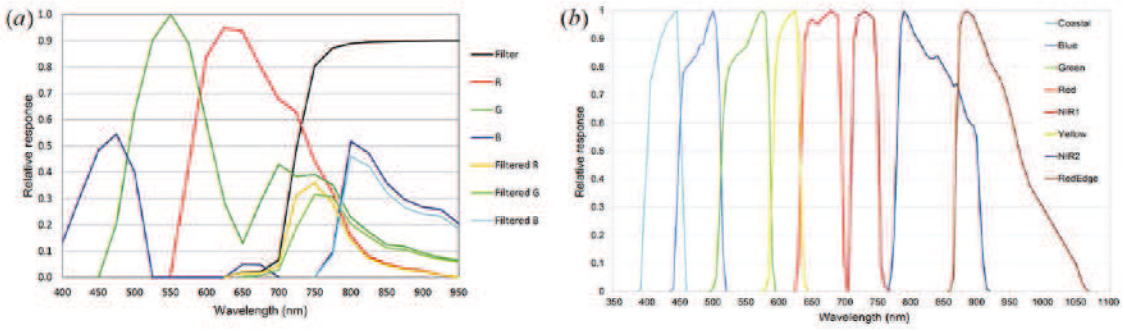


Figure 3. Spectral response of Sony A5100 camera – standard RGB and NIR version without IR-cut filter (a), compared to the spectral sensitivities of the WorldView-2 satellite sensors (b) based on DigitalGlobe datasheet (DigitalGlobe 2016).

low dynamic range of the pixels. The NIR modified camera was especially affected by this fact due to the longer wavelength of sensed light. The APS-C (23.5 × 15.6 mm) sized sensor of Sony A5100 camera provided nearly 8.8 times larger photosensitive area compared to the S100 camera. Fixed lens of Sony A5100 addressed the problems experienced with retractable zoom lens of Canon S100.

2.2.2. *Triggering*

The sensors were periodically triggered during the flight to cover the area of interest with sufficient image data. Significant overlap was required for robust mosaicking. Typically, the missions were flown with overlap and sidelap ranging between 80% and 85% of the image height and width, respectively.

To achieve homogenous coverage of the area, the following camera triggering strategies were employed:

- Constant time between images (intervalometer). This strategy has been implemented with the S100 cameras by means of modifying firmware (CHDK 2013). The firmware ran an in-house developed script based on KAP 3.4 (KAP 2015). The script triggered the camera in preset intervals (2 s intervals are proven to be the shortest interval the Canon S100 camera is able to maintain for prolonged periods). This approach provided homogenous coverage under ideal conditions. Wind and atmospheric turbulence caused the images to be spaced unevenly in real world application because of the varying ground speed of unmanned platform.
- Constant distance between images. Triggering was performed based on distance travelled by the UAV – a value computed by an autopilot from GPS data. This approach ensured homogenous image coverage even with a strong wind during the mapping flight. The cameras needed to be capable to capture the imagery with sufficient frequency – Sony A5100 cameras achieved 1 s intervals for prolonged periods.

2.2.3. *Georeferencing*

Structure-from-motion approach (SfM; Dandois and Ellis 2010; Westoby et al. 2012) was used to generate the digital surface model (DSM) and resulting orthomosaic using Agisoft PhotoScan software (Agisoft 2016). The SfM approach identifies similar features in conjugate

images, tolerating large variations in scale and image acquisition geometry. Even though PhotoScan has a simple interface with no possibility to control all the parameters, it is able to generate very dense and accurate three-dimensional point cloud (Turner, Lucieer, and Watson 2012; Whitehead and Hugenholtz 2014).

Using UAV data for monitoring of invasive species brings a principal advantage of very high spatial resolution. On the other hand, this resolution poses significant demand for geometrical accuracy to fit other ancillary or reference data such as aerial orthophoto or satellite VHR imagery or to carry out change detection using repeated data. Since low-cost components are primarily preferred in our project, precise georeferencing of the final image mosaics may be an issue, leading to unacceptable geometrical distortions and/or positional shifts. Several inputs influence the precision of final orthomosaic. Besides quality and type of the GPS receiver and the measurement method itself, further limitations such as shutter lag or availability of GPS corrections have to be considered.

To overcome such deficiencies and for the overall improvement of the final geometrical accuracy, different procedures were tested to evaluate the best setup balancing the accuracy and costs. At the first phase, only GPS built in the camera was used with original EXIF-based GPS information. Accuracy achieved by such low-end camera GPS burdened by high error rate up to several metres resulting in expected shifts of the processed orthomosaic. Influence of random misplacement of GPS coordinates led to local differences up to ×10 m.

Alternatively, an aircraft/autopilot GPS receiver (u-blox LEA 6 H) with assumed higher accuracy was considered. All trigger events were recorded by the camera with 10 ms accuracy by means of the in-house CHDK script. The resultant data log was synchronized with GPS position log from autopilot during post-processing. In this case, the proper synchronization of exact GPS position record and the image acquisition time is questionable, since the time coherence of the two independent devices may differ slightly resulting in a varying amount of misplacement.

As an optimal solution, a GPS module capable of raw data output (u-blox M8 T) was added to the autopilot. Triggering of the cameras was performed by the autopilot based on the distance travelled between the two consecutive images. Subsequently an automated approach of image geotagging was developed: the flight log records are used as a base to derive the correct coordinates. The employed SONY A5100 cameras are characterized by a stable 90 ms lag between the trigger event and the instant the shutter is actually released. This lag is accounted for by the post-processing procedure. Besides the time stamp of the camera trigger event, the GPS position is continuously recorded during the flight with a 5 Hz frequency. Due to the above mentioned shutter lag effect, a linear interpolation between two closest GPS log records is introduced to the final calculation of each image coordinates. In addition, the GPS coordinates were improved by post-processing using the RTKlib – an open-source package (RTKLIB 2016) and the respective correction data from the local Czech Reference Station Network (CZEPOS). Different settings were evaluated including the application of ionospheric map. An overview of positional variability is illustrated by Figure 4, comparing original, enhanced and post-processed GPS coordinates of the flight path and geo-tagged images. The overall positional accuracy was evaluated on the resulting orthomosaics only, based on signalized GCP with independently measured coordinates using

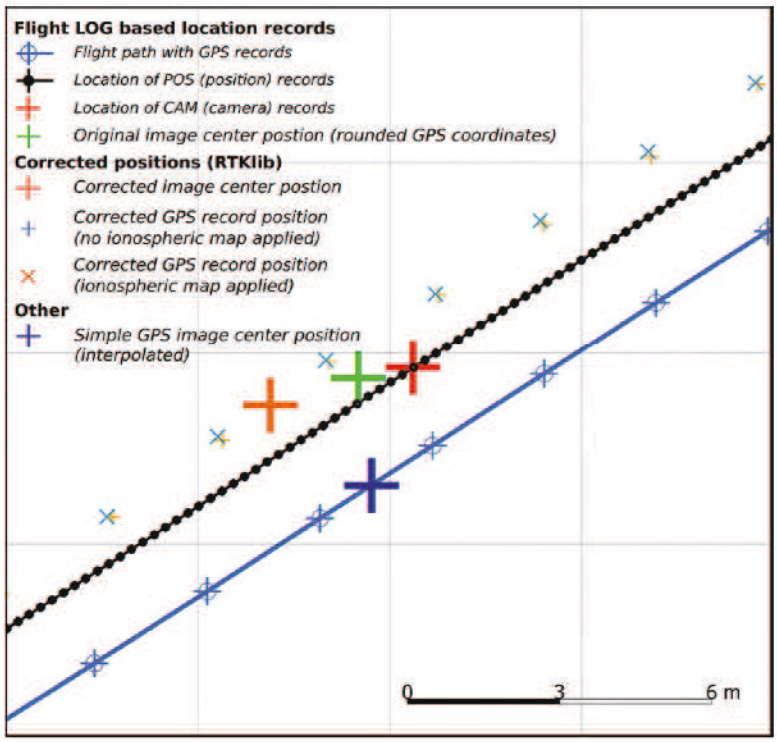


Figure 4. Overview of different settings for correction of GPS data and geotagged images.

reference data obtained with Trimble GeoExplorer GeoXH 6000 differential GNSS with post-processing in Trimble Pathfinder Office using CZEPOS correction data (Figure 5).

SfM method implemented within Agisoft PhotoScan (Agisoft 2016) for generation of RGB + NIR orthomosaic enables different parametrization to adapt the processing workflow according to the required purpose. This may lead to balanced procedure reflecting the required radiometric and geometric quality at reasonable processing time. Since two separate cameras were used continuously for RGB and NIR, separate or co-processed option for computation is an option. Separate RGB processing results in appropriate image quality (Figure 5(a)) with no visible artefacts in DSM (Figure 6(a)). However, for proper vegetation mapping and monitoring the NIR spectrum is crucial and, therefore, NIR band needs to be co-registered with the other bands. Several tests of co-processed RGB and NIR imagery revealed an obvious error in DSM generation causing 'islands' of unrealistic elevations and noisy point clouds (Figure 6(b)). Such artefacts are directly projected to orthomosaic generation causing blurred and deformed areas within the imagery with influence on classification, reduced reliability (Figure 6(e)) and higher spatial error (Figure 5(b)). Even the fastest processing option using sparse point cloud method from RGB imagery results in better spatial accuracy (Figure 5(a)). Dense point cloud method applied to RGB data also produces more accurate results (Figure 5(b)) and is still faster than RGB and NIR co-processing.

Aggressive depth filtering during the dense point cloud generation can be used to alleviate the aforementioned problems (Figure 6(c)). However, highly detailed DSM based on the dense point is prone to create mosaic artefacts in areas of complex patterns and steep DSM transitions. To minimize the distortions, the generated DSM can be exported with significantly lower spatial resolution (a factor of 100 seems to ensure balanced results) and re-imported for the orthomosaic creation – resulting in a smoother surface

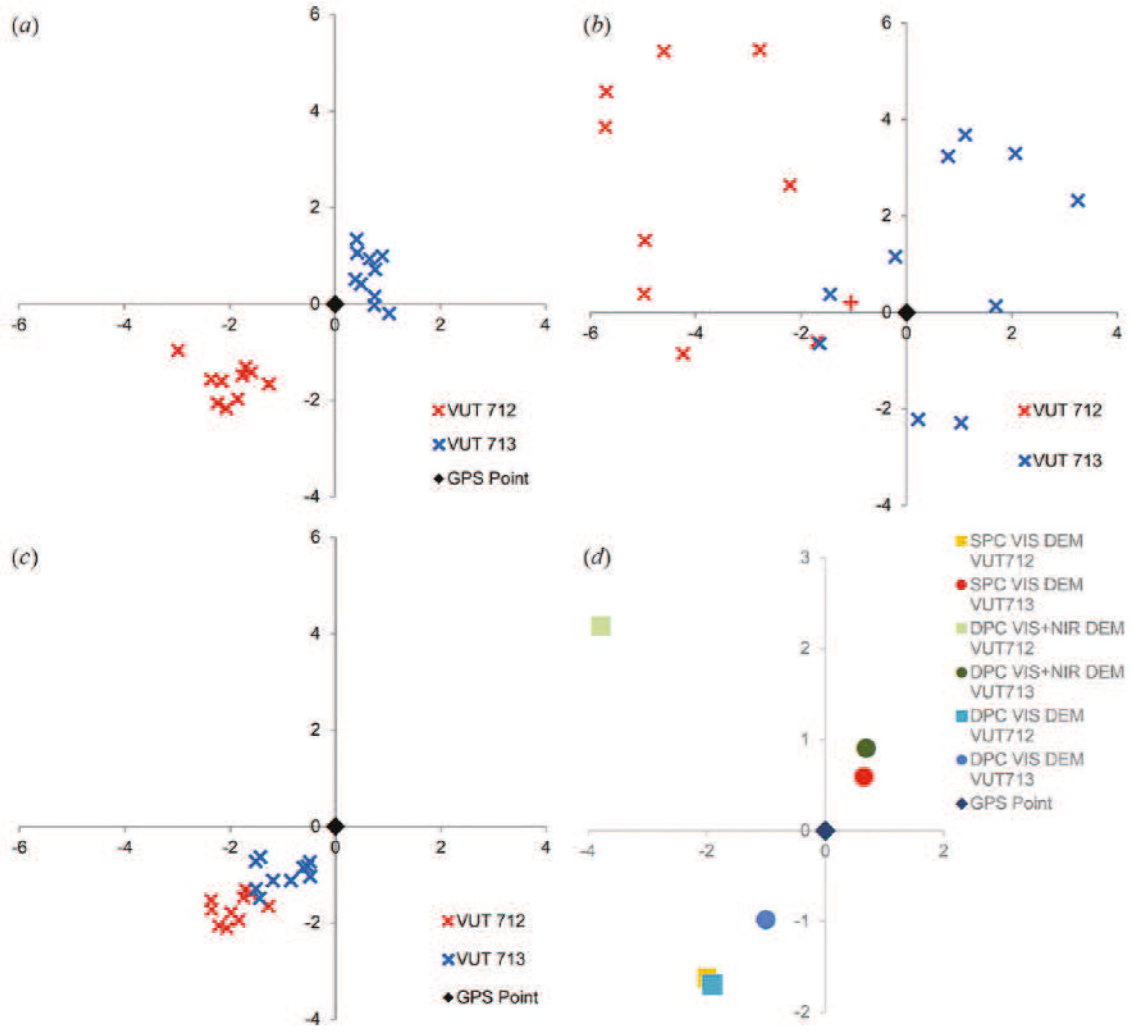


Figure 5. Errors of image projection (in metres) from two different unmanned systems (VUT 712 with Canon S100 Camera and internal GPS; and VUT 713 with Sony A5100 camera and autopilot differential GPS) compared to 10 GCP targets measured in the field with differential GPS (estimated error <0.1 m). Orthomosaics were generated using sparse point cloud based DSM from VIS images (a); dense point cloud based DSM from VIS and NIR images (b), and from VIS images only (c). The mean error of orthomosaics for VUT 712 was 2.56 m ± 0.38 (a), 4.82 m ± 2.07 (b), and 2.56 m ± 0.35 (c), whereas for VUT 713 it was 0.99 m ± 0.26 (a), 2.60 m ± 1.03 (b), and 1.44 m ± 0.40 (c). X and Y shifts are summarized in (d). SPC: sparse point cloud, DPC: dense point cloud.

representation (Figure 6(d)). Alternatively, an external standard image processing software or package can be used for resampling combined with further filtering (extreme or missing values, etc.). As a result, most of the artefacts are eliminated and overall image quality is enhanced (Figure 6(f)), and the original detailed DSM is preserved as a suitable ancillary data source for classification (e.g. vegetation height and heterogeneity).

The VUT 713 equipped with Sony A5100 camera produced the most spatially precise results independent from the orthomosaic processing settings (Figure 5(d)).

2.3. *Field data collection*

Field data are crucial for successful training of automatic/semiautomatic algorithms and for validation purposes. Considering the resolution of the final UAV imagery, it is obvious that a classical field GPS and even a differential GPS is not precise enough. This is

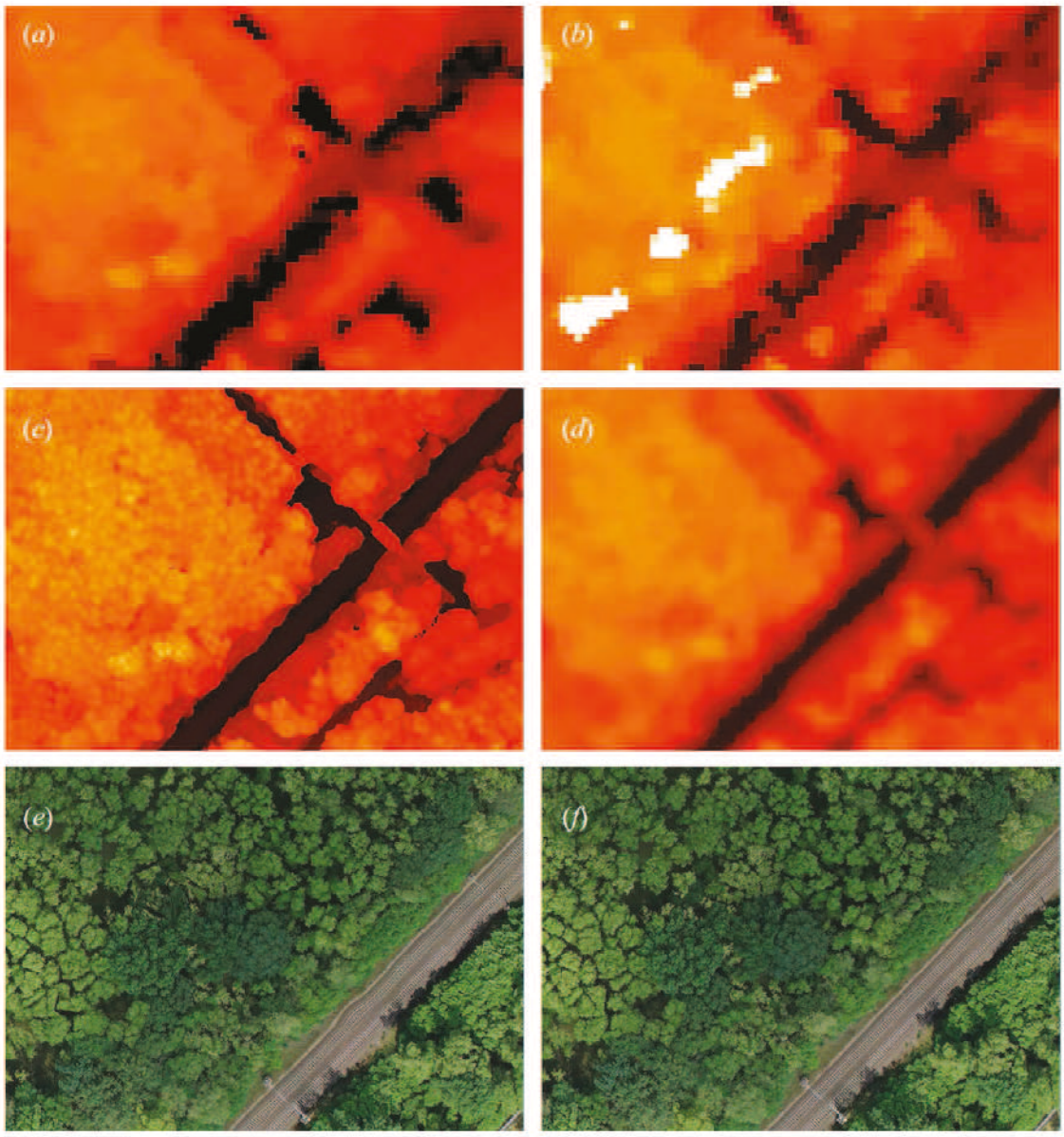


Figure 6. Digital elevation models (DEMs) resulting from different processing settings. Only RGB data processed – DSM based on sparse point cloud (a); RGB + NIR images co-processed – DSM based on sparse point cloud displaying artefacts (b); dense point cloud with aggressive depth filtering applied to RGB + NIR co-processed data (c); resampled DSM in order to provide smooth base for orthomosaic texture (d); visual artefacts resulting from distorted DSM shown in (b) (e); final mosaic based on resampled DSM shown in (d) (f).

especially true in forested environment where the estimated precision drops to several decimetres or even metres. The differential GPS would also be costly and time consuming option for large scale field data collection.

To overcome mentioned problems, we decided to use a field computer (a tablet with Android OS to decrease the costs) with UAV imagery or other available orthomosaics as a base for manual delineation of invasive species patches in the field with a help of integrated GPS. UAV imagery proved to be the most useful source of data for this purpose, because its high resolution provided enough detail necessary for precise delineation of vegetation polygons. To choose the best application/software for field data collection, we made a short review (Table 4), and after initial testing, chose collector for ArcGIS as the most viable alternative since

Table 4. A review of available applications/software for collection of field data.

Name	Operating system	Price	Offline use	Custom maps	Multi-user environment	Easy to use	Easy to prepare	HW Price	Comments
Trimble TerraSync	Windows Mobile	Fixed	Yes	Yes	No	Yes	Yes	Medium/ high	Precise measurements based on expensive GPS
Trimble TerraFlex	Multiple	Subscriptionbased			Yes			Low	Not tested in the field
Collector for ArcGIS	Multiple	Free with ArcGIS maintenance	Yes	Yes	Yes	Yes	Yes	Low	Works well in ArcGIS workflow
NextGIS Mobile	Android	Free	Yes	No			No	Low	Limited English documentation
QField, QGIS Mobile	Android	Free				No	No	Low	Complicated
ODK Collect	Android	Free	Yes	No	Yes	Yes	Yes	Low	Simple app for citizen science

it allowed us to: (i) collect the data offline (i.e. independent from the internet availability); (ii) use our own imagery as a background; (iii) attach photographs and several attributes to the collected polygons in the field; (iv) distribute data to multiple users in the field, which collect data to a centralized database; (v) use other supporting data overlays; and (vi) sync the data afterwards and make them directly accessible in ArcGIS for further processing including field photographs.

2.4. *Invasive species*

In our study, we focused on BL. This deciduous tree has thick and deeply furrowed bark with stipular spines and alternate pinnately compound leaves. It flowers in May with distinct pendant large racemes of white flowers. In ideal conditions, it can grow up to 30 m tall, however, if water limited can take the shrubby dwarf appearance with unshaped crown and deformed trunk of 3–5 m.

It is native to the southeastern USA, listed amongst the 40 most invasive woody angiosperms globally (Richardson and Rejmánek 2011), categorized as highly invasive in several international databases (DAISIE, CABI, NOBANIS, EPPO, ISSG) and mentioned in national Black Lists in many countries (Nehring et al. 2013; Pergl et al. 2016). It was introduced to Europe at the beginning of the seventeenth century as an ornamental and soon became planted mainly thanks to its quality durable timber, fast growth, honey production, and ability to stabilize and restore sandy or degraded soils (Vítková et al. 2017). Its area is still increasing; currently, it is planted across Europe, temperate Asia, temperate South America, northern and southern Africa, Australia, and New Zealand (Cierjacks et al. 2013; Li et al. 2014). Despite economic benefits, it represents a serious threat to nature conservation.

BL is a light-demanding pioneer species able to disperse quickly over short distances (2 m per year; Crosti et al. 2016) by numerous root suckers forming a connected system with the mother plant (Kowarik 1996; Cierjacks et al. 2013). Deliberate planting and transport of soil containing seeds and roots represent the main vectors for its long-distance dispersal (Pyšek et al. 2012). It is extremely resistant to disturbance; mechanical damage of roots or trunks causes an increase in stem density and rejuvenation (Kowarik 1996). Moreover, it colonizes a broad range of xeric to mesic habitats, including steep rocks or toxic man-made substrata (Vítková and Kolbek 2010; Vítková, Tonika, and Müllerová 2015; Cierjacks et al. 2013). As a nitrogen fixing species living in symbiosis with *Rhizobium* bacteria (Batzli, Graves, and Berkum 1992) it increases soil nitrogen (Van Miegroet and Cole 1984; Vítková, Tonika, and Müllerová 2015), supporting expansion of nitrophilous plants (Vítková and Kolbek 2010). If invading grasslands, it can cause scrub encroachment and canopy closure due to its fast growth, influencing considerably the light and microclimatic conditions of invaded habitats. This is especially true for dry and semi-dry grasslands, sites of high natural value, where it can cause extinction of many endangered light-demanding plants and invertebrates (Kowarik 1996; Matus, Tóthmérész, and Papp 2003; Vítková and Kolbek 2010). Other threatened habitat types are open dry forests, scrublands, alluvial habitats, agrarian landscapes, urban and industrial environments, and disturbed sites, such as post-fire sites, forest clearings, and degraded forestry plantations. Removal of the species is costly and time-consuming, and requires repeated eradication measures and monitoring for at least three years due

to its exceptional resprouting ability. In central Europe, it is limited by late spring frost and short vegetation period (Vítková et al. 2017).

2.5. *Study area and analysed data*

Study area is located in central part of Czech Republic in typical central European agricultural landscape of flat lowlands surrounding the river Elbe. It consists of managed mixed forests surrounded by arable fields. Forests are composed of native oak forests with variable proportion of elm, Scots pine and lime, and plantations of Scots pine and BL (both in monocultures and admixture). Two sites named Kozlovice (site 1) and Podvlčí (site 2) were covered by repeated UAV campaigns using VUT 712 and VUT 713; Figure 7). In flat terrain of the study site 1 (37 ha; BL was used for stabilization of aeolian sands and is therefore planted in monocultures altered by monocultures of Scots pine or mixed stands with old native oaks. BL plantations are regenerated by coppicing in stripes. The study site 2 (30 ha) is a reclamation dump site from a nearby power station. BL stands are located on both slope and flat parts of the spoil tip, mostly in mixed stands with admixture of Scots pine, poplar, willow and birch. BL stands are unmanaged and younger compared to the site 1.

In classification, UAV imagery from 6 June 2015 was analysed for both sites (Figure 7). As a reference WorldView-2 (WV-2) satellite multispectral data were used with nominal spatial resolution of 2 m consisting of four standard bands (red, green, blue, and near-infrared), four additional bands (coastal, yellow, red edge, and near-infrared2) and

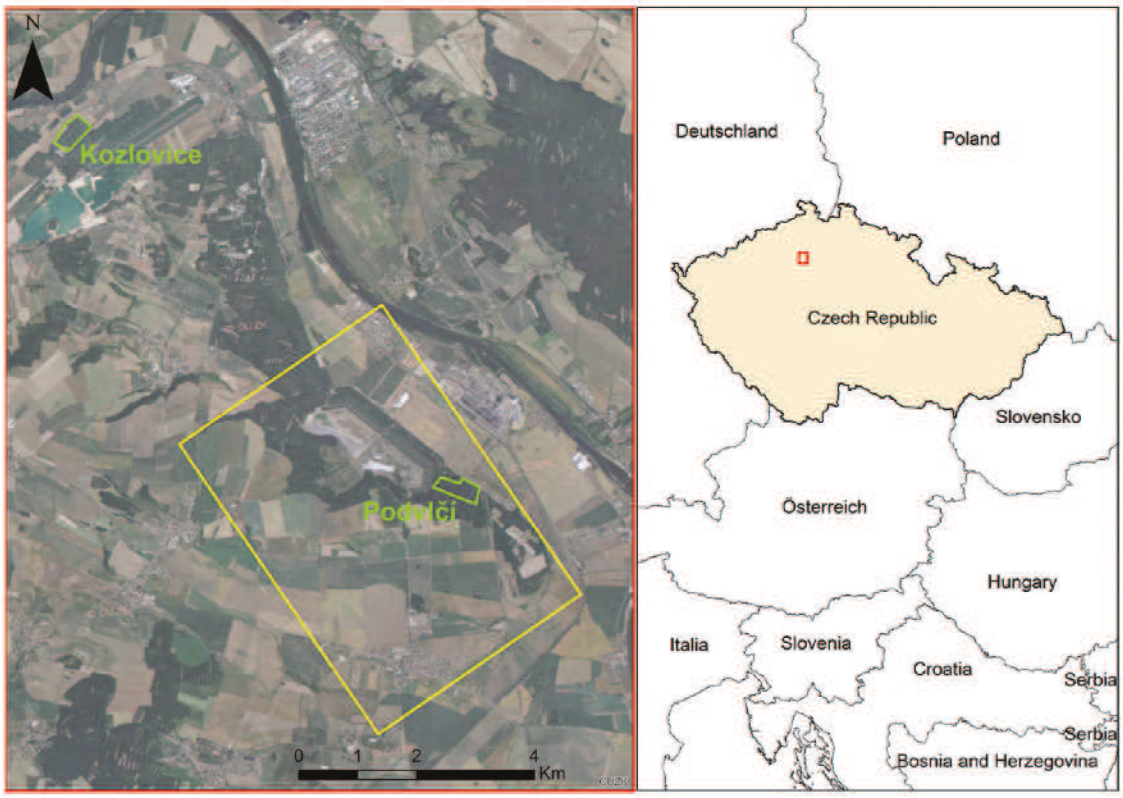


Figure 7. Study area with delineated areas of interest – Kozlovice (site 1) and Podvlčí (site 2). In green are UAV flights acquired on 6 July 2015 (both sites), in yellow is WorldView-2 imagery from 30 August 2013.

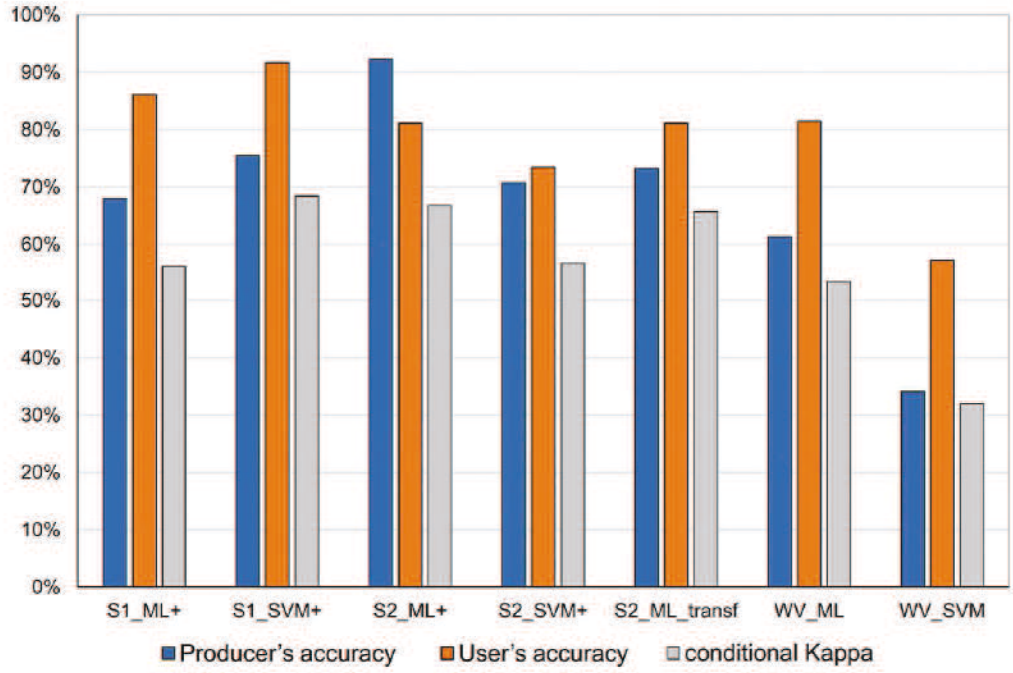


Figure 8. Classification accuracies of different data origin (UAV imagery of site 1 – S1 – and site 2 – S2, and WorldView 2 imagery – WV) and classification algorithms (ML: Maximum Likelihood; SVM: Support Vector Machines; +: DSM roughness included; 'transf': algorithm transferred from the site 1).

panchromatic channel with 0.5 m spatial resolution. The image was acquired on 30 August 2013 and covered the site 2 (Figure 8). RPC (Rational Polynomial Coefficients) metadata provided with the imagery and detailed DSM were used for orthorectification. The quality of spatial accuracy of the orthomosaic was visually inspected by comparison to national aerial orthophoto (CUZK 2015).

2.6. *Classification and validation*

Pixel-based approach was explored for classification. Supervised Maximum Likelihood (ML) and Support Vector Machines (SVM) algorithms were tested. Reason for choosing SVM was that this algorithm is supposed to be less susceptible to the noise and unbalanced or limited number/size of training sites (see Camps-Valls and Bruzzone 2009). Training classes were selected with the main purpose to distinguish amongst invasive BL and other types of vegetation. For each site and data, separate class signatures were generated, and subsequently the site 1 class signatures were applied to the UAV data from the site 2 acquired at the same day.

To include the texture (surface heterogeneity/roughness) and context of the classified pixel into the classification process, information on surface structure were derived from DSM generated as a by-product of UAV processing. Standard deviation and range of surface elevations parameters were tested using moving window of 5 × 5, 10 × 10, 50 × 50, and 100 × 100 pixels with range of 50 × 50 pixel window being the most informative. This information was included in classification as an additional layer. Due to geolocation inaccuracies of DSM and unavailability of detailed digital terrain model (DTM), precise vegetation height could not be calculated.

Validation was performed using 200 randomly distributed points at each site outside the training areas, with ca. half within the BL stands. User's accuracy (UA; ratio of the correctly classified and total classified, evaluating reliability of the results for the user), producer's accuracy (PA; ratio of the correctly classified and observed), and kappa analysis (conditional kappa index evaluating the statistical significance of the classifications, considers the actual agreement of the class in relation to the chance agreement, Congalton and Green 1999; Foody 2002) of BL detection were calculated from error matrices. Kappa statistics, despite the strong criticism due to the randomness used as a baseline (Pontius and Millones 2011), is still a widely used mean of the accuracy measure providing an opportunity to compare our results with other studies.

3. Detection results

The accuracies achieved for the invasive BL were very high, with UAV imagery providing better results (up to 92/81% and 75/92% PA/UA for site 1 and 2, respectively) compared to the satellite imagery (WV-2; up to 61/81% PA/UA). ML and SVM algorithms reached similarly high accuracies in most cases (Figures 8 and 9), still SVM seem to be less prone to the distortion artefacts of orthomosaic. Including surface roughness derived from DSM of UAV origin helped in discriminating forests from arable fields, since BL was sometimes misclassified as arable land; still it did not improve discrimination of BL and other tree species with similar surface heterogeneity values.

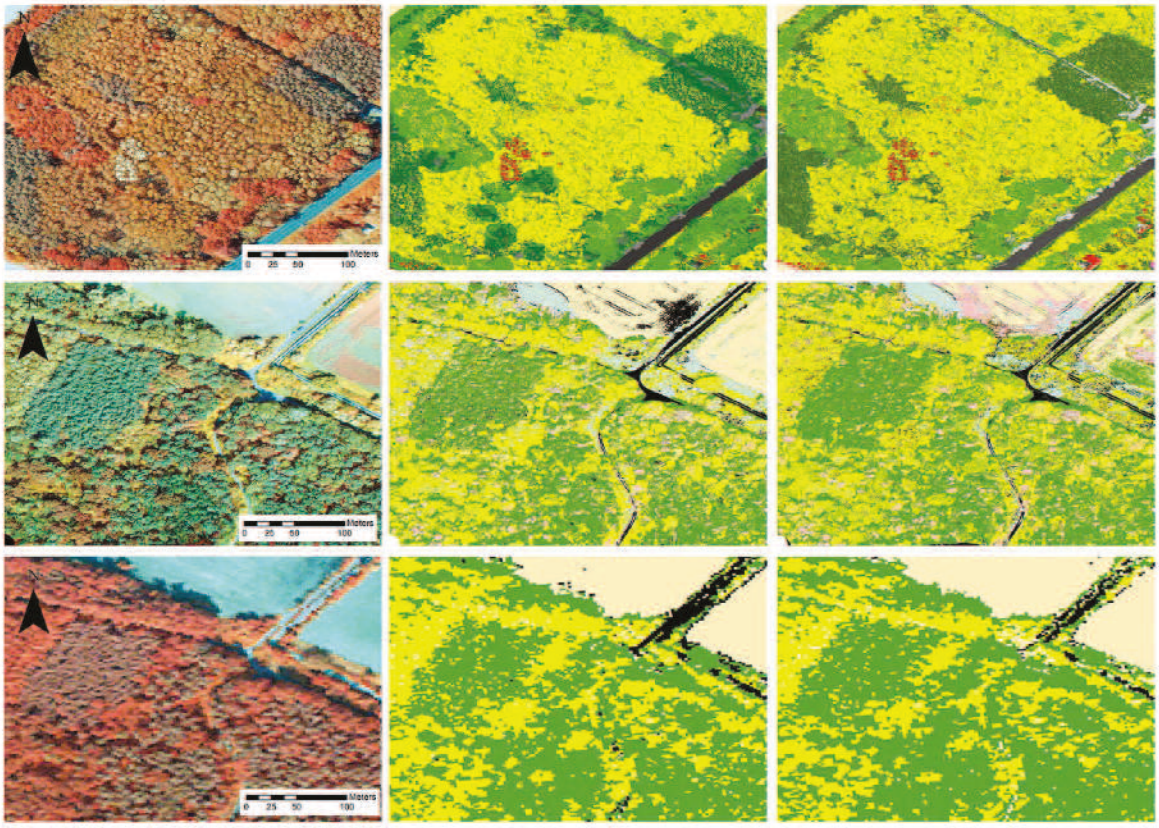


Figure 9. Classification of UAV site 1 and 2 (upper and middle rows, respectively) and WV-2 satellite imagery (lower row). False colour composites of the original imagery (NIR-G-B, left column), and results of ML classification (central column), and SVM (right column) are shown. BL yellow, BL flowering red, other tree species green, non-forest light brown, shadows grey and roads black.

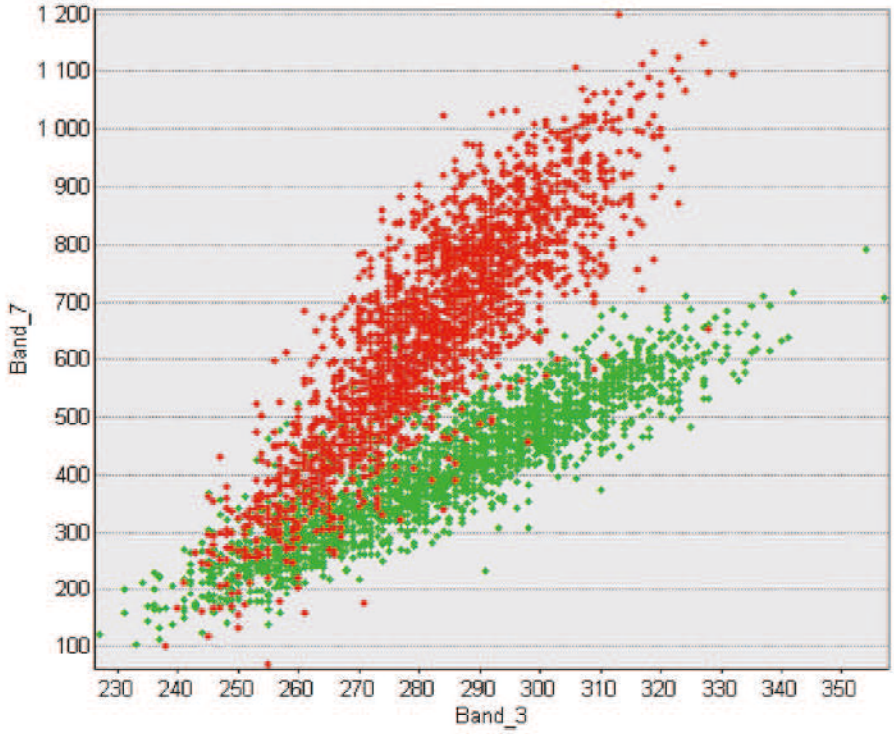


Figure 10. Separability of classes (BL: red; other tree species: green) shown on the scatterplot of green (band_3) and NIR 1 (band_7) bands of WV-2 satellite.

The spectral signatures derived from training classes at site 1 were applied to the classification of site 2 with moderate agreement of 73/81% PA/UA and 0.66 conditional kappa (for ML algorithm; SVM gave very poor results). Due to the differences in spectral sensitivities of sensors the signatures could not be transferred between UAV and satellite data. Also the class signatures incorporating the surface roughness did not give satisfactory results if applied from one site to the other.

The UAV flight campaign in 2015 was organized to capture BL in flower, however since the trees did not flower simultaneously even at the same site, only several trees were actually flowering on the orthomosaic (visible in white on Figure 9, uppermost part). Nevertheless this fact did not deteriorate the detection results, probably thanks to good separability from other tree species in NIR part of the spectrum based on leave and not only flower signatures (Figure 10).

4. Discussion

An important step in application of UAV approach in invasive monitoring seem to be generation of precise combined RGB + NIR orthomosaic from UAV images acquired during the flight campaign. This is because the NIR part of the spectrum is very important for the plant recognition as demonstrated here on case of BL. For further processing such as classification and validation, it is important to achieve high precision in both co-registration of the channels and geolocation of the imagery. The target accuracy should therefore meet the condition of possible inter-comparison with other EO sources as satellite imagery or repeated acquisition to avoid possible mismatches within the given target resolution for change monitoring.

In our research, we replaced an initial setup of separate RGB and NIR acquisition by continuous imaging of both spectra on the newer unmanned platform VUT 713. Since the image quality and positional accuracy were still not satisfactory, further adaptations were introduced to improve the overall quality. A differential global positioning system (DGPS) module was added to the autopilot setup to increase positional accuracy of camera stations. Raw GPS data stored in the autopilot log served as an input into the automated geotagging workflow along with CZEPOS correction data, ionosphere map, and shutter lag correction. This approach belongs to the post-processed kinematics (PPK) class of methods being currently employed by a growing number of commercial and academic bodies (Kais et al. 2005). Compared to the real-time kinematics approach, it is more robust, not relying on the datalink between rover and base stations. It also features lower cost due to less hardware required. The overall aim of the developed geotagging workflow is to eliminate laborious GCP collection and measurements for operational service. The distribution of reference GCPs may be limited by site disposition, for example, continuous tree cover may restraint the selection excluding the central forested part of the site.

The tests of different settings of DSM generation proved the advantage of our concept of DSM resampling to eliminate various defects caused by highly detailed DSM. Such procedure expelled most of the artefacts and thus reduced subsequent classification errors. Still further evaluation of parametrization during the data processing is needed to comprehensively evaluate the influence of partial processing steps on final imagery used for classification. Co-processing of both RGB and NIR imagery results in lower spatial accuracy than RGB orthomosaic alone and extend the time needed for its processing. However as demonstrated here, the NIR data are indispensable for BL classification and proper co-registration with RGB data is more important than the temporal co-registration.

Accuracy of invasive BL detection from UAV orthomosaics was very high, although values of acceptable classification accuracy presented in the literature differ considerably, ranging from 70% (Pringle et al. 2009) to 85% for PA and UA (Foody 2002), and 0.61 for kappa (Landis and Koch 1977). Our accuracies felt within this range, signifying good to excellent agreement. Lower accuracies for satellite WV-2 imagery were probably due to lower spatial resolution; still different timing could also play a role. This must be proved by further tests analysis of UAV imagery acquired in different periods of the vegetation season.

Measures of textural and spatial context can augment results of classification in case the spectral information is not sufficient (Wang et al. 2015), such as mixing arable land and BL stands (Somodi et al. 2012). Using range of elevation values instead of vegetation height derived by subtraction of DSM to existing DTM can overcame the problem of geolocation impreciseness, since it only defines relative differences within the defined neighbourhood. In case of abrupt change in surface height, such as at the border of forest/non forest, it brought noise into the classification, however since in our case non forest areas at the borders with forest were shaded (and classified as 'shade'), it did not influence the quality of the final results.

The timing of the data acquisition can be crucial in plant detection, since plants are often best recognized during flowering time (Everitt, Escobar, and Davis 2001; Müllerová,

Pergl, and Pyšek 2013). According to Somodi et al. (2012), BL is the best separable during flowering however this approach has following drawbacks impeding practical application: (a) BL individuals do not flower exactly at the same time even at the same site, and (b) the time window for flowering is very short (1–2 weeks) and difficult to predict (depending very much on May temperatures in particular year). In our study we found that if the data provide high spatial detail (UAV) and include NIR band, the species is separable very well even if not flowering. Importance of NIR band for discrimination of vegetation was reported from previous studies (Everitt, Yang, and Deloach 2005; Wang et al. 2015).

In our further research we would like to explore the potential benefits of sequence of orthomosaics with different timing in discriminating tree species (such as in Hill et al. 2010). For this approach precise georeferencing is indispensable, therefore, we will continue testing the methodology of data pre-processing to make the workflow as simple and automatic as possible (reducing the manual input such as GCP collection) and robust at the same time. Reduction of geometric distortions on the UAV orthomosaics will enable us to test the object-based approach accounting for the spatial structure and context information (Blaschke 2010). This approach is expected to improve the results by reducing the effects of shadows, within-class spectral variation and miss-registration (Laliberte, Browning, and Rango 2012; Tewkesbury et al. 2015).

5. Conclusions

The article presents and discusses application of low cost UAV technology in environmental monitoring. Our study showed that UAV data are well suitable for detection of selected invasive species (BL in our case), still processing of the data (mainly creation of the orthomosaic) can be problematic and must be handled with care. We provide evidence that good results can be obtained using a low cost solution of unmanned system composed from affordable off-the-shelf components such as radio controlled (RC) airplanes and consumer cameras modified for RGB/NIR spectrum in case the right methodology is applied to the important steps of image acquisition, pre-processing (mosaicking and georeferencing), ground-truthing and classification. For practical application of this novel, flexible and cheap tool in plant invasion management as well as other environmental actions, well proven and tested methodology is crucial, and our study brings insights in this area.

Acknowledgements

The research was supported by TAČR TA0402045, the Praemium Academiae award to P. Pyšek from the Czech Academy of Sciences, was part of long-term research development project number RVO 67985939 and received funding from the MEYS under the National Sustainability Programme I (project LO1202).

Disclosure statement

No potential conflict of interest was reported by the authors.

Funding

The research was supported by TAČR TA0402045, the Praemium Academiae award to P. Pyšek from the Czech Academy of Sciences, was part of long-term research development project number RVO 67985939 and received funding from the MEYS under the National Sustainability Programme I (project LO1202).

ORCID

Tomáš Bartaloš http://orcid.org/0000-0003-3270-0995

References

Agisoft. 2016. Agisoft PhotoScan. Accessed September 25 2016. http://www.agisoft.com/

Batzli, J. M., W. R. Graves, and P. Berkum. 1992. "Diversity among Rhizobia Effective with Robinia Pseudoacacia." *Applied and Environmental Microbiology* 58 (7): 2137–2143.

Blaschke, T. 2010. "Object Based Image Analysis for Remote Sensing." *ISPRS Journal of Photogrammetry and Remote Sensing* 65 (1): 2–16. doi:10.1016/j.isprsjprs.2009.06.004.

Bradley, B. A. 2014. "Remote Detection of Invasive Plants: A Review of Spectral, Textural and Phenological Approaches." *Biological Invasions* 16 (7): 1411–1425. doi:10.1007/s10530-013-0578-9.

Buchanan, G. M., A. B. Brink, A. K. Leidner, R. Rose, and M. Wegmann. 2015. "Advancing Terrestrial Conservation through Remote Sensing." *Ecological Informatics* 30: 318–321. doi:10.1016/j.ecoinf.2015.05.005.

C., H., and G. P. Asner. 2009. "Applications of Remote Sensing to Alien Invasive Plant Studies." *Sensors* 9: 4869–4889. doi:10.3390/s90604869.

Camps-Valls, G., and L. Bruzzone, eds. 2009. *Kernel Methods for Remote Sensing Data Analysis*. UK: Wiley & Sons. doi:10.1002/9780470748992.fmatter.

CHDK. 2013. Canon Hack Development Kit. Accessed September 7 2013 http://chdk.wikia.com/wiki/CHDK

Cierjacks, A., I. Kowarik, J. Joshi, S. Hempel, M. Ristow, M. Von Der Lippe, and E. Weber. 2013. "Biological Flora of the British Isles: Robinia Pseudoacacia." *The Journal of Ecology* 101: 1623–1640. doi:10.1111/1365-2745.12162.

Colomina, I., and P. Molina. 2014. "Unmanned Aerial Systems for Photogrammetry and Remote Sensing: A Review." *ISPRS Journal of Photogrammetry and Remote Sensing* 92: 79–97. doi:10.1016/j.isprsjprs.2014.02.013.

Congalton, R. G., and K. Green. 1999. *Assessing the Accuracy of Remotely Sensed Data: Principles and Practices*. New York:: Lewis Publishers.

Crosti, R., E. Agrillo, L. Ciccarese, R. Guarino, P. Paris, and A. Testi. 2016. "Assessing Escapes from Short Rotation Plantations of the Invasive Tree Species Robinia Pseudoacacia L. in Mediterranean Ecosystems: A Study in Central Italy." *Iforest-Biogeosciences and Forestry* 743. doi:10.3832/ifor1526-009.

CUZK. 2015. Orthophoto of the Czech Republic 2015. Accessed July 25 2016. http://geoportal.cuzk.cz/WMS_ORTOFOTO_PUB/WMService.aspx

Dandois, J. P., and E. C. Ellis. 2010. "Remote Sensing of Vegetation Structure Using Computer Vision." *Remote Sensing* 2: 1157–1176. doi:10.3390/rs2041157.

DigitalGlobe. 2016. Accessed September 25 2016. http://global.digitalglobe.com/sites/default/files/DigitalGlobe_Spectral_Response_1.pdf

Dvořák, P., J. Müllerová, T. Bartaloš, and J. Brůna. 2015. "Unmanned Aerial Vehicles for Alien Plant Species Detection and Monitoring." *International Archives Photogramm Remote Sens Spatial Information Sciences* XL-1/W4: 83–90. doi:10.5194/isprsarchives-XL-1-W4-83-2015.

Ehrenfeld, J. G. 2010. "Ecosystem Consequences of Biological Invasions." *Annual Review of Ecology, Evolution and Systematics* 41: 59–80. doi:10.1146/annurev-ecolsys-102209-144650.

European Commission. 2008. "Towards an EU Strategy on Invasive Species." COM 789. Brussels: EC.
European Commission. 2014. "Regulation on the Prevention and Management of the Introduction and Spread of Invasive Alien Species." COM 1143/2014. Brussels: EC.
Everitt, J. H., D. E. Escobar, and M. R. Davis. 2001. "Reflectance and Image Characteristics of Selected Noxious Rangeland Species." *Journal Range Manage* 54: A106–A120. doi:10.2307/4003193.
Everitt, J. H., C. Yang, and C. J. Deloach. 2005. "Remote Sensing of Giant Reed with Quickbird Satellite Imagery." *Journal of Aquatic Plant Management* 43: 81–85.
Foody, G. M. 2002. "Status of Land Cover Classification Accuracy Assessment." *Remote Sensing of Environment* 80: 185–201. doi:10.1016/S0034-4257(01)00295-4.
Hamada, Y., D. A. Stow, L. L. Coulter, J. C. Jafolla, and L. W. Hendricks. 2007. "Detecting Tamarisk Species (Tamarix Spp.) in Riparian Habitats of Southern California Using High Spatial Resolution Hyperspectral Imagery." *Remote Sensing of Environment* 109: 237–248. doi:10.1016/j.rse.2007.01.003.
Hantson, W., L. Kooistra, P. A. Slim, and G. Henebry. 2012. "Mapping Invasive Woody Species in Coastal Dunes in the Netherlands: A Remote Sensing Approach Using LIDAR and High-Resolution Aerial Photographs." *Appl Veg Sci* 15 (4): 536–547. doi:10.1111/j.1654-109X.2012.01194.x.
Hill, R. A., A. K. Wilson, M. George, and S. A. Hinsley. 2010. "Mapping Tree Species in Temperate Deciduous Woodland Using Time-Series Multi-Spectral Data." *Applied Vegetation Science* 13: 86–99. doi:10.1111/j.1654-109X.2009.01053.x.
Hulme, P. E., P. Pyšek, W. Nentwig, and M. Vilà. 2009. "Will Threat of Biological Invasions Unite the European Union?" *Science* 324: 40–41. doi:10.1126/science.1171111.
Kais, M., P. Bonnifait, D. Bétaille, and F. Peyret. 2005. "Development of Loosely-Coupled FOG/DGPS and FOG/RTK Systems for ADAS and a Methodology to Assess Their Real-Time Performances." In *IEEE Proceedings, Intelligent Vehicles Symposium*, 358–363. IEEE.
KAP. 2015. KAP UAV Exposure Control Script. Accessed April 12 2015. http://chdk.wikia.com/wiki/KAP_UAV_Exposure_Control_Script
Kowarik, I. 1996. "Funktionen Klonalen Wachstums Von Bäumen Bei Der Brachflächen-Sukzession Unter Besonderer Beachtung Von." *Robinia Pseudoacacia. Verhandlungen Der Gesellschaft Für Ökologie* 26: 173–181.
Laliberte, A. S., D. M. Browning, and A. Rango. 2012. "A Comparison of Three Feature Selection Methods for Object-Based Classification of Sub-Decimeter Resolution Ultracam-L Imagery." *International Journal of Applied Earth Observation and Geoinformation* 15: 70–78. doi:10.1016/j.jag.2011.05.011.
Landis, J., and G. Koch. 1977. "The Measurement of Observer Agreement for Categorical Data." *Biometrics* 33: 159–174. doi:10.2307/2529310.
Lawes, R. A., and J. F. Wallace. 2008. "Monitoring an Invasive Perennial at the Landscape Scale with Remote Sensing." *Ecological Management & Restoration* 9 (1): 53–59. doi:10.1111/j.1442-8903.2008.00387.x.
Li, G., G. Xu, K. Guo, and S. Du. 2014. "Mapping the Global Potential Geographical Distribution of Black Locust (Robinia Pseudoacacia L.) Using Herbarium Data and a Maximum Entropy Model." *Forests* 5: 2773–2792. doi:10.3390/f5112773.
Marvin, D. C., L. P. Koh, A. J. Lynam, S. Wich, A. B. Davies, R. Krishnamurthy, E. Stokes, R. Starkey, and G. P. Asner. 2016. "Integrating Technologies for Scalable Ecology and Conservation." *Global Ecology and Conservation* 7: 262–275. doi:10.1016/j.gecco.2016.07.002.
Matus, G., B. Tóthmérész, and M. Papp. 2003. "Restoration Prospects of Abandoned Species-Rich Sandy Grassland in Hungary." *Applied Vegetation Science* 6 (2): 169–178. doi:10.1111/j.1654-109X.2003.tb00577.x.
Müllerová, J., J. Brůna, P. Dvořák, T. Bartaloš, and M. Vítková. 2016. "Does the Data Resolution/Origin Matter? Satellite, Airborne and Uav Imagery to Tackle Plant Invasions." *International Archives Photogramm Remote Sens Spatial Information Sciences* XLI-B7: 903–908. doi:10.5194/isprsarchives-XLI-B7-903-2016.

Müllerová, J., J. Pergl, and P. Pyšek. 2013. "Remote Sensing as a Tool for Monitoring Plant Invasions: Testing the Effects of Data Resolution and Image Classification Approach on the Detection of a Model Plant Species Heracleum Mantegazzianum (Giant Hogweed)." *International Journal of Applied Earth Observation and Geoinformation* 25: 55–65. doi:10.1016/j.jag.2013.03.004.

Müllerová, J., P. Pyšek, V. Jarošík, and J. Pergl. 2005. "Aerial Photographs as a Tool for Assessing the Regional Dynamics of the Invasive Plant Species Heracleum Mantegazzianum." *Journal of Applied Ecology* 42: 1042–1053. doi:10.1111/j.1365-2664.2005.01092.x.

Nehring, S., I. Kowarik, W. Rabitsch, and F. Essl. 2013. "Naturschutzfachliche Invasivitätsbewertungen Für in Deutschland Wild Lebende Gebietsfremde Gefäßpflanzen. Naturschutzfachliche Invasivitäts-Bewertungen Für in Deutschland Wild Lebende Gebietsfremde Gefäßpflanzen. Bonn: Bundesamt Für Naturschutz." *BfN-Skripten* 352: 168–169.

Pergl, J., J. Sádlo, A. Petrusek, Z. Laštůvka, J. Musil, I. Perglová, R. Šanda, et al. 2016. "Black, Grey and Watch Lists of Alien Species in the Czech Republic Based on Environmental Impacts and Management Strategy." *NeoBiota* 28: 1–37. doi:10.3897/neobiota.28.4824.

Pimentel, D., R. Zuniga, and D. Morrison. 2005. "Update on the Environmental and Economic Costs Associated with Alien-Invasive Species in the United States." *Ecological Economics* 52 (3): 273–288. doi:10.1016/j.ecolecon.2004.10.002.

Pluess, T., R. Cannon, V. Jarošík, J. Pergl, P. Pyšek, and S. Bacher. 2012. "When are Eradication Campaigns Successful? A Test of Common Assumptions." *Biological Invasions* 14: 1365–1378. doi:10.1007/s10530-011-0160-2.

Pontius, R. G., and M. Millones. 2011. "Death to Kappa: Birth of Quantity Disagreement and Allocation Disagreement for Accuracy Assessment." *International Journal of Remote Sensing* 32: 4407–4429. doi:10.1080/01431161.2011.552923.

Pringle, R. M., M. Syfert, J. K. Webb, and R. Shine. 2009. "Quantifying Historical Changes in Habitat Availability for Endangered Species: Use of Pixel- and Object-Based Remote Sensing." *Journal of Applied Ecology* 46: 544–553. doi:10.1111/j.1365-2664.2009.01637.x.

Pyšek, P., M. Chytrý, J. Pergl, J. Sádlo, and J. Wild. 2012. "Plant Invasions in the Czech Republic: Current State, Introduction Dynamics, Invasive Species and Invaded Habitats." *Preslia* 84: 575–629.

Pyšek, P., and D. M. Richardson. 2010. "Invasive Species, Environmental Change and Management, and Health." *Annual Review of Environment and Resources* 35: 25–55. doi:10.1146/annurev-environ-033009-095548.

Rejmánek, M. 2000. "Invasive Plants: Approaches and Predictions." *Austral Ecology* 25: 497–506. doi:10.1046/j.1442-9993.2000.01080.x.

Richardson, D. M., and M. Rejmánek. 2011. "Trees and Shrubs as Invasive Alien Species–A Global Review." *Diversity and Distributions* 17 (5): 788–809. doi:10.1111/j.1472-4642.2011.00782.x.

Rocchini, D., V. Andreo, M. Förster, C. X. Garzon-Lopez, A. P. Gutierrez, T. W. Gillespie, H. C. Hauffe, et al. 2015. "Potential of Remote Sensing to Predict Species Invasions: A Modelling Perspective." *Progress in Physical Geography* 39: 283–309. doi:10.1177/0309133315574659.

RTKLIB: An Open Source Program Package for GNSS Positioning. Accessed July 20 2016. http://www.rtklib.com.

Somodi, I., A. Čarni, D. Ribeiro, and T. Podobnikar. 2012. "Recognition of the Invasive Species Robinia Pseudacacia from Combined Remote Sensing and GIS Sources." *Biological Conservation* 150: 59–67. doi:10.1016/j.biocon.2012.02.014.

Tewkesbury, A. P., A. J. Comber, N. J. Tate, A. Lamb, and P. F. Fisher. 2015. "A Critical Synthesis of Remotely Sensed Optical Image Change Detection Techniques." *Remote Sensing of Environment* 160: 1–14. doi:10.1016/j.rse.2015.01.006.

Turner, D., A. Lucieer, and C. Watson. 2012. "An Automated Technique for Generating Georectified Mosaics from Ultra-High Resolution Unmanned Aerial Vehicle (UAV) Imagery, Based on Structure from Motion (Sfm) Point Clouds." *Remote Sensing* 4 (5): 1392–1410. doi:10.3390/rs4051392.

Van Kleunen, M., W. Dawson, F. Essl, J. Pergl, M. Winter, E. Weber, H. Kreft, et al. 2015. "Global Exchange and Accumulation of Non-Native Plants." *Nature* 525: 100–103. doi:10.1038/nature14910.

Van Miegroet, H., and D. W. Cole. 1984. "The Impact of Nitrification on Soil Acidification and Cation Leaching in a Red Alder Ecosystem." *Journal of Environment Quality* 13: 586–590. doi:10.2134/jeq1984.00472425001300040015x.

Vilà, M., and I. Ibáñez. 2011. "Plant Invasions in the Landscape." *Landscape Ecology* 26: 461–472. doi:10.1007/s10980-011-9585-3.

Vítková, M., and J. Kolbek. 2010. "Vegetation Classification and Synecology of Bohemian *Robinia Pseudacacia* Stands in a Central European Context." *Phytocoenologia* 40 (2–3): 205–241. doi:10.1127/0340-269X/2010/0040-0425.

Vítková, M., J. Müllerová, J. Sádlo, J. Pergl, and P. Pyšek. 2017. "Black Locust (Robinia Pseudoacacia) Beloved and Despised: A Story of an Invasive Tree in Central Europe." *Forest Ecology and Management* 384: 287–302. doi:10.1016/j.foreco.2016.10.057.

Vítková, M., J. Tonika, and J. Müllerová. 2015. "Black Locust-Successful Invader of a Wide Range of Soil Conditions." *Science of the Total Environment* 505: 315–328. doi:10.1016/j.scitotenv.2014.09.104.

Wang, H., Y. Zhao, R. Pu, and Z. Zhang. 2015. "Mapping *Robinia Pseudoacacia* Forest Health Conditions by Using Combined Spectral, Spatial, and Textural Information Extracted from IKONOS Imagery and Random Forest Classifier." *Remote Sensing* 7 (7): 9020–9044. doi:10.3390/rs70709020.

Westoby, M. J., J. Brasington, N. F. Glasser, M. J. Hambrey, and J. M. Reynolds. 2012. "Structure-From-Motion Photogrammetry: A Lowcost, Effective Tool for Geoscience Applications." *Geomorphology* 179: 300–314. doi:10.1016/j.geomorph.2012.08.021.

Whitehead, K., and C. H. Hugenholtz. 2014. "Remote Sensing of the Environment with Small Unmanned Aircraft Systems (Uass), Part 1: A Review of Progress and Challenges 1." *Journal of Unmanned Vehicle Systems* 2 (3): 69–85. doi:10.1139/juvs-2014-0006.

Whitehead, K., C. H. Hugenholtz, S. Myshak, O. Brown, A. LeClair, A. Tamminga, T. E. Barchyn, B. Moorman, and B. Eaton. 2014. "Remote Sensing of the Environment with Small Unmanned Aircraft Systems (Uass), Part 2: Scientific and Commercial Applications 1." *Journal of Unmanned Vehicle Systems* 2 (3): 86–102. doi:10.1139/juvs-2014-0007.

Zweig, C. L., M. A. Burgess, H. F. Percival, and W. M. Kitchens. 2015. "Use of Unmanned Aircraft Systems to Delineate Fine-Scale Wetland Vegetation Communities." *Wetlands* 35: 303–309. doi:10.1007/s13157-014-0612-4.

Paper V



Müllerová, J., Brůna, J., Bartaloš, T., Dvořák, P., Vítková, M., Pyšek, P. (2017)

Timing is important: unmanned aircraft versus satellite imagery in plant invasion monitoring

Frontiers in Plant Science 8 (May):1-13. doi: 10.3389/fpls.2017.00887

frontiers in Plant Science

ORIGINAL RESEARCH
published: 31 May 2017
doi: 10.3389/fpls.2017.00887

Timing Is Important: Unmanned Aircraft vs. Satellite Imagery in Plant Invasion Monitoring

Jana Müllerová[1], Josef Brůna[1,2], Tomáš Bartaloš[3], Petr Dvořák[4], Michaela Vítková[1] and Petr Pyšek[1,5]*

[1] Institute of Botany, The Czech Academy of Sciences, Průhonice, Czechia, [2] Faculty of Science, Institute for Environmental Studies, Charles University, Prague, Czechia, [3] GISAT Ltd., Prague, Czechia, [4] Institute for Aerospace Engineering, Brno University of Technology, Brno, Czechia, [5] Department of Ecology, Faculty of Science, Charles University, Prague, Czechia

The rapid spread of invasive plants makes their management increasingly difficult. Remote sensing offers a means of fast and efficient monitoring, but still the optimal methodologies remain to be defined. The seasonal dynamics and spectral characteristics of the target invasive species are important factors, since, at certain time of the vegetation season (e.g., at flowering or senescing), plants are often more distinct (or more visible beneath the canopy). Our aim was to establish fast, repeatable and a cost-efficient, computer-assisted method applicable over larger areas, to reduce the costs of extensive field campaigns. To achieve this goal, we examined how the timing of monitoring affects the detection of noxious plant invaders in Central Europe, using two model herbaceous species with markedly different phenological, structural, and spectral characteristics. They are giant hogweed (*Heracleum mantegazzianum*), a species with very distinct flowering phase, and the less distinct knotweeds (*Fallopia japonica*, *F. sachalinensis,* and their hybrid *F.* × *bohemica*). The variety of data generated, such as imagery from purposely-designed, unmanned aircraft vehicle (UAV), and VHR satellite, and aerial color orthophotos enabled us to assess the effects of spectral, spatial, and temporal resolution (i.e., the target species' phenological state) for successful recognition. The demands for both spatial and spectral resolution depended largely on the target plant species. In the case that a species was sampled at the most distinct phenological phase, high accuracy was achieved even with lower spectral resolution of our low-cost UAV. This demonstrates that proper timing can to some extent compensate for the lower spectral resolution. The results of our study could serve as a basis for identifying priorities for management, targeted at localities with the greatest risk of invasive species' spread and, once eradicated, to monitor over time any return. The best mapping strategy should reflect morphological and structural features of the target plant and choose appropriate spatial, spectral, and temporal resolution. The UAV enables flexible data acquisition for required time periods at low cost and is, therefore, well-suited for targeted monitoring; while satellite imagery provides the best solution for larger areas. Nonetheless, users must be aware of their limits.

Keywords: alien species, giant hogweed, knotweed, plant phenology, remote sensing detection, UAV

OPEN ACCESS

Edited by:
Nancy F. Glenn,
Boise State University, United States

Reviewed by:
Francisco Artigas,
Meadowlands Environmental Research Institute, United States
Vicky M. Temperton,
Lüneburg University, Germany

****Correspondence:***
Jana Müllerová
jana.mullerova@ibot.cas.cz

Specialty section:
This article was submitted to Functional Plant Ecology, a section of the journal Frontiers in Plant Science

Received: *15 December 2016*
Accepted: *11 May 2017*
Published: *31 May 2017*

Citation:
Müllerová J, Brůna J, Bartaloš T, Dvořák P, Vítková M and Pyšek P (2017) Timing Is Important: Unmanned Aircraft vs. Satellite Imagery in Plant Invasion Monitoring. Front. Plant Sci. 8:887. doi: 10.3389/fpls.2017.00887

INTRODUCTION

Invasive species are considered among the major drivers of global change and are threats to biodiversity, ecosystem services, the economy, and human health (Pyšek and Richardson, 2010; Vilà et al., 2010). Early monitoring and rapid action at the operational level are therefore needed to mitigate the consequences of plant invasions (Kaiser and Burnett, 2010). Thanks to the availability of high spatial-resolution data, remote sensing (RS) is being increasingly used to study and model the spread of invasive plant species (Pergl et al., 2011; Somers and Asner, 2013; Rocchini et al., 2015), their phenology (Ge et al., 2006), and impacts (Asner et al., 2008). Most of the RS studies focus on invasive trees and shrubs (e.g., Frazier and Wang, 2011; Masocha and Skidmore, 2011), but the accurate detection of herbaceous plant species is challenging owing to their smaller size and patchiness. In this sense, invasive plant species are easier to handle compared to native ones since they usually grow vigorously, produce a great amount of biomass, and dominate the canopy, often forming extensive monospecific stands (Maheu-Giroux and de Blois, 2004; Huang and Asner, 2009; Müllerová et al., 2013). There continues to be a need for data of sufficient quality and resolution, especially where the target species is less distinct from other vegetation, or covered by it.

It has been shown that the timing of data acquisition plays an important role (Laba et al., 2005) since plants are often more distinct from the surrounding vegetation at certain times of the vegetation season (Andrew and Ustin, 2008; Rocchini et al., 2015), mostly during flowering (Müllerová et al., 2005, 2013; Andrew and Ustin, 2006; Ge et al., 2006) or leaf coloring (Shouse et al., 2013). Using a change detection approach, some species can be recognized by the differences in their life cycle compared to the background vegetation (Peterson, 2005; McEwan et al., 2009). Such adaptation is quite common in plant invasions, since the mismatch of phenology between native and exotic species can provide benefit to invaders outcompeting the natives by using the time window available via extending or shifting the growing season (Wolkovich and Cleland, 2011; Fridley, 2012; Gioria et al., 2016). Phenological differences influencing the RS detection include also the seasonal development of broad-leaved tree canopies, because the target species in the understory may be detectable only before emergence and after the leaf senescence of the canopy vegetation (Resasco et al., 2007; Wilfong et al., 2009). Thus, the seasonal dynamics and spectral behavior of the target species and their surrounding constitute important parameters in the RS detection process.

To study the role of phenology on RS detection of invasive species, it is necessary to acquire data at certain phenological phases, as well as with suitable spatial and spectral resolution. Freely available satellite data such as MODIS, Landsat or Sentinel do not provide appropriate spatial resolution for a highly heterogeneous Central European landscape where the occurrence of invasive plant populations is rather patchy. Very high resolution (VHR) satellites such as Pleiades, QuickBird, Ikonos, or WorldView are costly to acquire, and in all cases the acquisition of suitable data is constrained by clouds and the regular trajectory of the satellite. Aerial campaigns offer some flexibility, but they must still be planned in advance, with uncertainty in weather forecasting being a factor, and they are also costly. If relying on the archives of aerial imagery, the choice of phenology phases is limited and spectral resolution is usually low. New means such as unmanned aircraft vehicles (UAV) provide high flexibility, low price, and easy deployment (Watts et al., 2012), but rather low spectral resolution (RGB + modified NIR bands with modified consumer cameras if cheap solution is considered), and due to geometric and radiometric irregularities they require complex processing (Rango et al., 2009; Laliberte et al., 2010; Salamí et al., 2014; Müllerová et al., 2017). At the same time, the large amount of data collected by UAVs brings about the need for automatic processing. Legal constraints limiting use of UAVs only to unpopulated areas further reduce their applicability (Watts et al., 2012). This is especially problematic for invasive species that tend to prefer urban areas (Pyšek, 1998; Kowarik, 2008). Moreover, extremely high detail of UAV data generates problems with precise location of validation data due to the limits of available GNSS instruments (especially in forested or hilly environments). Still, despite these limits, the UAV technology holds great potential for invasive species assessment and monitoring (Calviño-Cancela et al., 2014; Michez et al., 2016; Müllerová et al., 2016, 2017; **Table 1**).

To demonstrate the role of timing and resolution for the RS detection of invasive plants, we chose two model herbaceous species with markedly different phenological, structural, and spectral characteristics. They are the giant hogweed (*Heracleum mantegazzianum*), a species with a very distinct flowering phase, during which it forms large white circular inflorescences, and knotweeds (*Fallopia japonica, F. sachalinensis,* and their hybrid *F.* × *bohemica*), lacking such distinct features. High flexibility of the data acquisition provided by small UAV (in our case a custom-built one producing imagery of 5 cm spatial and multispectral resolution of RGB + modified NIR) enabled us to study the role of phenology. The results were compared with those of multispectral satellite imagery of 50 cm resolution using several approaches (pixel- and object-based) and data from different parts of the vegetation season to find a repeatable, efficient, and low-cost monitoring strategy (in terms of data source, processing approach and target species' phenological stage). Our aims were to: (a) assess the role of timing and both the spectral and spatial resolution in detection of the two structurally and phenologically different invasive species, (b) define the optimal phenological stage (time window) and data resolution, and (c) describe the computer-assisted workflow of the image-processing to achieve the highest detection rate. Our recommended methodology, operational in environmental monitoring and applicable over large areas, can be used for nature conservation, with the potential to reduce the costs of extensive field campaigns.

METHODS

Study Species

To study the different aspects important for their recognition, we chose model herbaceous invasive species differing in

Abbreviations: GNSS, Global Navigation Satellite System; PA, producer's accuracy; RF, random forests; RS, remote sensing; SVM, support vector machine; UA, user's accuracy; VHR, very high resolution.

TABLE 1 | Advantages and constraints of different types of remote sensing imagery in invasive species monitoring.

	NASA and ESA satellites	VHR satellites	Aerial	UAV
Timing (flexibility)	No flexibility, but extensive archive	Low	Medium	**High**
Resolution	Down to 10 m	Down to 0.3–0.4 m	0.1–0.5 m	**up to 1 cm**
Financial costs of imagery	**No**	High	High	**Low**
Acquisition	**Easy—available for download**	**Easy—commercial order**	**Easy—commercial order**	Some expertise needed
Pre-processing	**Standardized**	**Standardized**	**Standardized**	Not standardized, complex
Weather constraints—cloudy sky	Impossible	Impossible	Impossible	**Only possible in case of high clouds and no rain**
Weather constraints—wind	**No influence**	**No influence**	Strong wind is problematic	Very problematic
Legal constraints	**No**	**No**	Few	Many constraints (e.g., in urban areas, private land, commercial zones, around airports...)
Data volume	**Moderate**	High	High	High/very high
Spectral resolution	**High**	**High**	Low (medium)	Medium (depend on camera)
Temporal resolution	**High**	Moderate	Low	**High**

The best options are highlighted in bold.

TABLE 2 | Remote sensing detection of the two target species—their important characteristics, imagery required for the analysis and the best processing approach.

Species		*Heracleum mantegazzianum* (giant hogweed)	*Fallopia* sp. (knotweeds)
Foliage structure		Large, deeply incised leaves	Variable leaves, forming dense stands
Inflorescence		Large, distinct	Small, insignificant
Type of habitat infested		Unmanaged grasslands, abandoned land, riverbanks, sparse forest and field edges, ruderal habitats	Riverbanks, unmanaged grasslands, disturbed sites, sparse forests, urban areas
Optimal phenological stage for RS detection		Peak of flowering	Senescence
Optimal period of the data acquisition (CR)		2nd half of June—1st half of July	End of October, beginning of November
Detection efficiency		Very high	High
Imagery tested		UAV (RGB+NIR; 5 cm); Pleiades 1B (MSS; 50 cm); color orthophoto (RGB; 25 cm)	UAV (RGB+NIR; 5 cm and 50 cm); Pleiades 1B (MSS; 50 cm)
Data resolution required	Spatial	<50 cm	<50 cm
	Spectral	Low	Moderate (NIR)
	Temporal	Right timing important (1 month period)	Right timing important (1 month period)
Optimal approach		Object-based	Pixel-based

plant architecture and spectral dynamics: giant hogweed and knotweeds (**Table 2**). These plants are among the most serious plant invaders in Europe (DAISIE, 2012).

The giant hogweed (*H. mantegazzianum* Sommier and Levier, Apiaceae family), native to Caucasus Mountains, is an example of a species that is distinct from both the spectral and the structural point of view, with pronounced dynamics of seasonal development (flowering). It is the biggest herbaceous plant in Central Europe (2–5 m in height with leaves up to 2.5 m long), forming large white circular inflorescences of compound umbels (up to 80 cm wide; Page et al., 2006; Perglová et al., 2006). As a perennial monocarpic species it flowers once in a lifetime, mostly in the third year (Pergl et al., 2006); in the Czech Republic, the flowering season is from late June to early August (Perglová et al., 2006). The white inflorescences are distinct, but non-flowering plants are problematic to detect. Although, the species invades mostly unmanaged grasslands and anthropogenic habitats, and forms large monospecific populations, it also occurs at forest margins or in forest interiors where RS detection is difficult (**Table 2**). The same is true for grazed or mown plants, that survive as ground rosettes that do not flower or, if they do, it is late in the season and inflorescences are very small (Müllerová et al., 2013).

Knotweeds [*F. japonica* Houtt., *F. sachalinensis* (F. Schmidt) Nakai, and their hybrid *F.* × *bohemica* Chrtek and Chrtková] are example of species that are difficult to recognize by RS means because they form dense stands, relatively indistinct from similar vegetation types; the flowers are in white clustered racemes that appear from July to September in the Czech Republic. Morphological differences between the above-listed knotweeds are too subtle from the RS perspective to separate the two species and their hybrid. They are stout herbaceous perennials with

robust erect stems up to 4 m tall and with highly heterogeneous canopy architecture. New leaves are dark red; stems and leaves turn orange/brown in late autumn. Although, knotweeds are considered as light-demanding species (Beerling et al., 1994; Bímová et al., 2003), they can grow under the forest canopy especially in areas disturbed by flooding, which makes the detection particularly difficult (**Table 2**). Still, the differences in phenology between knotweeds and the tree canopy (mainly the knotweed stem coloration late in the season after the canopy leaf abscission) could possibly allow for their detection using imagery from specific time or multitemporal, remotely-sensed imagery (cf. Shouse et al., 2013).

Study Area

Three study sites were chosen in Czech Republic, Central Europe (**Figure 1**). For giant hogweed detection, these were: site 1 at a hilly landscape near Louny town (59 ha; 370 m a.s.l.), and site 2 in uplands near Sokolov town (70 ha; 600 m a.s.l.). Knotweeds were studied at site 3, situated in the lowland river floodplain around the Bečva river near Hranice na Moravě (96 ha; 250 m a. s. l.; **Figure 1**). RS data covered the variety of spectral, spatial, and temporal resolution (**Table 3**), such as the satellite imagery of Pleiades 1B (50 cm pan sharpened resolution; 4 channels; sites 1 and 3), color orthophoto (25 cm; site 1 and 2; CUZK, 2015), and UAV imagery (5 cm, RGB + NIR; all sites). For giant hogweed, we studied three phenological phases: the peak of flowering (beginning of July, site 2, UAV and aerial data), the end of flowering and the start of the fruit ripening (2nd half of July, site 1, all types of data), and post-flowering period (September, site 2, UAV, **Table 3**). For knotweeds, spring acquisition (May—UAV) captured early knotweed growth when many trees did not yet have leaves, summer one (July—UAV, August—satellite) captured the top of the vegetation season, and the autumn- (September—satellite, October—UAV) and late autumn acquisitions (November—UAV) recorded orange/red decaying knotweeds while most of the tree species were again without leaves. Availability of satellite imagery from the dates of the UAV acquisition was limited by cloudy weather.

Unmanned Aircraft System Deployed

For the purpose of this study, we designed a low-cost UAV capable of performing fully-automated mapping missions controlled by the APM ArduPlane/PixHawk autopilot. Its aerial segment is propelled by an electric BLDC motor, features a flying wing design and carries two modified consumer cameras (Sony Alpha A5100 with APS-C sensor and Sony E 20/2.8 lens). The first camera acquired standard RGB, and the second was modified to be sensitive in the NIR band by the removal of the built-in IR-cut filter and the addition of a Hoya R72 filter. This setup was used as a low-cost alternative to a more expensive multispectral camera (for more details on the UAV description see Müllerová et al., 2017). Using this UAV, we could test a suitable period in the seasonal development of the target species, focusing on times when it is possibly distinct from the background, such as, flowering for giant hogweed and autumn senescence for knotweeds.

Image Processing

Pre-processing

During the UAV flight mission, the sensors were periodically triggered with an overlap and sidelap ranging between 80 and 85% of the image height and width, respectively. This setting

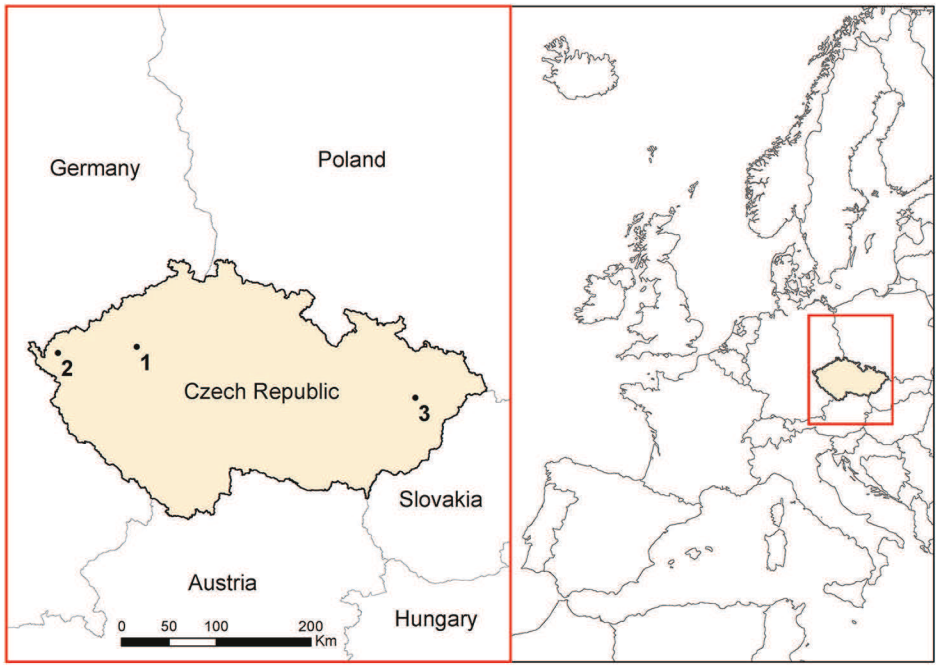


FIGURE 1 | Study areas for both invasive species. Sites 1 and 2 account for giant hogweed, site 3 for knotweeds.

TABLE 3 | Overview of study sites and imagery used.

Site No.	Name	Species	Area (ha)	Latitude	Longitude	Acquisition date			Phenological stage
						UAV	Satellite	Aerial	
1.	Domoušice	*H. mantegazzianum*	59	50.23404	13.71937	15.7.2015 20.7.2016	17.7.2015	17.7.2013	End of flowering Ripening
2.	Anenská Ves	*H. mantegazzianum*	70	50.20937	12.53582	4.9.2014 9.7.2016	–	1.7.2015	Peak of flowering Out of bloom
3.	Skalička	*Fallopia* sp.	96	49.5318	17.7944	27.8.2015 20.10.2015	7.7.2015 9.9.2016 25.5.2016 8.11.2016	–	First leaves Top of vegetation season Early senescence Late senescence

Gaps in the UAV imagery dataset are due to the technical problems with UAV.

assured a robust mosaicking. Georeferencing was carried out using structure-from-motion approach (SfM; Dandois and Ellis, 2010; Westoby et al., 2012) in Agisoft PhotoScan Professional (Agisoft, 2016). This approach identifies similar features in conjugate images, tolerating large variations in scale and image acquisition geometry, generating very dense and accurate three-dimensional point clouds (Whitehead and Hugenholtz, 2014). Since the data are often linked to other field or remote sensing data either as a reference or for change detection, very high spatial resolution of UAV data implies the need for extremely accurate georeferencing. To assure high georeferencing accuracy, a GPS module capable of RAW data output (u-blox M8T) was connected to the autopilot. Triggering the two cameras was performed by the autopilot based on the distance traveled between two consecutive images (for more details see Müllerová et al., 2017).

Imagery from Pleiades 1B satellite was orthorectified using the Rational Polynomial Coefficients metadata provided and a digital surface model, and pan-sharpened to 0.5 m resolution. All imagery was afterwards visually checked and if necessary orthorectified using a national aerial orthophoto (CUZK, 2015) to ensure that the training areas and validation points cover the same areas in all UAV and satellite data.

Classification Algorithms

Considering the inconsistent results in the comparison of different approaches to image classification (see e.g., Duro et al., 2012), we decided to test a large variety of algorithms (both pixel and object based) on both species and all three study sites. Whereas, the pixel-based approach uses only spectral information, the object-based approach takes into account also the spatial structure and context information. This approach is expected to improve the results by reducing the effects of shadows, within-class spectral variation and mis-registration, and is especially beneficial for detecting targets that take specific shape/form (Blaschke, 2010; Blaschke et al., 2014), such as giant hogweed inflorescences. It is also expected to be suitable for very high spatial resolution imagery (Laliberte and Rango, 2009). For the pixel-based classification, maximum likelihood (ML), a baseline classification method with equal probability of class assignment, and machine learning algorithms Support Vector Machine (SVM; Vapnik, 1995) and Random Forests (RF; Breiman, 2001) were employed in an ArcGIS 10.4.1 environment. Machine learning algorithms are assumed to be less sensitive to imbalanced training data sets (often the case in invasive ecology) since no assumptions are made about the distribution of input variables (Atkinson and Tatnall, 1997; Masocha and Skidmore, 2011). SVM is supposed be less susceptible to noise and correlated bands, especially useful for UAV pseudo NIR bands, and to better detect subtle and non-linear patterns (Foody and Mathur, 2004) whereas, RF classifier combining multiple classification trees (Breiman, 2001) is thought to be resistant to overfitting, strong interactions among the variables and small perturbations of the data (Pal, 2005; Cutler et al., 2007). For the object-based approach, several types of segmentation (multiresolution and contrast split) and classification (rule-based, SVM, and RF) were tested in eCognition Developer software. Multiresolution segmentation consecutively merges pixels or existing image objects minimizing the heterogeneity, whereas the contrast split segmentation divides the image into dark and bright objects based on the threshold, maximizing the contrast by an edge ratio algorithm (eCognition Developer 9.2 Reference Book, 2016). The parameters used to classify segmented objects in an iterative, rule-based classification were length/width ratio, maximum object size, brightness, mean channel value, circular standard deviation and layer mean, maximum pixel values, hue, saturation, and intensity transformation, and mean difference to darker neighbors. To train the machine learning algorithms, the following object features were used: mean, maximum, and minimum layer values and their standard deviation—both normal and circular, contrast to neighboring pixels, the geometry of objects such as extent and shape (area, border length, length/width ratio, asymmetry, compactness), textural measures (Haralick and Shanmugam, 1973) based on spatial relationships of pixels in a gray-level co-occurrence matrix, such as GLCM homogeneity, contrast, dissimilarity, and entropy. For the giant hogweed, we also tested the template matching function in eCognition, where objects are detected based on prior created "templates" generated from the imagery.

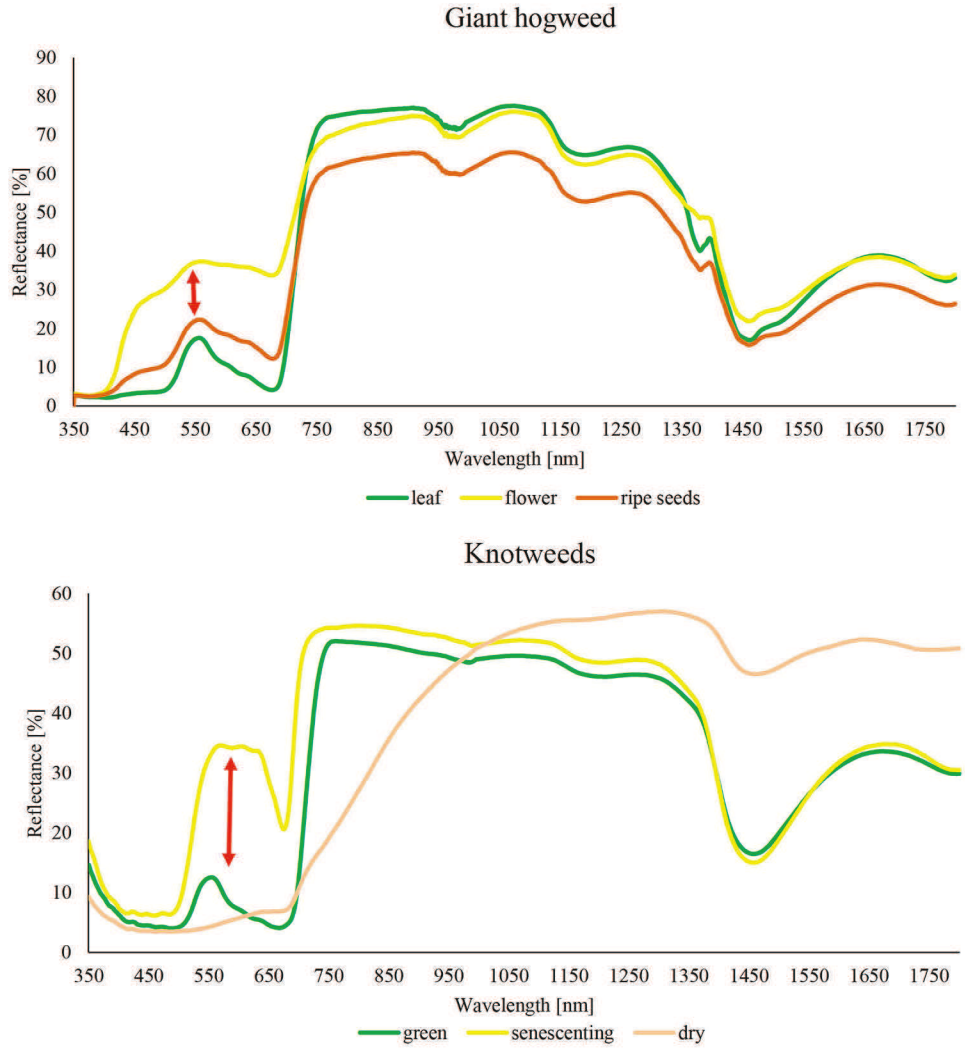


FIGURE 2 | Reflectance curves of target species *H. mantegazzianum* and *F. japonica* measured by portable spectrometer Spectral Evolution RS-3500.

To separate the role of spectral and spatial resolution, coarser spatial resolution similar to Pleiades 1B satellite was simulated by resampling UAV data to 50 cm resolution and performing the same classification algorithms (in case of knotweeds). The same training areas were used for all classifiers (inspected visually and in the field). To account for knotweeds hidden within the canopy, knotweed validation points were stratified to 50 in open areas and 50 among the canopy or in shadows, although still visible on all imagery. This allowed us to disentangle the role of the canopy in determining success in classification at different parts of vegetation season.

Field Data and Accuracy Assessment

In case of extremely high spatial resolution of the UAV imagery, geometrical precision of the field data can be problematic. Differential GNSS with centimeter precision is costly and time-consuming, especially for larger scales. Moreover, in some cases, such as a forested environment or with complex geomorphology, the estimated precision drops to several decimeters or even meters. To overcome the problem we used an Android-based application Collector for ArcGIS (ESRI, 2016) installed on a tablet with an integrated GPS. This enabled manual delineation of patches of invasive species using custom base maps, such as UAV imagery or other available high resolution orthophotos, increasing the precision of collected data. Field data collected in 2015 and 2016 were divided into the training and validation part to make the two sets independent. The reflectance spectra of the target invasive and co-occurring species were collected at midday with a portable spectrometer, Spectral Evolution RS-3500 (spectral range 350–2500 nm) using a pistol grip and calibrated, using a 99% white reference panel. Spectra were averaged from 10 measurements, repeated 10 times per species at each site and at the same distance apart, where possible.

Validation was performed using 200 randomly-distributed points (stratified sampling, 50% within the target species polygons delineated in the field) outside the training areas. For this purpose, we merged all classes without the target species into one class ("background"). All validation points were visually inspected on all images to ensure they cover the target species. In cases where the land cover changed, the points were removed and new random points were generated. Some training areas had to be reduced to cover the species on all images, because the extent of the target species changed between the acquisitions. For accuracy, assessment and comparison of the role of imagery timing and resolution, user's (UA) and producer's accuracy (PA) were used (Congalton and Green, 1999; Foody, 2002).

RESULTS

Our results show that both the detection accuracy and the best classification approach depend strongly on the phenological stage of plants, and on the spectral resolution of data (**Table 2**). This was true for both model species regardless of their markedly different phenological, structural and spectral characteristics, and seasonal dynamics. While giant hogweed was best detected when plants were flowering, thanks to its large white inflorescences, knotweeds were distinct at the phase of senescence because of reddish-brown coloring of decaying plants (**Figure 2**). In other parts of the season, detection of any of the species was more problematic and higher spectral resolution of satellite imagery improved the detection. The object-based approach was successful for giant hogweed if (i) the species was sampled in the right phenological stage and (ii) the spatial resolution enabled the distinction of individual compound umbels. For less distinct knotweeds spectral resolution of the data and pixel-based approach played more important role.

Giant hogweed was detected with a very high accuracy when flowering (up to 100%), dropping down later in the vegetation season to ∼60% (September; **Table 4**). Flowering, undamaged individuals were detected with high accuracy, whereas non-flowering, fruiting, cut, sprayed, or grazed ones were more difficult to recognize due to their similarity with the surrounding vegetation. Further, the leaves surrounding flowering umbels were difficult to map (**Figures 2**, **3**). The best results were obtained for full flowering (UAV imagery; 9 July; site 2) using an object-based approach—contrast split segmentation followed by rule-based classification (**Figure 3**). Contrast split segmentation itself separated very well the white objects on the imagery, meaning that all flowering hogweeds were detected. They were, however, mixed with other bright objects such as some artificial surfaces or harvested fields and had to be filtered out by further rule-based classification. At peak flowering, the inflorescences were so distinct that they could be detected with reasonable success (42/100% PA/UA of the hogweed class) even

TABLE 4 | Classification accuracies (in %) for giant hogweed (*Heracleum mantegazzianum*) for UAV data (RGB, modified NIR; 5 cm), color orthophotos (RGB; 25 cm), and Pleiades (MSS; 2 m pan sharpened to 50 cm).

Site 1		**UAV**														**Pleiades**						**Ortho photo**
Classification		**Pixel-based**						**Object-based**								**Pixel-based**			**Object-based**			
		ML		**SVM**		**RF**		**MRS**		**CS**		**SVM**		**RF**		**ML**	**SVM**	**RF**	**CS**	**SVM**	**RF**	**CS**
Acquisition date		15-Jul-2015	20-Jul-2016	15-Jul-2015	20-Jul-2016	15-Jul-2015	20-Jul-2016	15-Jul-2015	20-Jul-2016	**15-Jul-2015**	20-Jul-2016	15-Jul-2015	20-Jul-2016	15-Jul-2015	20-Jul-2016	**17-Jul-2015**	17-Jul-2015	17-Jul-2015	17-Jul-2015	17-Jul-2015	17-Jul-2015	17-Jul-2013
Overall accuracy		78	71	76	72	75	72	**83**	65	**83**	Failed	65	71	76	75	**91**	85	89	72	63	85	79
Hogweed class	PA	59	55	64	55	64	59	66	31	66		**69**	49	64	58	**86**	79	86	46	25	70	57
	UA	94	80	83	83	82	80	99	94	**100**		17	89	83	88	**94**	90	91	96	100	99	94

Site 2		**UAV**												**Ortho photo**
Classification		**Pixel-based**						**Object-based**						
		ML		**SVM**		**RF**		**MRS**		**CS**		**SVM**		**RF**		**CS**
Acquisition date		4-Sep-2014	9-Jul-2016	4-Sep-2014	9-Jul-2016	4-Sep-2014	9-Jul-2016	4-Sep-2014	9-Jul-2016	4-Sep-2014	**9-Jul-2016**	4-Sep-2014	9-Jul-2016	4-Sep-2014	9-Jul-2016	8-Jul-2008
Overall accuracy		58	83	61	54	60	84	Failed	82	Failed	**100**	Failed	86	Failed	84	71
Hogweed class	PA	44	66	45	66	44	69		64		**99**		72		75	42
	UA	61	99	66	99	64	99		100		**100**		100		90	100

The best results are highlighted in bold. Object-based analysis did not work for imagery from later phenophases, such cases are marked as "failed." CS, contrast split segmentation followed by rule based classification; ML, Maximum Likelihood; MRS, multiresolution segmentation followed by rule based classification; PA, producer's accuracy; RF, Random Forests; SVM, Support Vector Machines; UA, user's accuracy.

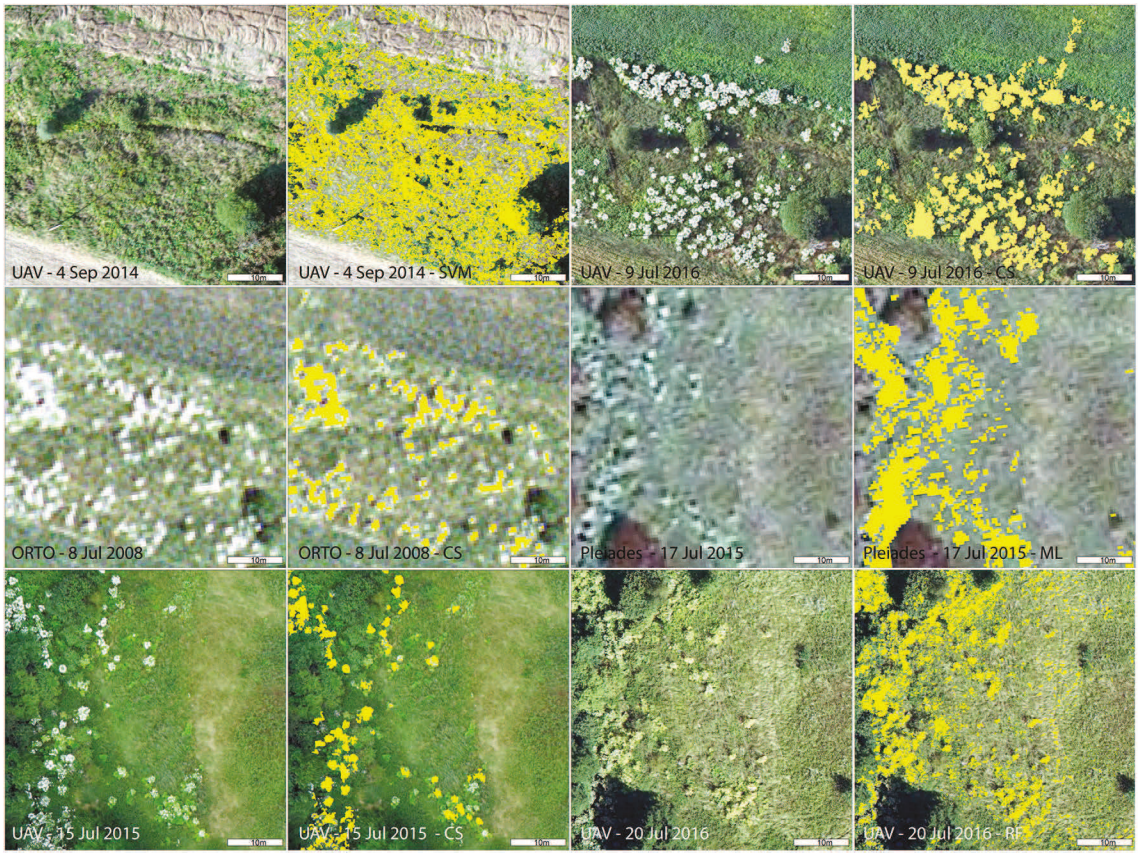


FIGURE 3 | Detail of giant hogweed at different phenophases captured by various imagery (UAV, aerial, and Pleiades) and results of the best performing classification for each imagery. CS, contrast split segmentation; ML, Maximum Likelihood; RF, Random Forests object-based.

from a low spectral resolution aerial orthophoto (25 cm) using the same approach. However, the template-matching approach incorporated in eCognition software failed to recognize the umbels even at the peak of flowering. Depending on the threshold, it either picked all the hogweed umbels and many other objects of similar shape, even of different color or, if the threshold was lower, it missed half of the plants. It could work well if the infested area was previously masked out and the algorithm ran with high threshold only inside the infested polygons. This approach would require substantial manual input and would, thus, not be feasible to apply over larger datasets. In case of site 1, the summer UAV imagery was obtained later in the season (15 and 20 July) and part of the umbels in hogweed compound inflorescences had already started to ripen, slightly decreasing the accuracy. The contrast split rule-based approach of 15 July 2015 was the most effective, but failed completely for the imagery from 20 July 2016, when hogweed was mostly out of bloom. In the case of ripening hogweed (site 1), pixel-based approach and ML algorithm of the satellite imagery provided higher accuracy measures when compared to those derived from UAV. Still the accuracies were lower compared to full flowering hogweed on UAV imagery from site 1. In autumn, the UAV imagery depicted only leaves and dry stems, and the accuracy was very low (**Table 4**, **Figure 3**). In this case, no distinct objects could be identified and the object-based approach failed.

The accuracies of knotweed classification varied considerably according to the phenology and spectral resolution (**Table 5**; **Figure 4**). The best results obtained were for the late-autumn UAV imagery (8 November; ML for both original and 50 cm resampled), when reddish-brown knotweeds stands were clearly visible (**Figure 4**). At other parts of the vegetation season, the PA derived from UAV imagery was low. Resampling of UAV data from 5 to 50 cm to simulate the Pleiades resolution slightly improved accuracies by eliminating salt and pepper effect, showing that spatial resolution does not limit species' recognition. Classification of summer Pleiades imagery using a RF classifier provided high accuracies (74/95% PA/UA of the knotweed class). Due to their architecture, knotweeds do not form objects of distinct shape or color, and object-based algorithms were therefore unsuccessful.

DISCUSSION

Our study addresses how different aspects of data quality (spatial, spectral, and temporal), costs, and operationality affect the methodology and practical application of the detection of invasive plants. Our two model species of different phenology and architecture, giant hogweed and knotweeds, showed different results reflecting their spectral characteristics and seasonal dynamics, still phenology played an important role in detection

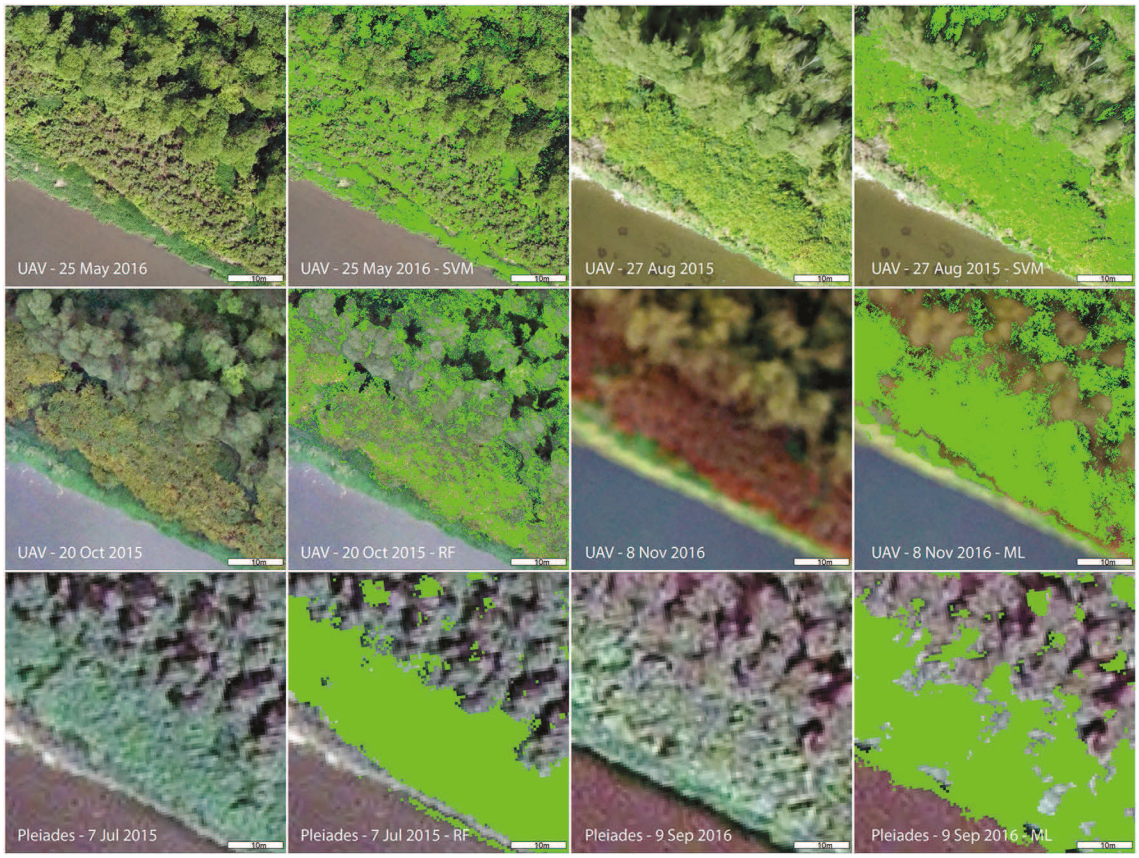


FIGURE 4 | Detail of *Fallopia* sp. at different phenophases captured by various imagery (UAV and Pleiades) and results of the best performing classification per each imagery. ML, Maximum Likelihood; RF, Random Forest; SVM, Support Vector Machine.

of both species (cf. Huang and Asner, 2009; Somodi et al., 2012; Müllerová et al., 2013; Bradley, 2014). The choice of the best data source (aerial color orthophoto, UAV with RGB + NIR modified consumer cameras, and Pleiades satellite MSS imagery) and classification approach (object or pixel based) depended strongly on the species' characteristics and their phenological stage.

We demonstrate that the spectral resolution of the low-cost solution, represented by an unmanned aircraft system, is limited (720–950 nm with variable response declining rapidly toward the longer wavelength; Müllerová et al., 2017), but that this limitation can to some extent be surpassed by identifying the right phenological stage when a more satisfactory detection rate is achievable even for the less distinct species such as knotweed. During the spring, when the knotweed stands are formed by the mixture of old red stems from the previous year and short emerging new regrowth stems, and summer acquisition, with dense, fully-developed indistinct stands, spectral resolution became more important for the detection. On the other hand, during the senescent phase the reddish color and better visibility of knotweeds under defoliated trees provided good detectability irrespective of the spectral quality. The problem with the canopy cover hiding knotweeds during the vegetation season was partly solved by using off-season imagery (from late autumn), but some individuals still remained hidden, covered by trunks or by their shadows.

The very fine spatial resolution of UAV imagery was not always beneficial. In case of hogweed, it actually overwhelmed the relevant spatial patterns and hampered the classification based on flowering objects since, in such a great detail, instead of the consistent white "dots" of hogweed inflorescences, individual umbels of each inflorescence were visible, eventually decreasing the classification accuracy (cf. Ustin and Santos, 2010). On the other hand, the fine detail enabled mapping of the hogweed leaves surrounding flowering umbels and, to some extent, non-flowering individuals. In case of knotweed (pixel-based approach), very fine spatial resolution of UAV data caused the salt and pepper effect, eliminated after resampling and being less pronounced in case of late autumn imagery and slightly blurred due to technical matters relating to cameras. Still, the resampling of summer UAV imagery lowered the success rate, probably because, in the forest, individual pixels of knotweeds visible among the canopy trees were merged into mixed pixels.

We achieved slightly higher giant hogweed detection rates compared to previous aerial photography analysis (Müllerová et al., 2013). Michez et al. (2016) used a similar approach,

TABLE 5 | Classification accuracies (in %) for knotweed (*Fallopia* sp.) for UAV data (RGB, modified NIR; 5 cm, and resampled to 50 cm), and Pleiades (MSS; 2 m pan sharpened to 50 cm).

Classification		**ML**				**SVM**				**RF**			
Site 3													
UAV (5 cm)													
Acquisition date		25-May-2016	27-Aug-2015	20-Oct-2015	8-Nov-2016	25-May-2016	27-Aug-2015	20-Oct-2015	8-Nov-2016	25-May-2016	27-Aug-2015	20-Oct-2015	8-Nov-2016
Overall accuracy		66	76	77	79	74	78	75	76	65	74	76	73
Knotweed	PA	44	53	63	80	55	60	57	54	37	57	67	47
Class	UA	77	77	86	78	87	92	88	95	82	86	82	96
UAV RESAMPLED TO (50 cm)													
Acquisition date		25-May-2016	27-Aug-2015	20-Oct-2015	8-Nov-2016	25-May-2016	27-Aug-2015	20-Oct-2015	8-Nov-2016	25-May-2016	27-Aug-2015	20-Oct-2015	8-Nov-2016
Overall accuracy		70	68	79	83	69	82	71	78	62	75	72	73
Knotweed	PA	47	43	74	82	47	67	51	60	31	55	56	50
class	UA	85	86	82	83	84	94	85	92	82	90	82	93
PLEIADES (2 M PAN SHARP. TO 50 cm)													
Classification				**ML**				**SVM**				**RF**	
Acquisition date				7-Jul-2015	9-Sep-2016			7-Jul-2015	9-Sep-2016			7-Jul-2015	9-Sep-2016
Overall accuracy				80	72			85	70			85	66
Knotweed	PA			68	54			74	49			74	43
Class	UA			89	83			94	83			95	78

The best results are highlighted in bold. Object-based analysis did not provide satisfactory results and is not shown. ML, Maximum Likelihood; PA, producer's accuracy; RF, Random Forests; SVM, Support Vector Machines; UA, user's accuracy.

applying multiresolution segmentation (an object-based approach) and RF classifier on UAV imagery gaining higher overall accuracy; still since the authors do not provide the hogweed class accuracy, it is difficult to compare their results with ours. In contrast to our research, earlier studies of knotweed detection did not achieve the accuracies sufficient for operational application (Dorigo et al., 2012; Michez et al., 2016). Dorigo et al. (2012), who detected knotweed using a ratio of spring and summer aerial photography, applied a random-forest classifier based on pixels combined with textural information derived from a moving kernel. Jones et al. (2011) performed a rule-based object-oriented classification of aerial photography but provide no assessment of accuracy so their results are difficult to compare. Michez et al. (2016) applied multiresolution segmentation (an object-based approach) and RF classifier of UAV imagery, but provided only overall accuracies and Kappa index, and admitted that they did not reach sufficient accuracies for operational application. These authors show that the best results were provided by using very small objects (~30 cm in size) and spectral indices, which is actually similar to the pixel-based methods. In some cases, ML performed slightly better compared to the learning algorithms, still the differences were minor. The commonly accepted principle of machine learning algorithms outcompeting ML cannot therefore be taken as a rule of thumb (but see Andermann and Gloaguen, 2009; Otukei and Blaschke, 2010). For object-based classification, a rule-based algorithm was more successful compared to the machine learning, still the method is highly case-specific, less universal, and requires substantially more expert knowledge.

Trade-offs exist between spatial, spectral, and temporal resolution while minimizing cost and making an approach operationally viable (Wiens et al., 2009; Willis, 2015). The demands for both spatial and spectral resolution depend largely on the target plant species; good results can be achieved with substantially lower resolution if the vegetation is sampled at the phenological phase when the species is at its most distinct. Our study shows that proper timing and high spatial resolution can to some extent compensate for the lower spectral resolution of a low-cost, unmanned aerial system, and help to decrease the error of omission. This is important for practical applications

as it minimizes the number of missed plants (Müllerová et al., 2013). Multispectral or even hyperspectral UAV sensors available on the market would definitely improve the resulting accuracy; our low-cost solution of modified consumer cameras provides substantially lower spectral quality (Müllerová et al., 2017). We believe, however, that such instruments would make the resulting methodology too costly and complex to be puts into operation for nature conservation or land management.

UAV technology with its high flexibility and low costs can provide an appropriate sampling method at a high spatio-temporal scale. We do, however, need to be aware of several limits for application in the management of invasive plants. Among these are legal constraints in those urban areas that are typically invaded by alien plants and under the focus of land managers (Pyšek and Hulme, 2005). UAV is well-suited for experimental studies, targeted monitoring and eradication control, yet the satellite imagery (if available at right phenological phases) provides more appropriate solution for larger areas. For species with distinct appearance aerial imagery should also be considered.

CONCLUSIONS AND LESSONS LEARNED

The variety of data and especially flexibility of the UAV approach enabled us to assess the effect of timing of the data acquisition (i.e., the phenological stage of the target invasive species) and both spectral and spatial resolution on the detection success. Our research establishes a methodology for targeted timely monitoring of invasive species, provides land managers and nature protection with information on spatial distribution of invaders and serves as a baseline for assessment and modeling of spatial patterns and future spread of invasive plants. Nevertheless, it is necessary to be aware of limits of the RS detection, for example, if the target plant is under dense tree canopies or heavily damaged by mowing, grazing, or spraying. Our results indicate that the choice of the best classification method is case-specific, depending largely on both the target plant and imagery characteristics. The results from one methodological comparison should not, therefore, be mechanically transposed to other target species and data types. A detailed methodological analysis and testing of possible approaches such as ours is therefore a necessary step in finding optimal mapping strategies. For practical implementation of the proposed monitoring approach, the recommended time window should be wide enough to allow for organizing a flight campaign, and highly-flexible, small UAVs are a great choice, providing an opportunity to carry out the mission at the right time and in a cost-effective manner.

AUTHOR CONTRIBUTIONS

JM contributed substantially to the conception of the work, data acquisition, processing, analysis and interpretation, and composing the manuscript. JB contributed substantially to the data acquisition, processing, analysis and interpretation, and composing the manuscript. TB contributed to the data acquisition and processing, and composing the manuscript. PD contributed to the data acquisition and processing, and composing the manuscript. PP contributed to the conception of the work and composing the manuscript. MV contributed to the field data acquisition, interpretation, and composing the manuscript.

FUNDING

The research was supported by the Centre of Excellence PLADIAS (project no. 14-36079G from the Czech Science Foundation), Praemium Academiae award to PP from The Czech Academy of Sciences, was part of long-term research development project no. RVO 67985939 and received funding from the MEYS under the National Sustainability Programme I (Project LO1202).

ACKNOWLEDGMENTS

We thank Lucie Šmejdová for her help with the collection of the field data, and Václav Vobora for help with the pre-processing of the UAV data.

REFERENCES

Agisoft (2016). *Agisoft PhotoScan*. Available online at: http://www.agisoft.com/ (Accessed September 25, 2016).

Andermann, C., and Gloaguen, R. (2009). Estimation of erosion in tectonically active orogenies. Example from the Bhotekoshi catchment, Himalaya (Nepal). *Int. J. Remote Sens.* 30, 3075–3096. doi: 10.1080/01431160802558733

Andrew, M. E., and Ustin, S. L. (2006). Spectral and physiological uniqueness of perennial pepperweed (*Lepidium latifolium*). *Weed Sci.* 54, 1051–1062. doi: 10.1614/WS-06-063R1.1

Andrew, M. E., and Ustin, S. L. (2008). The role of environmental context in mapping invasive plants with hyperspectral image data. *Remote Sens. Environ.* 112, 4301–4317. doi: 10.1016/j.rse.2008.07.016

Asner, G. P., Hughes, R. F., Vitousek, P. M., Knapp, D. E., Kennedy-Bowdoin, T., Boardman, J., et al. (2008). Invasive plants transform the three-dimensional structure of rain forests. *Proc. Natl. Acad. Sci. U.S.A.* 105, 4519–4523. doi: 10.1073/pnas.0710811105

Atkinson, P. M., and Tatnall, A. R. L. (1997). Introduction - neural networks in remote sensing. *Int. J. Remote Sens.* 18, 699–709. doi: 10.1080/014311697218700

Beerling, D. J., Bailey, J. P., and Conolly, A. P. (1994). *Fallopia japonica* (Houtt.) ronse decraene. *J. Ecol.* 82, 959–979. doi: 10.2307/2261459

Bímová, K., Mandák, B., and Pyšek, P. (2003). Experimental study of vegetative regeneration in four invasive Fallopia taxa (Polygonaceae). *Plant Ecol.* 166, 1–16. doi: 10.1023/A:1023299101998

Blaschke, T. (2010). Object based image analysis for remote sensing. *ISPRS J. Photogrammetry and remote sensing* 65, 2–16. doi: 10.1016/j.isprsjprs.2009.06.004

Blaschke, T., Hay, G. J., Kelly, M., Lang, S., Hofmann, P., Addink, E., et al. (2014). Geographic object-based image analysis–towards a new paradigm. *ISPRS J. Photogramm. Remote Sens.* 87, 180–191. doi: 10.1016/j.isprsjprs.2013.09.014

Bradley, B. A. (2014). Remote detection of invasive plants: a review of spectral, textural and phenological approaches. *Biol. Invasions* 16, 1411–1425. doi: 10.1007/s10530-013-0578-9

Breiman, L. (2001). Random forests. *Mach. Learn.* 45, 5–32. doi: 10.1023/A:1010933404324

Calviño-Cancela, M., Méndez-Rial, R., Reguera-Salgado, J., and Martín-Herrero, J. (2014). Alien plant monitoring with ultralight airborne imaging spectroscopy. *PLoS ONE* 9:e102381. doi: 10.1371/journal.pone.0102381

Congalton, R. G., and Green, K. (1999). *Assessing the Accuracy of Remotely Sensed Data: Principles and Practices*. New York, NY: Lewis Publishers.

Cutler, D. R., Edwards, T. C., Beard, K. H., Cutler, A., Hess, K. T., Gibson, J., et al. (2007). Random forests for classification in ecology. *Ecology* 88, 2783–2792. doi: 10.1890/07-0539.1

CUZK (2015). *Orthophoto of the Czech Republic 2015*. Available online at: http://geoportal.cuzk.cz/WMS_ORTOFOTO_PUB/WMService.aspx (Accessed July 25, 2016).

DAISIE (2012). *European Invasive Alien Species Gateway*. Available online at: http://www.europe-aliens.org/

Dandois, J. P., and Ellis, E. C. (2010). Remote sensing of vegetation structure using computer vision. *Remote Sens.* 2, 1157–1176. doi: 10.3390/rs2041157

Dorigo, W., Lucieer, A., Podobnikar, T., and Čarni, A. (2012). Mapping invasive *Fallopia japonica* by combined spectral, spatial, and temporal analysis of digital orthophotos. *Int. J. Appl. Earth Observ. Geoinform.* 19, 185–195. doi: 10.1016/j.jag.2012.05.004

Duro, D. C., Franklin, S. E., and Dubé, M. G. (2012). A comparison of pixel-based and object-based image analysis with selected machine learning algorithms for the classification of agricultural landscapes using SPOT-5 HRG imagery. *Remote Sens. Environ.* 118, 259–272. doi: 10.1016/j.rse.2011.11.020

eCognition Developer 9.2 Reference Book (2016). *Trimble Germany GmbH*. Available online at: http://www.ecognition.com/

ESRI (2016). *Collector for ArcGIS*. Available online at: https://doc.arcgis.com/en/collector (Accessed December 5, 2016).

Foody, G. M. (2002). Status of land cover classification accuracy assessment. *Remote Sens. Environ.* 80, 185–201. doi: 10.1016/S0034-4257(01)00295-4

Foody, G. M., and Mathur, A. (2004). Toward intelligent training of supervised image classifications: directing training data acquisition for SVM classification. *Remote Sens. Environ.* 93, 107–117. doi: 10.1016/j.rse.2004.06.017

Frazier, A. E., and Wang, L. (2011). Characterizing spatial patterns of invasive species using sub-pixel classifications. *Remote Sens. Environ.* 115, 1997–2007. doi: 10.1016/j.rse.2011.04.002

Fridley, J. D. (2012). Extended leaf phenology and the autumn niche in deciduous forest invasions. *Nature* 485, 359–362. doi: 10.1038/nature11056

Ge, S., Everitt, J., Carruthers, R., Gong, P., and Anderson, G. (2006). Hyperspectral characteristics of canopy components and structure for phenological assessment of an invasive weed. *Environ. Monit. Assess.* 120, 109–126. doi: 10.1007/s10661-005-9052-1

Gioria, M., Pyšek, P., and Osborne, B. A. (2016). Timing is everything: does early and late germination favor invasions by herbaceous alien plants? *J. Plant Ecol.* doi: 10.1093/jpe/rtw105

Haralick, R. M., and Shanmugam, K. (1973). Textural features for image classification. *IEEE Trans. Syst. Man Cybern.* 610–621. doi: 10.1109/TSMC.1973.4309314

Huang, C. Y., and Asner, G. P. (2009). Applications of remote sensing to alien invasive plant studies. *Sensors* 9, 4869–4889. doi: 10.3390/s90604869

Jones, D., Pike, S., Thomas, M., and Murphy, D. (2011). Object-based image analysis for detection of Japanese Knotweed s.l. taxa (Polygonaceae) in Wales (UK). *Remote Sens.* 3, 319–342. doi: 10.3390/rs3020319

Kaiser, B. A., and Burnett, K. M. (2010). Spatial economic analysis of early detection and rapid response strategies for an invasive species. *Resour. Energy Econ.* 32, 566–585. doi: 10.1016/j.reseneeco.2010.04.007

Kowarik, I. (2008). "On the role of alien species in urban flora and vegetation," in *Urban Ecology*, eds J. Marzluff, E. Shulenberger, W. Endlicher, M. Alberti, G. Bradley, C. Ryan, C. ZumBrunnen, and U. Simon (New York, NY: Springer), 321–338.

Laba, M., Tsai, F., Ogurcak, D., Smith, S., and Richmond, M. E. (2005). Field determination of optimal dates for the discrimination of invasive wetland plant species using derivative spectral analysis. *Photogramm. Eng. Remote Sensing* 71, 603–611. doi: 10.14358/PERS.71.5.603

Laliberte, A. S., Herrick, J. E., Rango, A., and Winters, C. (2010). Acquisition, orthorectification, and object-based classification of unmanned aerial vehicle (UAV) imagery for rangeland monitoring. *Photogramm. Eng. Remote Sensing* 76, 661–672. doi: 10.14358/PERS.76.6.661

Laliberte, A. S., and Rango, A. (2009). Texture and scale in object-based analysis of sub-decimeter resolution unmanned aerial vehicle (UAV) imagery. *IEEE Trans. Geosci. Remote Sens.* 47, 761–770. doi: 10.1109/TGRS.2008.2009355

Maheu-Giroux, M., and de Blois, S. (2004). Mapping the invasive species *Phragmites australis* in linear wetland corridors. *Aquat. Bot.* 83, 310–320. doi: 10.1016/j.aquabot.2005.07.002

Masocha, M., and Skidmore, A. K. (2011). Integrating conventional classifiers with a GIS expert system to increase the accuracy of invasive species mapping. *Int. J. Appl. Earth Observ. Geoinform.* 13, 487–494. doi: 10.1016/j.jag.2010.10.004

McEwan, R. W., Birchfield, M. K., Schoergendorfer, A., and Arthur, M. A. (2009). Leaf phenology and freeze tolerance of the invasive shrub *Amur honeysuckle* and potential native competitors. *J. Torrey Bot. Soc.* 136, 212–220. doi: 10.3159/08-RA-109.1

Michez, A., Piégay, H., Jonathan, L., Claessens, H., and Lejeune, P. (2016). Mapping of riparian invasive species with supervised classification of Unmanned Aerial System (UAS) imagery. *Int. J. Appl. Earth Observ. Geoinform.* 44, 88–94. doi: 10.1016/j.jag.2015.06.014

Müllerová, J., Bartaloš, T., Bråna, J., Dvořák, P., and Vítková, M. (2017). Unmanned aircraft in nature conservation – an example from plant invasions. *Int. J. Remote Sens.* 38, 2177–2198. doi: 10.1080/01431161.2016.1275059

Müllerová, J., Bråna, J., Dvořák, P., Bartaloš, T., and Vítková, M. (2016). Does the data resolution/origin matter? Satellite, airborne and UAV imagery to tackle plant invasions. *Int. Arch. Photogramm. Remote Sens. Spatial Inf. Sci.* XLI-B7, 903–908. doi: 10.5194/isprs-archives-XLI-B7-903-2016

Müllerová, J., Pergl, J., and Pyšek, P. (2013). Remote sensing as a tool for monitoring plant invasions: testing the effects of data resolution and image classification approach on the detection of a model plant species *Heracleum mantegazzianum* (giant hogweed). *Int. J. Appl. Earth Observ. Geoinform.* 25, 55–65. doi: 10.1016/j.jag.2013.03.004

Müllerová, J., Pyšek, P., Jarošík, V., and Pergl, J. (2005). Aerial photographs as a tool for assessing the regional dynamics of the invasive plant species *Heracleum mantegazzianum*. *J. Appl. Ecol.* 42, 1–12. doi: 10.1111/j.1365-2664.2005.01092.x

Otukei, J. R., and Blaschke, T. (2010). Land cover change assessment using decision trees, support vector machines and maximum likelihood classification algorithms. *Int. J. Appl. Earth Observ. Geoinform.* 12, S27–S31. doi: 10.1016/j.jag.2009.11.002

Page, N. A., Wall, R. E., Darbyshire, S. J., and Mulligan, G. A. (2006). The biology of invasive alien plants in Canada, 4. *Heracleum mantegazzianum* Sommier and Levier. *Can. J. Plant Sci.* 85, 569–589. doi: 10.4141/P05-158

Pal, M. (2005). Random forest classifier for remote sensing classification. *Int. J. Remote Sens.* 26, 217–222. doi: 10.1080/01431160412331269698

Pergl, J., Perglová, I., Pyšek, P., and Dietz, H. (2006). Population age structure and reproductive behaviour of the monocarpic perennial *Heracleum mantegazzianum* (Apiaceae) in its native and invaded distribution ranges. *Am. J. Bot.* 93, 1018–1028. doi: 10.3732/ajb.93.7.1018

Pergl, P., Müllerová, J., Perglová, I., Herben, T., and Pyšek, P. (2011). The role of long-distance seed dispersal in the local population dynamics of an invasive plant species. *Divers. Distrib.* 17, 725–738. doi: 10.1111/j.1472-4642.2011.00771.x

Perglová, I., Pergl, J., and Pyšek, P. (2006). Flowering phenology and reproductive effort of the invasive alien plant *Heracleum mantegazzianum*. *Preslia* 78, 265–285.

Peterson, E. B. (2005). Estimating cover of an invasive grass (*Bromus tectorum*) using tobit regression and phenology derived from two dates of Landsat ETM+ data. *Int. J. Remote Sens.* 26, 2491–2507. doi: 10.1080/01431160500127815

Pyšek, P. (1998). Alien and native species in Central European urban floras: a quantitative comparison. *J. Biogeogr.* 25, 155–163. doi: 10.1046/j.1365-2699.1998.251177.x

Pyšek, P., and Hulme., P. E. (2005). Spatio-temporal dynamics of plant invasions: linking pattern to process. *Ecoscience* 12, 302–315. doi: 10.2980/i1195-6860-12-3-302.1

Pyšek, P., and Richardson, D. M. (2010). Invasive species, environmental change and management, and health. *Annu. Rev. Environ. Resour.* 35, 25–55. doi: 10.1146/annurev-environ-033009-095548

Rango, A., Laliberte, A., Herrick, J. E., Winters, C., Havstad, K., Steele, C., et al. (2009). Unmanned aerial vehicle-based remote sensing for rangeland assessment, monitoring, and management. *J. Appl. Remote Sens.* 3:033542. doi: 10.1117/1.3216822

Resasco, J., Hale, A. N., Henry, M. C., and Gorchov, D. L. (2007). Detecting an invasive shrub in a deciduous forest understory using late-fall Landsat sensor imagery. *Int. J. Remote Sens.* 28, 3739–3745. doi: 10.1080/01431160701373721

Rocchini, D., Andreo, V., Förster, M., Garzon-Lopez, C. X., Gutierrez, A. P., Gillespie, T. W., et al. (2015). Potential of remote sensing to predict species invasions: a modelling perspective. *Progr. Phys. Geogr.* 39, 283–309. doi: 10.1177/0309133315574659

Salamí, E., Barrado, C., and Pastor, E. (2014). UAV flight experiments applied to the remote sensing of vegetated areas. *Remote Sens.* 6, 11051–11081. doi: 10.3390/rs61111051

Shouse, M., Liang, L., and Fei, S. (2013). Identification of understory invasive exotic plants with remote sensing in urban forests. *Int. J. Appl. Earth Observ. Geoinform.* 21, 525–534. doi: 10.1016/j.jag.2012.07.010

Somers, B., and Asner, G. P. (2013). Invasive species mapping in Hawaiian rainforests using multi-temporal *Hyperion spaceborne* imaging spectroscopy. *IEEE J. Sel. Topics Appl. Earth Observ. Remote Sens.* 6, 351–359. doi: 10.1109/JSTARS.2012.2203796

Somodi, I., Čarni, A., Ribeiro, D., and Podobnikar, T. (2012). Recognition of the invasive species *Robinia pseudacacia* from combined remote sensing and GIS sources. *Biol. Conserv.* 150, 59–67. doi: 10.1016/j.biocon.2012.02.014

Ustin, S. L., and Santos, M. J. (2010). "Spectral identification of native and non-native plant species," in *Proceedings of ASD and IEEEGRS; Art, Science and Applications of Reflectance Spectroscopy Symposium*, Vol. II (Boulder, CO), 17.

Vapnik, V. (1995). *The Nature of Statistical Learning Theory*. New York, NY: Springer-Verlag.

Vilà, M., Basnou, C., Pyšek, P., Josefsson, M., Genovesi, P., Gollasch, S., et al. (2010). How well do we understand the impacts of alien species on ecosystem services? A pan-European, cross-taxa assessment. *Front. Ecol. Environ.* 8, 135–144. doi: 10.1890/080083

Watts, A. C., Ambrosia, V. G., and Hinkley, E. A. (2012). Unmanned aircraft systems in remote sensing and scientific research: classification and considerations of use. *Remote Sens.* 4, 1671–1692. doi: 10.3390/rs4061671

Westoby, M. J., Brasington, J., Glasser, N. F., Hambrey, M. J., and Reynolds, J. M. (2012). Structure-from-motion photogrammetry: a lowcost, effective tool for geoscience applications. *Geomorphology* 179, 300–314. doi: 10.1016/j.geomorph.2012.08.021

Whitehead, K., and Hugenholtz, C. H. (2014). Remote sensing of the environment with small unmanned aircraft systems (UASs), part 1: a review of progress and challenges 1. *J. Unmanned Veh. Syst.* 2, 69–85. doi: 10.1139/juvs-2014-0006

Wiens, J., Sutter, R., Anderson, M., Blanchard, J., Barnett, A., Aguilar-Amuchastegui, N., et al. (2009). Selecting and conserving lands for biodiversity: the role of remote sensing. *Remote Sens. Environ.* 113, 1370–1381. doi: 10.1016/j.rse.2008.06.020

Wilfong, B. N., Gorchov, D. L., and Henry, M. C. (2009). Detecting an invasive shrub in deciduous forest understories using remote sensing. *Weed Sci.* 57, 512–520. doi: 10.1614/WS-09-012.1

Willis, K. S. (2015). Remote sensing change detection for ecological monitoring in United States protected areas. *Biol. Conserv.* 182, 233–242. doi: 10.1016/j.biocon.2014.12.006

Wolkovich, E. M., and Cleland, E. E. (2011). The phenology of plant invasions: a community ecology perspective. *Front. Ecol. Environ.* 9, 287–294. doi: 10.1890/100033

Conflict of Interest Statement: The authors declare that the research was conducted in the absence of any commercial or financial relationships that could be construed as a potential conflict of interest.

Copyright © 2017 Müllerová, Brůna, Bartaloš, Dvořák, Vítková and Pyšek. This is an open-access article distributed under the terms of the Creative Commons Attribution License (CC BY). The use, distribution or reproduction in other forums is permitted, provided the original author(s) or licensor are credited and that the original publication in this journal is cited, in accordance with accepted academic practice. No use, distribution or reproduction is permitted which does not comply with these terms.